UNIVERSIDADE FEDERAL DE SANTA CATARINA
CENTRO DE TECNOLOGIA
PROGRAMA DE PÓS-GRADUAÇÃO EM ENGENHARIA ELÉTRICA

Victoria Dala Pegorara Souto

APPLICATION OF EVOLUTIONARY COMPUTATION TECHNIQUES IN EMERGING OPTIMIZATION PROBLEMS IN 5G AND BEYOND WIRELESS SYSTEMS

Florianópolis
2021

Victoria Dala Pegorara Souto

APPLICATION OF EVOLUTIONARY COMPUTATION TECHNIQUES IN EMERGING OPTIMIZATION PROBLEMS IN 5G AND BEYOND WIRELESS SYSTEMS

Tese submetida ao Programa de Pós-Graduação em Engenharia Elétrica da Universidade Federal de Santa Catarina para a obtenção do título de Doutora em Engenharia Elétrica.
Orientador: Prof. Bartolomeu Ferreira Uchôa Filho, Dr.
Coorientador: Prof. Richard Demo Souza, Dr.

Florianópolis
2021

Ficha de identificação da obra elaborada pelo autor,
através do Programa de Geração Automática da Biblioteca Universitária da UFSC.

Souto, Victoria Dala Pegorara Souto
Application of evolutionary computation techniques in emerging optimization problems in 5G and beyond wireless systems / Victoria Dala Pegorara Souto Souto ; orientador, Bartolomeu Ferreira Uchôa Filho Uchôa Filho, coorientador, Richard Demo Souza Souza, 2021.
111 p.

Tese (doutorado) - Universidade Federal de Santa Catarina, Centro Tecnológico, Programa de Pós-Graduação em Engenharia Elétrica, Florianópolis, 2021.

Inclui referências.

1. Engenharia Elétrica. 2. 5G. 3. B5G. 4. Comunicações sem fio. I. Uchôa Filho, Bartolomeu Ferreira Uchôa Filho. II. Souza, Richard Demo Souza. III. Universidade Federal de Santa Catarina. Programa de Pós-Graduação em Engenharia Elétrica. IV. Título.

Victoria Dala Pegorara Souto

APPLICATION OF EVOLUTIONARY COMPUTATION TECHNIQUES IN EMERGING OPTIMIZATION PROBLEMS IN 5G AND BEYOND WIRELESS SYSTEMS

O presente trabalho em nível de doutorado foi avaliado e aprovado por banca examinadora composta pelos seguintes membros:

Prof. Glauber Gomes de Oliveira Brante, Dr.
Universidade Tecnológica Federal do Paraná

Prof. Natanael Rodrigues Gomes, Dr.
Universidade Federal de Santa Maria

Prof. Walter Pereira Casper Júnior, Dr.
Universidade Federal de Santa Catarina

Certificamos que esta é a **versão original e final** do trabalho de conclusão que foi julgado adequado para obtenção do título de Doutora em Engenharia Elétrica.

ICP-Edu
Documento assinado digitalmente
Telles Brunelli Lazzarin
Data: 05/04/2021 09:48:48-0300
CPF: 023.400.719-25
Verifique as assinaturas em https://v.ufsc.br

Coordenação do Programa de Pós-Graduação

GOV.BR
Documento assinado digitalmente
Bartolomeu Ferreira Uchoa Filho
Data: 30/03/2021 14:56:13-0300
CPF: 476.362.114-91
Verifique as assinaturas em https://v.ufsc.br

Prof. Bartolomeu Ferreira Uchôa Filho, Dr.
Orientador

Prof. Richard Demo Souza, Dr.
Coorientador

Florianópolis, 2021.

This work is dedicated to the memory of my beloved grandparents.

Acknowledgements

I thank Prof. Bartolomeu F. Uchôa Filho and Prof. Richard Demo Souza for the trust given to me and for all the opportunities entrusted to me. I am grateful for wise advice and for all the time dedicated to my personal and academic training. Their dedication and the opportunities given to me by you were unique, being essential for the accomplishment of this work. I feel honored to have been guided by these two great professionals during my doctorate.

I would like to express my unbounded love to my mother and my brother who always believe in me and gave me unconditional support to complete this work.

I thank Rafael Sanchotene Silva for accompanying me during the undergraduate, master, and doctorate courses. I would like to thank him for all the dedication, support, affection, and love. Your partnership was essential for me.

In special, I would like to thank and dedicate this thesis to the memory of my beloved grandparents. Thank you for your love. Thank you for your genuine and wise advice during part of my life. Thank you for make me who I am and being my examples and the strength that moves me to continue and achieve my goals. Thank you for making this journey possible.

Finally, with immense pleasure and gratitude, I would like to thank everyone who contributed in some way to me to complete this work.

"The saddest aspect of life right now is that science gathers knowledge faster than society gathers wisdom."
(Isaac Asimov)

RESUMO

Os sistemas comunicação sem fio 5G e além (B5G, do inglês *Beyong 5G*) permitirão a plena implantação de aplicações existentes, como carros autônomos, redes de sensores massivas e casas inteligentes. Para tornar essas aplicações possíveis, requisitos rigorosos, como alta eficiência espectral e ultra baixa latência de comunicação, devem ser atendidos. Para atender a esses requisitos, diferentes tecnologias-chave estão em desenvolvimento, como comunicações de Ondas Milimétricas (mmWave, do inglês *Millimeter Wave*) e Superfícies Refletivas Inteligentes (IRS, do inglês *Intelligent Reflecting Surfaces*). As comunicações mmWave têm atraído grande interesse devido ao abundante espectro de frequência disponível, ao contrário das bandas congestionadas adotadas nas redes 4G. No entanto, as bandas mmWave apresentam características de propagação desfavoráveis. Para superar tais problemas de propagação, o uso de *beamforming* altamente direcional é uma solução eficaz. Além disso, recentemente, uma tecnologia de baixo custo e alta eficiência energética denominada IRS, uma meta-superfície equipada com um grande número de elementos passivos de baixo custo, capaz de refletir o sinal incidente com uma dada mudança de fase/amplitude, foi desenvolvida para otimizar a capacidade da rede. Implantando densamente IRSs em redes de comunicação sem fio e coordenando seus elementos de maneira inteligente, os canais sem fio entre o transmissor e o receptor podem ser intencional e deterministicamente controlados para melhorar a qualidade do sinal no receptor. Embora essas tecnologias tenham inúmeros benefícios para o desempenho do sistema, elas apresentam muitos desafios em sua implantação. Mais especificamente, embora as bandas mmWave permitam considerar o uso de *beamforming* altamente direcional tanto na BS quanto no UE, isto pode representar um desafio para o processo de Acesso Inicial (IA, do inglês *Initial Access*) pois, uma vez que a transmissão omnidirecional não pode ser aplicada, devido ao seu baixo ganho de potência e SNR recebido, a duração geral do IA pode ser muito longa. O atraso causado pela busca direcional deve ser pequeno para atender a alguns dos requisitos das redes B5G como baixa latência de ponta-a-ponta. Além disso, apesar da capacidade das IRSs de controlar os canais sem fio, o projeto do *beamforming* na BS e na IRS é um problema desafiador devido à necessidade de estimar a informação de estado do canal (CSI, do inglês *Channel State Information*) de todos os links do sistema. No entanto, para estimar o CSI entre a IRS e a BS ou entre a IRS e o UE, cada elemento da IRS precisa ser equipado com uma cadeia de radiofrequência (RF, do inglês *Radio Frequency*), o que aumenta consideravelmente o custo e o consumo de energia do sistema e vai contra algumas das principais vantagens de utilizar IRSs em sistemas de comunicação sem fio. Portanto, motivados pelos problemas emergentes acima, nesta tese, pretendemos desenvolver novos métodos baseados em técnicas de Computação Evolutiva tais como, Algoritmos Genéticos (GA, do inglês *Genetic Algorithm*) e Otimização por Enxame de Partículas (PSO, do inglês *Particle Swarm*

Optimization), visando resolver o problema de IA e realizar o projeto do *beamforming* na BS e IRS sem conhecimento prévio do CSI na BS. Os resultados obtidos nesta tese mostram que os métodos desenvolvidos podem reduzir consideravelmente o atraso e alcançar um desempenho próximo ao ótimo no problema de projeto do *beamforming* na BS e IRS com sobrecarga de treinamento reduzida.

Palavras-chave: 5G, 5G e além, ondas milimétricas, acesso inicial, superfícies refletivas inteligentes.

RESUMO EXPANDIDO

Introdução

Como a 5G já iniciou a sua fase de implantação comercial, a indústria e a academia começaram a focar sua atenção no desenvolvimento da evolução das redes 5G e da próxima geração de sistemas de comunicação sem fio. Os sistemas sem fio B5G permitirão a plena implantação de aplicações emergentes já existentes, como carros autônomos, grandes redes de sensores, telemedicina e casas inteligentes. Para tornar essas aplicações possíveis, requisitos rigorosos como conectividade massiva, alta eficiência espectral, cobertura e taxa de dados, além de latência ultrabaixa, devem ser atendidos. A fim de atender a esses requisitos, várias tecnologias candidatas foram propostas, como comunicações mmWave e IRSs.

As comunicações mmWave têm atraído grande interesse da academia e da indústria devido ao abundante espectro disponível, ao contrário das bandas congestionadas em UHF e frequências sub-6GHz adotadas pelas redes 4G. No entanto, as bandas de mmWave apresentam características de propagação desfavoráveis devido à alta perda de percurso, atenuação atmosférica e de chuva, bloqueio e baixa difração em torno de obstáculos. Para superar esses problemas, o uso de *beamforming* altamente direcional é uma solução eficaz e pode ser obtida a partir do uso de grandes arranjos de antenas na BS e no UE.

As IRSs emergiram recentemente como um novo paradigma promissor para alcançar ambientes de propagação inteligentes e reconfiguráveis para sistemas de comunicação sem fio B5G. Uma IRS é uma meta-superfície que compreende um grande número de elementos refletivos, capazes de refletir o sinal incidente com um dado deslocamento de fase/amplitude. Ao implantar IRSs em redes de comunicação sem fio e coordenar de forma inteligente seus elementos, os canais sem fio entre o transmissor e o receptor podem ser intencional e deterministicamente controlados para melhorar a qualidade do sinal no receptor e, consequentemente, a capacidade e confiabilidade da rede.

Apesar de essas tecnologias-chave apresentarem inúmeras vantagens para o desempenho do sistema, sua implantação apresenta diversos desafios para os projetistas de redes de comunicação sem fio. Mais especificamente, embora as bandas mmWave permitam a melhoria da capacidade do sistema através da implantação de um grande número de antenas na BS e no UE, isso pode ser desafiador para o processo de IA, pelo qual o UE estabelece um link físico com a BS. A duração geral do processo IA pode ser muito longa devido ao atraso causado pela busca direcional. No entanto, o atraso de IA deve ser pequeno para atender a alguns os requisitos emergentes das redes B5G, como por exemplo baixa latência ponto-a-ponto. Além disso, embora a implantação de IRSs em redes sem fio permita que os canais sem fio sejam deterministicamente controlados, projetar o beamforming na BS e na IRS é um problema desafiador devido

ao *overhead* necessário para estimar os canais do sistema. Além deste grande *overhead*, estimar o CSI entre IRS e BS ou entre IRS e UE requer que cada elemento da IRS seja equipado com uma cadeia de radiofrequência o que aumenta consideravelmente o custo e o consumo de energia do sistema, além de contrariar as principais motivações para a implantação de IRSs em redes B5G

Portanto, motivados pelos problemas previamente apresentados, nesta tese, novos métodos baseados em técnicas de Computação Evolutiva, isto é, GA e PSO, são apresentados. Essas técnicas têm sido amplamente aplicadas nos mais diversos problemas de otimização devido à sua simplicidade de implementação, baixos custos operacionais e fácil paralelização. A partir dos métodos desenvolvidos o problema de IA em sistemas mmWave e o projeto de *beamforming* na BS e IRS foram resolvidos com sucesso, demonstrando a relevância e eficiência dessas técnicas na resolução de problemas emergentes das redes B5G.

Objetivos

O objetivo principal desta tese é o desenvolvimento de novos métodos baseados em técnicas de Computação Evolutiva para a resolução de problemas emergentes de sistemas de comunicação B5G. Além disso, os objetivos específicos desta tese são:

- Desenvolver um novo método baseado em técnicas de Computação Evolutiva para resolver o problema de IA em sistemas MIMO mmWave.
- Desenvolver um novo método baseado em técnicas de Computação Evolutiva visando realizar o projeto de *beamforming* na BS e na IRS sem a necessidade de estimar o CSI instantâneo de todos os links do sistema.

Em relação à Computação Evolutiva, o objetivo é demonstrar que esses métodos podem ser usados com sucesso para resolver problemas emergentes relevantes e complexos das redes B5G. Assim, o foco não é ajustar os parâmetros dos algoritmos propostos para atingir um desempenho ótimo, mas demonstrar que eles são capazes de atingir um desempenho próximo ao ótimo com complexidade razoável e configuração padrão. A otimização detalhada dos parâmetros do PSO e GA é deixada como um potencial trabalho futuro.

Metodologia

A pesquisa desenvolvida para elaboração desta tese iniciou-se com uma revisão bibliográfica dos principais problemas encontrados na implantação das redes B5G. Motivados pelos problemas apresentados na literatura, dois problemas emergentes foram selecionados para serem alvo de estudo nesta tese, são eles: IA em sistemas mmWave e projeto de beamforming em redes assistidas por IRS.

Após definido os problemas a serem abordados, foi realizada uma revisão bibliográfica das técnicas de IA existentes na literatura, visando elencar suas principais características, vantagens e desvantagens. Além disso, foi realizado um estudo das características de propagação em sistemas *mmWave* e de técnicas de *beamforming* a serem utilizadas com o objetivo de otimizar o desempenho do sistema.

Ademais, realizou-se um amplo estudo das características físicas das IRSs e dos principais desafios existentes para sua plena implantação em redes B5G. Tendo em vista que ambos os problemas de otimização, alvo de estudo nesta tese, são não convexos, ou seja, não existe um método padrão para resolvê-los, foi realizado um estudo aprofundado das principais técnicas de Computação Evolutiva existentes e da viabilidade de utilizá-las na resolução dos problemas abordados.

Para finalizar, foi realizado o desenvolvimento de métodos baseados em técnicas de Computação Evolutiva capazes de reduzir o atraso inserido pela busca celular no procedimento de IA e realizar o projeto sub-ótimo do beamforming na BS e IRS reduzindo o consumo de energia do sistema e otimizando o seu desempenho. Os métodos desenvolvidos foram avaliados em diferentes cenários, visando comprovar sua eficiência e aplicabilidade em aplicações práticas.

Resultados e Discussão

Nesta tese, tanto o problema de IA em sistemas mmWave quanto o projeto de *beamforming* em sistemas sem fio assistidos por IRS são abordados. Uma das principais contribuições desta tese é mostrar que a Computação Evolutiva pode ser usada com sucesso para resolver tais problemas de otimização os quais são relevantes para o pleno desenvolvimento das redes B5G.

Nesta tese, diferentes problemas de otimização são apresentados e resolvidos com sucesso usando técnicas de Computação Evolutiva. Mais especificamente, um método de refinamento de feixe baseado em GA é proposto a fim de reduzir o atraso da busca direcional no procedimento de IA em sistemas mmWave, considerando cenários com e sem restrições de atraso. O método proposto foi avaliado em diferentes cenários. Através dos resultados obtidos foi possível concluir que o método proposto apresenta um excelente desempenho quando comparado a outras heurísticas apresentadas na literatura e pode atingir os mesmos resultados que a Busca Exaustiva (ES, do inglês *Exhaustive Search*). Além disso, o algoritmo proposto pode reduzir o atraso de busca celular introduzido pelo uso de *beamforming* na BS e UE.

Ademais, a implantação de IRSs em sistemas de comunicação sem fio é estudada e diferentes abordagens são avaliadas. Incialmente, um novo método baseado em PSO é proposto a fim de minimizar a potência de transmissão na BS, otimizando conjuntamente o *beamforming* na BS e na IRS considerando fases contínuas na IRS e

restrição de taxa mínima no UE. A solução proposta alcançou um desempenho próximo ao ideal com uma quantidade razoável de feedback do UE, permitindo o uso de IRS sem a necessidade de implantar uma cadeia de RF por elemento, já que não é necessário realizar a aquisição do CSI, reduzindo, assim, o custo e o consumo de energia do sistema. Para finalizar, um cenário mais realista o qual considera fases discretas na IRS, é avaliado. Em seguida, duas soluções diferentes são propostas. Primeiramente, um novo método baseado em GA é proposto, o qual não considera nenhum conhecimento do CSI na BS. Um projeto sub-ótimo de *beamforming* na BS e na IRS, considerando mudanças de fase discretas, é apresentado. Para finalizar, outra solução baseada em GA é proposta com o objetivo de resolver o problema de projeto do *beamforming* explorando apenas o conhecimento estatístico do canal. As novas soluções foram avaliadas considerando diferentes configurações de parâmetros do sistema e, a partir dos resultados obtidos, pôde-se concluir que os métodos propostos apresentam um ótimo desempenho considerando fases discretas com um pequeno números de bits de controle em cada elemento e com uma quantidade razoável de feedback do UE. Portanto, as soluções propostas são muito atrativas na prática.

A partir dos resultados apresentados nesta tese, é possível confirmar a eficiência das técnicas de Computação Evolutiva na solução de problemas emergentes de otimização não convexa relacionados a sistemas sem fio B5G.

Considerações Finais

Nesta tese diferentes problemas emergentes das redes B5G são abordados a partir da aplicação de técnicas de Computação Evolutiva. Mais expecificamente, esta tese demostra que a Computação Evolutiva pode ser usada com sucesso para resolver o problema de IA em sistemas de comunicação mmWave e otimizar o projeto de *beamforming* em sistemas sem fio assistidos por IRS. No entanto, alguns cenários práticos, otimização de parâmetros e outros problemas de otimização emergentes não são investigados e são propostos em trabalhos futuros.

Palavras-chave: 5G, 5G e além, ondas milimétricas, acesso inicial, superfícies refletivas inteligentes.

ABSTRACT

Beyond 5G (B5G) wireless systems will enable the deployment of demanding applications such as autonomous cars, massive sensor networks, and smart homes. To make these applications possible, stringent requirements such as improved spectrum efficiency and low communication latency must be fulfilled. In order to meet these requirements, different key technologies are in development such as millimeter Wave (mmWave) communications and Intelligent Reflecting Surfaces (IRS). The mmWave communications have attracted great interest due to the abundant available spectrum, unlike the congested bands adopted in the 4G networks. However, the mmWave bands present poor propagation characteristics. To overcome these propagation issues, the use of highly directional beamforming is an effective solution. In addition, recently, an energy-efficient and low-cost technology named IRS, which is a meta-surface equipped with a large number of low-cost passive elements, capable of reflecting the incident signal with a given phase/amplitude shift, was developed to increase the network capacity. By densely deploying IRSs in wireless communication networks and intelligently coordinating their elements, the wireless channels between the transmitter and receiver can be intentionally and deterministically controlled to improve the signal quality at the receiver. Although these technologies have uncountable benefits for the system performance, they present many challenges in their deployment. More specifically, although the mmWave bands allow to consider highly directional beamforming at the BS and UE, this can be challenging for the Initial Access (IA) process. Since omnidirectional transmission may not be applied, due to its low power gain and received SNR, the overall duration of IA can be very long. The delay caused by directional search must be small to meet some of the B5G requirements for low end-to-end latency. Moreover, despite the capacity of controlling the wireless channels of the IRSs, designing the beamforming at the BS and at the IRS is a challenging problem due to the necessity of estimating the channel state information (CSI) of all system links. However, to estimate the CSI between IRS and BS or between IRS and UE, each element of the IRS needs to be equipped with one radio-frequency (RF) chain which greatly increases the cost and energy consumption of the system and goes against some of the original advantages of using an IRS. Therefore, motivated by the above emerging problems, in this thesis, we intend to develop new methods based on Evolutionary Computation techniques, *i.e.*, Genetic Algorithms (GA) and Particle Swarm Optimization (PSO), to solve the IA problem and to design the beamforming at the BS and IRS without CSI. Results show that the developed methods can reduce the IA delay and achieve a close-to-optimal performance in the IRS beamforming problem with reduced training overhead.

Keywords: 5G, 5G and beyond (B5G), Millimeter Wave, Initial Access, Intelligent Reflecting Surfaces.

LIST OF FIGURES

LIST OF TABLES

LIST OF ABBREVIATIONS AND ACRONYMS

5G	Fifth Generation
AoA	Angle of Arrival
AoD	Angle of Departure
B5G	Beyond 5G
BS	Base Station
CSI	Channel State Information
DFT	Discrete Fourier Transform
ES	Exhaustive Search
GA	Genetic Algorithm
IA	Initial Access
I-CSI	Instantaneous Channel State Information
MIMO	Multiple-Input Multiple-Output
mmWave	Millimeter Wave
MRT	Maximum-Ratio Transmission
PSO	Particle Swarm Optimization
RF	Radio Frequency
S-CSI	Statistical Channel State Information
UDN	Ultra-Dense Networks
UE	User Equipment
ULA	Uniform Linear Array
UPA	Uniform Planar Array

List of Symbols

N_{vec}	Codebook size
P_{T}	Total transmit power
p_{mut}	Mutation probability
α	Delay cost for running each iteration
T_{tourn}	Number of individuals selected to participate in each tournament
p_{c}	Crossover probability
N_{f}	Number of elements selected by the elitism process
g_{best}	The swarm experience
p_{best}	The individual experience
$\mathbf{v}$	Particle velocity
$\mathbf{x}$	Particle position
ℓ_1	Learning factor of the swarm experience
ℓ_2	Learning factor of the individual experience
ω	Inertia velocity weight
ω_{max}	Maximum inertia velocity weight
ω_{min}	Minimum inertia velocity weight
N_{it}	Number of iterations
M	Number of transmit antennas at the BS
N	Number of receive antennas at the UE
$\mathbf{H}$	mmWave channel matrix between the BS and UE
$\mathbf{W}$	Beamforming array at the BS
$\mathbf{U}$	Beamforming array at the UE

N_l	Number of propagation paths
N_c	Number of spreading paths
β^{L}	Small-scale complex fading gain
$\mathbf{a}_{\mathrm{r}}(\cdot)$	Normalized receive antenna array response
ϑ^{r}	Azimuth AoA
ϕ^{r}	Elevation AoA
$\mathbf{a}_{\mathrm{t}}(\cdot)$	Normalized transmit antenna array response
ϑ^{r}	Azimuth AoD
ϕ^{r}	Elevation AoD
d_{array}	Distance between the array elements
λ	Wavelength
$\mathbf{C}_{\mathrm{T}}$	Transmitter codebook
$\mathbf{C}_{\mathrm{R}}$	Receiver codebook
$\mathcal{C}$	Shannon capacity
B	System bandwidth
Γ	Signal-to-noise ratio
N_0	Noise power spectral density
$\Gamma_{\min}$	Minimum Signal-to-noise ratio
P_{out}	Outage probability
L	Number of elements at each iteration
K	Number of reflecting elements at the IRS
$\mathbf{h}_{\mathrm{r}}$	Channel vector from the IRS to the UE
$\mathbf{G}$	Channel vector from the BS to the IRS
$\mathbf{h}_{\mathrm{d}}$	Channel vector from the BS to the UE
$\mathbf{w}$	Beamforming vector at the BS
ξ	Amplitude reflection coefficient
$\mathbf{G}^{\mathrm{LoS}}$	LoS components of the channel vector from the BS to the IRS
$\mathbf{h}_{\mathrm{r}}^{\mathrm{LoS}}$	LoS components of the channel vector from the IRS to the UE
$\mathbf{h}_{\mathrm{d}}^{\mathrm{LoS}}$	LoS components of the channel vector from the BS to the UE
$\mathbf{h}_{\mathrm{d}}^{\mathrm{NLoS}}$	NLoS components of the channel vector from the BS to the UE
$\mathbf{h}_{\mathrm{r}}^{\mathrm{NLoS}}$	NLoS components of the channel vector from the IRS to the UE
θ	Phase shift vector
p_{PSO}^{*}	Mutation probability of the proposed PSO

p_{PSO}	Probability of changing a column in the proposed PSO
β_{BU}	Rician factor of the BS-UE link
β_{IU}	Rician factor of the IRS-UE link
β_{BI}	Rician factor of the BS-IRS link
α_{BI}	Path loss exponent of the BS-UE link
α_{BI}	Path loss exponent of the BS-IRS link
α_{BI}	Path loss exponent of the IRS-UE link
C_0	Path loss at the reference distance
d_{v}	BS-UE vertical distance
d_{h}	BS-IRS distance
T	Number of discrete phase-shift levels
b	Number of bits per each element at the IRS
ϕ^{AoA}	AoA to the ULA at the IRS from the BS
ϕ^{AoD}	AoD from the ULA at the BS towards the IRS
φ^{AoD}	AoD from the ULA at the BS towards the UE
ψ^{AoD}	AoD from the ULA at the IRS towards the UE
β	Rician factor of all channel links
$\overline{\mathbf{G}}^{\mathrm{LoS}}$	Imperfect estimation of the LoS component of the BS-IRS link
$\mathbf{E}$	Estimation error
τ	Estimation accuracy

CONTENTS

Chapter 1

Introduction

As the fifth generation (5G) of wireless cellular systems is being deployed commercially, the industry and academy focused their attention to the development of its evolution and the next generation, named Beyond 5G (B5G). The B5G wireless systems will enable the deployment of demanding applications such as autonomous cars, massive sensor networks, telemedicine, and smart homes. To make these applications possible, stringent requirements such as massive connectivity, improved spectrum, higher efficiency, coverage, and data rate, besides ultra-low latency must be fulfilled. In order to meet these requirements, various candidate technologies have been proposed such as millimeter wave (mmWave) communications and Intelligent Reflecting Surfaces (IRS).

The mmWave communications have attracted great interest from academy and industry due to the abundant available spectrum, unlike the congested bands in UHF and sub-6GHz frequencies adopted in 4G networks [1]. However, the mmWave bands present poor propagation characteristics due to the high path-loss, atmospheric and rain attenuation, blockage and low diffraction around obstacles [2]. To overcome these propagation issues, the use of highly directional beamforming is an effective solution. Advances in the CMOS RF circuits together with the small wavelengths of mmWave allow for the use of antenna arrays formed by a large number of antennas at the Base Station (BS) and at the User Equipment (UE) [2, 3]. These large arrays allow for high-performance beamforming, which can improve range, directivity, and spatial multiplexing, thus obtaining a large capacity [4, 5].

Intelligent reflecting surfaces, also called *reconfigurable intelligent surfaces* [6],

large intelligent surfaces [7], and *software-controlled metasurfaces* [8], have recently emerged as a promising new paradigm to achieve smart and reconfigurable radio propagation environments for B5G wireless communication systems [9]. An IRS is a meta-surface comprising a large number of reflecting elements, capable of reflecting the incident signal with a given phase/amplitude shift. By densely deploying IRSs in wireless communication networks and intelligently coordinating their elements, the wireless channels between the transmitter and receiver can be intentionally and deterministically controlled to improve the signal quality at the receiver, and consequently the network capacity and reliability [10–13].

Despite these key technologies have countless advantages for the system performance, their deployment presents many challenges to the designer. More specifically, although the mmWave bands allow the improvement of the system capacity by the deployment of a huge number of antennas at the BS and UE, *i.e.*, the use of high-performance beamforming at the BS and UE, this can be challenging for the Initial Access (IA) process, whereby the UE establishes a physical link with the BS [14]. Since omnidirectional transmission may not be applied, due to its low power gain and received SNR, while the best pair of beams between BS and UE is not known a priori, the overall duration of IA can be very long, as in principle multiple preambles must be transmitted repeatedly with all transmit/receive beam pairs. The delay caused by directional search must be small to meet some of the B5G requirements for low end-to-end latency [15–17].

Moreover, although the capacity of controlling the wireless channels presented by the IRSs, designing the beamforming at the BS and the phase shifts at the IRS is a challenging problem due to the system overhead necessary to estimate all channels link. It is notable that, most works in the literature consider perfect Channel State Information (CSI) at the BS [12, 18–22]. Estimating the CSI between IRS and BS or between IRS and UE requires that each element of the IRS be equipped with one radio-frequency (RF) chain. However, the low cost of the reflecting elements is key in the IRS paradigm and installing multiple RF chains leads to high cost and energy consumption, going against some of the original motivations of using an IRS.

Therefore, driven by the previous issues, in this thesis, new methods based on Evolutionary Computation techniques, *i.e.*, Genetic Algorithm (GA) and Particle Swarm Optimization (PSO), are presented. These techniques have been widely applied in the

most diverse optimization problems [23–26], due to their simplicity of implementation, low operating costs, and easy parallelization [27]. With the developed methods the IA in mmWave bands and the beamforming at the BS and IRS were successfully solved, demonstrating the relevance and efficiency of these techniques in solving emerging problems of B5G.

1.1 THESIS GOALS

The main goal of this thesis is the development of new methods based on Evolutionary Computation techniques in order to solve emerging problems of B5G. In addition, the specific goals of this thesis are:

1. To develop a new method based on Evolutionary Computation in order to solve the IA problem in mmWave Multiple-Input Multiple-Output (MIMO) systems.
2. To develop a new method based on Evolutionary Computation in order to jointly design the beamforming at the BS and the phase shifts at the IRS without the need of estimating the instantaneous CSI (I-CSI).

Regarding Evolutionary Computation, the goal is to show that these methods can be successfully used to solve relevant and complex emerging problems in B5G systems. Thus, the focus is not to tune the parameters of the proposed algorithms to achieve the ultimate performance, but to demonstrate that they are able to achieve close-to-optimal performance with reasonable complexity and standard configuration. The detailed optimization of the parameters involved in the PSO and GA algorithms is left as a potential future work.

1.2 CONTRIBUTIONS

The contributions of this thesis can be divided in two parts as follows.

1. *With respect to IA in mmWave communications:*
    - The development of a meta-heuristics method based on GA to solve the IA problem in mmWave systems using analog beamforming, reducing the

IA delay compared to [23–25]. Consequently, the proposed method also outperforms Link-by-Link search [28], Two-Level search [29, 30], and Tabu search [31].

2. *Regarding IRS beamforming design:*

   - The development of a meta-heuristics method based on PSO to design the beamforming at the BS and the phase shifts at the IRS, without requiring any CSI acquisition and considering continuous phases at the IRS, while achieving close-to-optimal performance.
   - The development of a meta-heuristics method based on GA to design the beamforming at the BS and the phase shifts at the IRS, exploring the Statistical Channel State Information (S-CSI) knowledge and considering discrete phases at the IRS, while achieving close-to-optimal performance with very limited training and control overhead.

1.3 PUBLISHED PAPERS

From the results obtained in this thesis the following papers were published.

- V. D. P. Souto, R. D. Souza, B. F. Uchôa-Filho, A. Li and Y. Li, ***"Beamforming Optimization for Intelligent Reflecting Surfaces without CSI,"*** in IEEE Wireless Communications Letters, vol. 9, no. 9, pp. 1476-1480, Sept. 2020, doi: 10.1109/LWC.2020.2994218.

- V. D. P. Souto, R. D. Souza, B. F. Uchôa-Filho and Y. Li, ***"A Novel Efficient Initial Access Method for 5G Millimeter Wave Communications Using Genetic Algorithm,"*** in IEEE Transactions on Vehicular Technology, vol. 68, no. 10, pp. 9908-9919, Oct. 2019, doi: 10.1109/TVT.2019.2935695.

- V. D. P. Souto, R. D. Souza and B. F. Uchôa-Filho, ***"Tx-Rx Initial Access and Power Allocation for Uplink NOMA-mmWave Communications,"*** *XXXVIII Simpósio Brasileiro de Telecomunicações e Processamento de Sinais (SBrT2020)*, Florianópolis, SC, Brasil, 22-25th November 2020,

- V. D. P. Souto, R. D. Souza and B. F. Uchôa-Filho, ***"Power Allocation and Initial Access Using PSO for Uplink NOMA mmWave Communications,"*** *2019 IEEE 30th Annual International Symposium on Personal, Indoor and Mobile Radio Communications (PIMRC)*, Istanbul, Turkey, 2019, pp. 1-6, doi: 10.1109/PIMRC.2019.8904292.

- V. D. P. Souto, R. D. Souza and B. F. Uchôa-Filho, ***"Acesso Inicial Utilizando Algoritmos Genéticos para Redes Celulares 5G mmWave,"*** *XXXVI Simpósio Brasileiro de Telecomunicações e Processamento de Sinais (SBrT2018)*, Campina Grande, PB, Brasil, 16-19th September 2018.

1.4 DOCUMENT STRUCTURE

The rest of this thesis is organized as follows.

- **Chapter 2** presents the basics concepts and operation of different metaheuristic algorithms (GA and PSO).

- **Chapter 3** discusses the initial access optimization problem, the proposed solution, and the obtained results.

- **Chapter 4** introduces the beamforming optimization problem for IRS-assisted network, the approaches proposed in this thesis, and the obtained results.

- **Chapter 5** concludes this thesis.

1.5 HOW TO READ THIS THESIS

Chapters 3 and 4 present two different emerging problems in B5G wireless systems, *i.e.*, mmWave communications and IRS beamforming, respectively. Both chapters bring a short description of the Evolutionary Computation method used to solve their respective optimization problem. Therefore, they are somewhat self-contained and they may be read independently, based on the reader's interest. However, if the reader has no familiarity with Evolutionary Computation Methods, then reading Chapter 2 is recommended.

Chapter 2

Evolutionary Computation Techniques

Evolutionary Computation techniques have attracted great interest due to their ability to solve complex optimization problems from different fields. These techniques are inspired by biological evolution process, swarm behavior, and physics [32]. Among the main Evolutionary Computation techniques, Genetic Algorithm (GA) and Particle Swarm Optimization (PSO) are algorithms widely used for handling optimization problems. Their main concepts and operation are presented in this chapter.

2.1 GENETIC ALGORITHMS

GA are based on the Theory of Evolution by natural selection proposed by Charles Darwin [33], which proves that the individuals change over time and these changes help them to survive and to reproduce in order to generate more descendants in the next generations. GAs have been widely applied in the most diverse optimization problems, due to their simplicity of implementation, low operating costs, and easy parallelization [27].

2.1.1 Basic Concepts and Operation

Many concepts and terminologies from Biology are used as a theoretical basis in GAs. The main terms used in this work are: gene, chromosome, parents, children,

Table 2.1 – The meaning of the main GA parameters.

GA Parameter	**Meaning**
Chromosome	Optimization variable.
Individual	The set of all optimization variables in the problem.
Population	A set of all possible solutions for the optimization problem.
Parents	Individuals selected in the Selection Method.
Children	Individuals generated by the Crossover Operator.
Fitness Function	Performance metric defined by the optimization problem.
Fitness	Output of the fitness function.
Generation	Iteration of the algorithm.

and fitness function. A gene is defined as an optimization variable which is represented in coded form. A chromosome represents a finite number of genes that characterize an individual. Parents are the individuals selected by the process of natural selection to participate in the reproduction process. Children are the resulting individuals of this operator, and the value of the fitness function represents the degree of suitability of each individual in the environment in which they live [27, 34]. In order to improve the understanding about this terms, Table 2.1 presents the meaning of theses terms in the optimization process. In addition, the basic operation of a GA can be described by the following steps [27, 35]:

1. Randomly generate the individuals of the first generation;
2. Compute the fitness of each individual;
3. **Elitism:** Create a set with some of the fittest individuals of the current generation and perpetuate these individuals to the next generation;
4. Select some individuals (named parents) by the **Selection Method**, which will be submitted to the Reproduction Process (Crossover and Mutation Operators).
5. **Crossover Operator:** This operator makes the permutation of the genetic material of the selected parents with probability p_{c} and generates children.
6. **Mutation Operator**: The individuals generated in the previous step are submitted to the *Mutation Operator* with probability p_{mut}.

7. Generate the new population by the union of the of individuals selected in Steps 3 and the new individuals generated in Step 6.

8. The GA finishes if the stop criterion is fulfilled. Otherwise, return to Step 2.

2.1.2 Selection Methods

As in the Theory of Evolution where the fittest individuals are more likely to be selected to reproduce and generate more decedents, GAs implement selection methods where each individual's fitness value is considered so that they are selected to participate in the reproduction process. In the current literature, several selection methods are described [27, 36]. However, in this work, only the Tournament Method [27] is considered and its operation is described next.

The *Tournament Method* takes some individuals to participate in a tournament, where the selection criterion is the fitness value of each individual, that is, the individual with the highest fitness wins the tournament and is selected to participate in the reproduction process [27, 34, 36]. Moreover, the tournament size (T_{tourn}) defines how many individuals must be selected to participate in each tournament [27]. As can be seen, in this method, there is no favoritism for the fittest individuals due to the fact that individuals with low fitness can be selected in some tournaments. Consequently, this selection method can help to improve the genetic diversity of the next generation. In order to improve the understanding of the reader, Figure 2.1 exemplifies the operation of this method for $T_{\text{tourn}} = 2$.

2.1.3 Genetic Operators

After applying the selection method, the remaining individuals are submitted to probabilistic modifications through the genetic operators. The main goal of these operators is to optimize the individuals' fitness through successive generations. The main genetic operators presented in the literature are the crossover and mutation operators [27, 34, 35], which are described next.

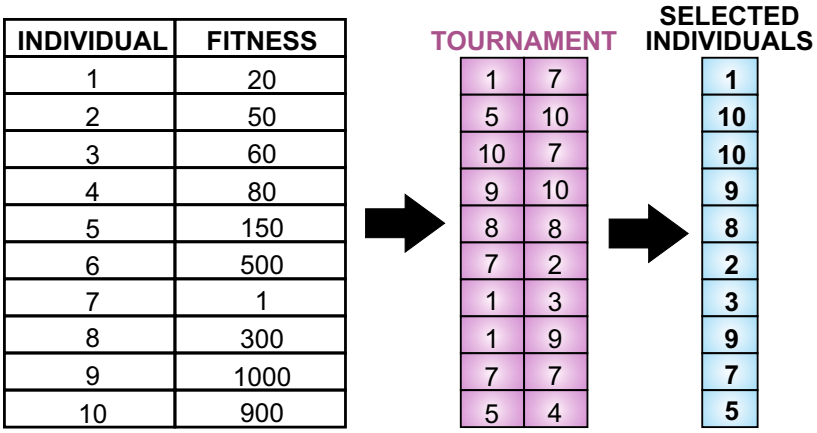

Figure 2.1 – Tournament method example.

2.1.3.1 Crossover Operator

In this operator, the characteristics of two or more selected parents are exchanged to form descendants. This operator is applied according to a given crossover probability p_c, which must be high to guarantee the genetic diversity of the next generation. There are many crossover operators described in the literature. In this work, only the Discrete Crossover Operator [27] is considered, as described next.

After selecting the individuals who will participate in the reproduction process, a binary value (0 or 1) is drawn for each gene. If the value is "1" (resp., "0") then the first child receives the gene from the current position of the first (resp., second) parent and the second child receives the gene from the current position of the second (resp., first) parent. The discrete crossover operator is used to create only two children, if the designer needs to create more than two children it is recommended to choose another crossover operator. Figure 2.2 exemplifies the discrete crossover operator.

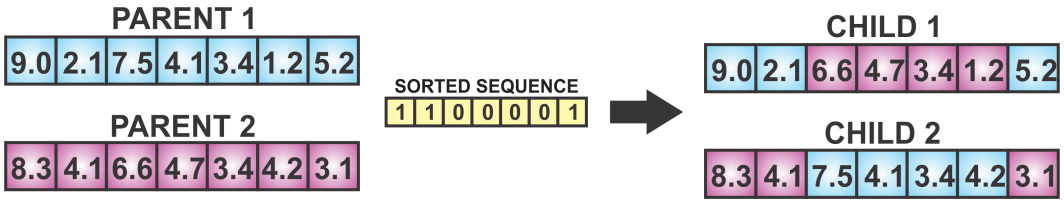

Figure 2.2 – Discrete crossover operator example.

2.1.3.2 Mutation Operator

Mutation operates on the individuals resulting from the crossover operator, inserting new genetic material in the population. This operator is considered in order to increase the genetic variability of the next generations and to avoid the GA from being stuck in a local optimum solution. In addition, this operation improves the performance and accuracy of the GA. There are many crossover operators described in the literature [27, 36]. In this work, the Real Random Mutation Operator is evaluated and its basic operation is described next.

The real random mutation operator randomly selects a value belonging to a predetermined range and replaces the current value of a randomly selected gene with the previous selected value. This operator is applied according to a given mutation probability p_{mut} [27, 34], which should be low to avoid that the GA becomes a random search. Figure 2.3 illustrates this operation.

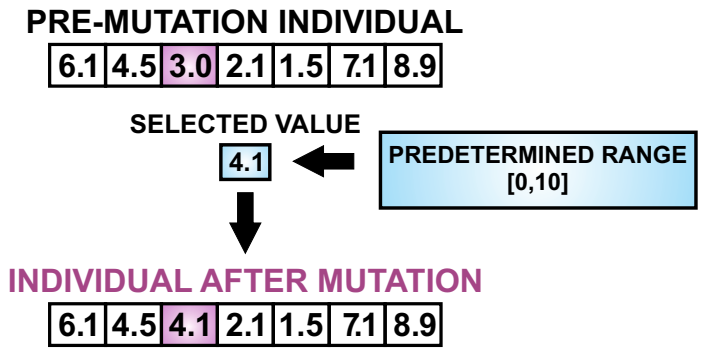

Figure 2.3 – Real random mutation operator example.

2.1.4 Elitism

Elitism is a method that is used to ensure that the genetic material of the fittest individuals of the current generation will be perpetuated to the next generation, improving the GA convergence. In Elitism, the N_{f} best individuals of a population are selected and kept to the next generation without going through the crossover and mutation operators. This method guarantees that the quality of the solution obtained by the GA does not decrease in the next generation. In addition, elitism improves the

performance of GA because this concept ensures that the GA does not waste time re-discovering good solutions previously analyzed [27, 36].

2.1.5 Stop Criterion

In order to avoid to simulate indefinitely, it is necessary to define a stop criterion. There are some possible approaches: (*i*) Maximum number of iterations; (*ii*) When the diversity of the population is very small or non-existent, *i.e.*, the individuals present similar fitness and keep these fitness for at least a predefined number of iterations; (*iii*) A predetermined fitness value is reached. In this work, the maximum number of iterations is used as a stop criterion.

2.2 PARTICLE SWARM OPTIMIZATION

PSO technique is a stochastic optimization approach based on the social behavior of some animal species, which present the capacity to work collectively [37]. Although PSO does not consider any concept of natural selection, it is classified as an evolutionary method as PSO makes use of populations of individual solutions and presents similar aspects to evolutionary operators implemented by GAs. In addition, PSO also considers collaboration strategies in order to evolve its population [38]. It is important to emphasize that PSO is effective in optimizing non-convex problems with continuous variables and it has been widely applied in several optimization problems [26], due to its simplicity of implementation and low computational complexity [37].

2.3 BASIC CONCEPTS AND OPERATION

PSO uses some terminologies for its main parameters that need to be clearly understood. The main terms used by this technique are: particle, swarm, velocity, position, g_{best}, and p_{best}. A *particle* is a possible solution to the optimization problem and represents a *position* in the search space, as particle represents the set of optimization variables in the optimization problem. The *swarm* is the set of all particles in the current iteration, *i.e.*, it represents all possible solutions in the current iteration. The *velocity* is the speed that one particle changes its position. In addition, PSO explores the experience of its particles. Thus, g_{best} is defined as the swarm experience, and

p_{best} denotes the individual experience, which are obtained by evaluating the position of each particle through a fitness function. Each particle presents its own p_{best} value and all particles present the same g_{best} value. In order to improve the understanding about these terms, Table 2.2 presents their meaning in the optimization process. In addition, the basic operation of a PSO is described by the following steps [37]:

Table 2.2 – The meaning of the main PSO parameters.

PSO Parameter	**Meaning**
Particle	The set of all optimization variables in the problem.
Swarm	A set of all possible solutions for the optimization problem.
Fitness Function	Performance metric defined by the optimization problem.
Fitness	Output of the fitness function.
g_{best}	The best fitness value reached by the swarm up to the current iteration.
p_{best}	The best fitness value reached by each particle up to the current iteration.
Position	The value of the optimization variables (particle) given by (2.2).
Velocity	A value computed by (2.1) to change the value (position) of the optimization variables (particles).

1. Randomly initialize the first swarm, *i.e.*, the initial velocity and position of each particle.

2. Compute the fitness of each particle;

3. Update p_{best} and g_{best} from the fitness computed in the previous step: p_{best} is the best position visited for each particle up to the current iteration, and g_{best} is the best position visited for all particles.

4. Update the new velocity and position of each particle based on [37]

$$[\mathbf{v}]_i^{t+1} = \omega[\mathbf{v}]_i^t + \ell_1 \text{rand}() \times ([p_{\text{best}}]_i^t - [\mathbf{x}]_i^t) + \ell_2 \text{rand}() \times ([g_{\text{best}}]^t - [\mathbf{x}]_i^t), \tag{2.1}$$

$$[\mathbf{x}]_i^{t+1} = [\mathbf{x}]_i^t + [\mathbf{v}]_i^{t+1} \tag{2.2}$$

where $[\mathbf{v}]_i^t$ and $[\mathbf{x}]_i^t$ represent the velocity and the position of particle i at iteration t, respectively, ℓ_1 and ℓ_2 are the particle learning factors, which define the influence of individual and collective experience on the motion of particles, respectively, while the function $\mathrm{rand}()$ returns a random number between 0 and 1 with uniform distribution. Moreover, ω is the inertia velocity weight, which defines the influence of the current velocity on the update velocity of each particle, being

$$\omega = \left(\omega_{\max} - \frac{(\omega_{\max} - \omega_{\min})t}{N_{\mathrm{it}}}\right) \tag{2.3}$$

where N_{it} is the maximum number of iterations, and $\omega_{\max}$ and $\omega_{\min}$ are the maximum and minimum value of ω, respectively.

5. Generate a new swarm from the particles (**x**,**v**) computed in the Step 4.

6. The PSO finishes if the stop criterion is fulfilled. Otherwise, return to Step 2.

Although both GA and PSO are able to successfully solve different complex problems, they present some relevant differences that need to be taken into account by the designer. First, GA is discrete by nature, *i.e.*, it is preferable to use GA to solve discrete optimization problems. In contrast, PSO is suited to continuous optimization problems. PSO needs to be deeply modified to solve discrete optimization problems and usually does not present a great performance for complex problems of such kind. Similarly, GA can be applied in continuous optimization problems, however, GA presents a higher computational cost and a larger number of parameters that need to be tuned when compared to PSO in such cases. Finally, it is important to deeply evaluate the optimization problem in order to choose the technique to be applied [27, 34, 37, 39].

Chapter 3

IA in mmWave Communications

3.1 INTRODUCTION

mmWave communications have attracted great interest from the academy and industry due to the abundant available spectrum, unlike the congested bands in UHF and sub-6GHz frequencies adopted in the 4G networks [1]. However, the mmWave bands present poor propagation characteristics due to the high path-loss, atmospheric and rain attenuation, blockage, and low diffraction around obstacles [2]. To overcome these issues, the use of highly directional beamforming is an effective solution. However, the use of beamforming at the BS and/or UE is challenging for the IA process.

The IA can be defined as the process whereby the UE establishes a physical link with the BS [14]. Both the BS and UE need to determine their appropriate beam directions to establish a directional communication. Due to the huge number of antennas at the BS and UE and, consequently, the high directivity beamforming, the search space greatly increases and the duration of the IA process can be prohibitively long, as in principle multiple preambles must be transmitted repeatedly with all transmit/receive beam pairs. The delay caused by directional search must be small to meet some of the B5G requirements for low end-to-end latency [15–17].

Basically, the IA process in mmWave systems can be divided into three steps as presented in Figure 3.1 and described next [14].

1. **Cellular Search:** The BS periodically transmits synchronization signals in different beam directions to the UE. If the UE detects the signal, the beam direction

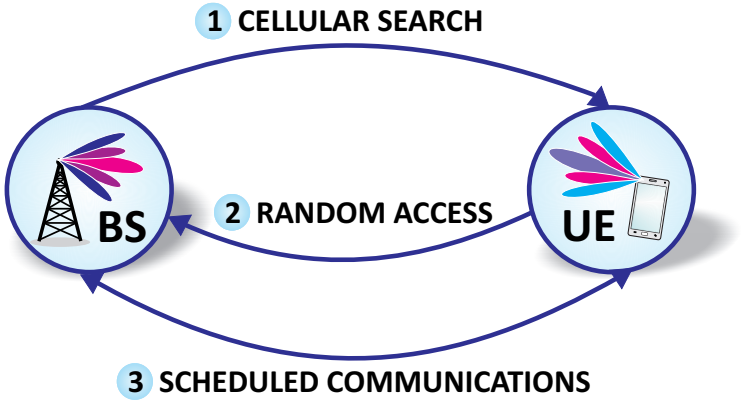

Figure 3.1 – IA process.

of the UE and BS are defined.

2. **Random Access:** In this step, the beam directions are known at the BS and UE and they exchange random access messages to establish a physical link.

3. **Scheduled Communications:** In this step, the beam refinement process can be applied to further optimize the beam directions and the UE mobility can be addressed. After this step, the communication between the UE and BS can be effectively established with maximum beamforming gain using scheduled channels.

Due to the complexity of the IA problem, in this chapter, a novel efficient method based on GA is presented. As explained in Chapter 2, the GAs provide an alternative to traditional optimization techniques by using directed random searches to locate optimal solutions in complex problems. This evolutionary technique shows high efficiency to solve problems that do not have feasible analytical solutions, for example, efficient antenna [40, 41] and communication systems design [42, 43].

3.1.1 Related Work

Most IA techniques can be classified into six groups: Exhaustive, Iterative/ Hierarchical, Statistical/Probabilistic, Meta-Heuristics, Context-Information Based, and Machine Learning. Table 3.1 lists the main works related to these groups, as well as some of their distinguishing characteristics.

Table 3.1 – Some relevant literature on IA for mmWave networks.

Techniques	**Low Search Delay**	**Low Outage Prob.**	**Context-Information Based**	**Generic/ Flexible**
Exhaustive [14, 15, 17, 44–46]		√		
Iterative/Hierarchical [14, 17, 28–30, 45]	√			
Statistical/Probabilistic [47–49]	√	√		
Meta-Heuristic [23–25, 31]	√	√		√
Context-Information Based [17, 50–55]	√	√	√	
Machine Learning [55–57]	√	√	√	

Exhaustive Search (ES) is a brute force sequential beam search technique [14, 17, 45], where both BS and UE scan sequentially all the beamspace, adding a significant delay to the IA process [14, 15, 17, 44–46]. However, ES shows low misdetection probability and is indicated for use in scenarios with large cells and edge users [14, 17]. Moreover, the Iterative Search techniques scan the beamspace in some steps. These techniques use codebooks with different sizes. In the first step, the BS scans the beamspace using macro beams, while in the subsequent steps the search is performed only in the best sector found, but then using narrower beams [14, 17, 28–30, 45, 46].

In [14, 17, 45] the authors compare ES with Iterative Search, showing that Iterative Search reduces the IA delay, but increases the misdetection probability and should be used only for short distances between BS and UE. In addition, the results demonstrate that Iterative Search is not indicated for edge users because its performance decreases with the distance between BS and UE, and also due to the low beamforming gain present in the first step. Furthermore, this technique presents a high outage probability as compared to ES.

In [28], the authors proposed an Iterative Search method where the BS-UE beam pair is settled user-by-user by considering the interference from the other links. However, this method cannot find a better transmit/receive beam set by conducting beamforming link-by-link. Therefore, the method in [28] can obtain only a locally optimal solution and cannot ensure global optimality.

In a different approach, some works in the literature consider statistical knowledge about the mobility and connection probability of users [47, 48]. Probabilistic methods can be used to perform the beam refinement in order to reduce the IA delay [49]. These techniques depend on prior knowledge of the system's and users' behaviors. In addition, these methods are not generic. Yet it is possible to model the problem mathematically and ensure the method's convergence.

Techniques using Context Information aim at exploiting knowledge about UE and/or BS positions [17, 51, 52], user profiles, application quality requirements, network status, and traffic prediction [17, 51, 52]. From the exploration of this type of information many IA methods have been developed. These methods can, for instance, handle the presence of obstacles inside the service area [50, 53, 54], showing a good performance and reduced delay. However, in many cases it may be very difficult to obtain such amount of prior information, limiting the applicability of this strategy.

In another group, IA based on Machine Learning normally exploits context information for the learning process. Currently, these techniques have been applied to the beam refinement problem in order to reduce the IA delay in complex scenarios, e.g., considering mobile users [55–57], multiple users [55], multiple BSs [56, 57] and/or obstacles [55]. In [55–57] techniques based on Machine Learning are used for cell search using different context information and the results show that these techniques improve the IA performance. However, the system's performance depends on the level of accuracy of the information and it is necessary to maintain, access, and update these databases in real time.

Finally, Meta-Heuristic techniques are often used to solve an optimization problem generically. For the IA problem this means that the method can be used for different system models and performance metrics, which is very relevant. In addition, these techniques present low search delay and outage probability, because they scan the search space intelligently and with few iterations. In [23–25] an IA method was proposed using GA. The results show that the method achieves the same capacity as the ES and considerably reduces the IA delay. However, the method almost totally consists of random operations that do not follow some of the basic principles of a GA. In [31] an IA method based on Tabu search was proposed and simulation results verify that it can achieve near-optimal performance and reduced delay with low complexity. Even so, the method in [23–25] achieves a superior result in comparison to the Tabu search in [31].

In conclusion, among the techniques presented in Table 3.1, and described above, the Meta-Heuristics techniques are generic, *i.e.*, they can be applied in different scenarios without deep modifications. Furthermore, unlike ES, Meta-Heuristic techniques achieve a low IA delay and low outage probability in mmWave communication systems when compared to Iterative Search [23–25, 31]. In addition, unlike Machine Learning techniques and those based on Context-Information, Meta-Heuristic techniques do not require context information. Therefore, in this chapter, a new meta-heuristic beam refinement method based on GA is proposed. The proposed method differs from the techniques in Table 3.1 in several ways, such as:

- It is generic, *i.e.*, it can be applied to different scenarios without considerable modifications;
- It does not use context information, such as prior knowledge on channel state or users' behavior;
- It is based on GA, as [23–25], but with a different implementation with respect to selection, crossover, mutation, and elitism. Such differences lead to a better performance, *e.g.*, the proposed GA reduces the number of antennas at the BS and UE, power consumption and IA delay when compared to the method in [23–25].

Next, we present in details the system model, the proposed method and the obtained simulation results.

3.2 SYSTEM MODEL

The system model illustrated in Figure 3.2 where the BS and the UE are equipped with an Uniform Planar Array (UPA) with M and N antennas, respectively, is considered. Beamforming is considered at both the BS and the UE. For each time interval t, the received signal at the UE is [25]

$$\mathbf{y}(t) = \sqrt{\frac{P_{\mathrm{T}}}{M}} \left[\mathbf{U}(t)^{\mathrm{H}} \mathbf{H}(t) \mathbf{W}(t) \right] \mathbf{s}(t) + \mathbf{n}(t), \tag{3.1}$$

where P_{T} is the total transmit power, $\mathbf{W}(t) \in \mathbb{C}^{M \times M}$ and $\mathbf{U}(t) \in \mathbb{C}^{N \times N}$ denote the beamforming arrays at the BS and UE, respectively, $\mathbf{s}(t) \in \mathbb{C}^{M \times 1}$ is the intended

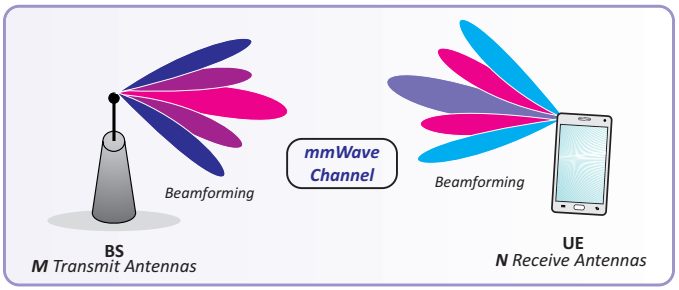

Figure 3.2 – System Model.

message, $\mathbf{n}(t) \in \mathbb{C}^{N\times 1}$ denotes the independent and identically distributed (IID) Gaussian noise vector, and $\mathbf{H}(t) \in \mathbb{C}^{M\times N}$ is the channel matrix. For simplicity, the time index t is omitted in the rest of this chapter.

In this work, the Saleh-Valenzuela extended geometric channel model is assumed [4, 58]. This channel model is often used in mmWave scenarios [59–61]. The channel is composed of N_l grouped propagation paths in N_c clusters, each cluster corresponding to a spreading path at a macro level and each path or subcluster being composed of several subpaths. The channel matrix $\mathbf{H} \in \mathbb{C}^{M\times N}$ is given by

$$\mathbf{H} = \sqrt{\frac{MN}{N_c N_l}} \sum_{i=1}^{N_c} \sum_{l=1}^{N_l} \beta_{il}^{\mathrm{L}} \mathbf{a}_{\mathrm{r}}(\phi_{il}^{\mathrm{r}}, \theta_{il}^{\mathrm{r}}) \mathbf{a}_{\mathrm{t}}^{\mathrm{H}}(\phi_{il}^{\mathrm{t}}, \theta_{il}^{\mathrm{t}}), \tag{3.2}$$

where β_{il}^{L} is the small-scale complex fading gain of the l-th subpath in the i-th cluster, $\mathbf{a}_{\mathrm{r}}(\cdot)$ denotes the normalized receive antenna array response as a function of the azimuth and elevation angles of arrival (AoA), $\vartheta_{il}^{\mathrm{r}}$ and ϕ_{il}^{r}, respectively, and $\mathbf{a}_{\mathrm{t}}(\cdot)$ denotes the normalized transmit antenna array response, expressed as a function of the azimuth and elevation angles of departure (AoD), $\vartheta_{il}^{\mathrm{r}}$ and ϕ_{il}^{r}, respectively, which are given by

$$\mathbf{a}_{\mathrm{r}}(\phi_{il}^{\mathrm{r}}, \theta_{il}^{\mathrm{r}}) = \frac{1}{N}\Bigg[1, e^{j\frac{2\pi}{\lambda} d_{\mathrm{array}}\left(\sin(\phi_{il}^{\mathrm{r}})\sin(\theta_{il}^{\mathrm{r}})+\cos(\theta_{il}^{\mathrm{r}})\right)}, \ldots, e^{j\frac{2\pi}{\lambda} d_{\mathrm{array}}\left((N-1)\sin(\phi_{il}^{\mathrm{r}})\sin(\theta_{il}^{\mathrm{r}})+(N-1)\cos(\theta_{il}^{\mathrm{r}})\right)}\Bigg], \tag{3.3}$$

$$\mathbf{a}_{\mathrm{t}}(\phi_{il}^{\mathrm{t}},\theta_{il}^{\mathrm{t}}) = \frac{1}{M}\Bigg[1, e^{j\frac{2\pi}{\lambda}d_{\mathrm{array}}\left(\sin(\phi_{il}^{\mathrm{t}})\sin(\theta_{il}^{\mathrm{t}})+\cos(\theta_{il}^{\mathrm{t}})\right)},\ldots, e^{j\frac{2\pi}{\lambda}d_{\mathrm{array}}\left((M-1)\sin(\phi_{il}^{\mathrm{t}})\sin(\theta_{il}^{\mathrm{t}})+(M-1)\cos(\theta_{il}^{\mathrm{t}})\right)}\Bigg], \tag{3.4}$$

where d_{array} is the distance between the array elements and λ is the wavelength. Although it is not so realistic, in our simulations, we consider $d_{\mathrm{array}} = \lambda/2$ for the BS and UE. Moreover, discrete fourier transform (DFT)-based codebooks [62] at the BS and at the UE are considered. The BS codebook $\mathbf{C}_{\mathrm{T}} \in C^{M\times N_{\mathrm{vec}}}$ is defined as

$$\mathbf{C}_{\mathrm{T}}(m,u) = \mathrm{e}^{(-j2\pi(m-1)(u-1)/N_{\mathrm{vec}})}, \tag{3.5}$$

while the UE codebook $\mathbf{C}_{\mathrm{R}} \in C^{N\times N_{\mathrm{vec}}}$ is

$$\mathbf{C}_{\mathrm{R}}(n,u) = \mathrm{e}^{(-j2\pi(n-1)(u-1)/N_{\mathrm{vec}})}, \tag{3.6}$$

where $m = 1,\ldots,M$, $u = 1,\ldots N_{\mathrm{vec}}$ and $n = 1,\ldots,N$. In this work, $\mathbf{C}_{\mathrm{T}}$ and $\mathbf{C}_{\mathrm{R}}$ are refered as codebooks, and N_{vec} $\left(N_{\mathrm{vec}} \geq \max(M,N)\right)$ denotes the size of the codebooks. N_{vec} must be chosen carefully, because large codebooks increase the IA delay, although it improves the capacity of beam refinement. This is because the codebook defines the radiation pattern of the antenna array, so the proper choice of a codebook allows to define the width of the main beam, directivity, and array gain. Such features directly influence the IA delay and misdetection probability. Therefore, the design of an optimal codebook is very relevant and is an open problem in the literature [63, 64].

3.2.1 Performance Metrics

In the following, the capacity and outage probability are defined as the performance metrics considered in the optimization problem. Let N_{it} be the maximum number of iterations of the beam search procedure, which is defined by the system designer. For the k-th iteration, where $k = 1, 2, ..., N_{\mathrm{it}}$, the Shannon capacity in bits per second (bits/s) is given as [23]

$$\mathcal{C}(k) = (1-\alpha k)\cdot B\log_2(1+\Gamma_k), \tag{3.7}$$

where α denotes the delay cost for running each iteration of the particular search algorithm ($\alpha N_{\mathrm{it}} < 1$), B is the system bandwidth, and Γ_k is the user SNR in the k-th iteration,

$$\Gamma_k = \frac{\frac{P_{\mathrm{T}}}{M}||\mathbf{U}_k^{\mathrm{H}}\mathbf{H}\mathbf{W}_k||^2}{BN_0}, \tag{3.8}$$

where N_0 is the noise power spectral density, and for the sake of simplicity, $BN_0 = 1$. From the system capacity in (3.7) it is possible to observe that the larger the number of iterations, the larger the IA delay and consequently the greater the penalty in (3.7).

Any application demands a minimum SNR, denoted as $\Gamma_{\min}$, to deliver an acceptable quality of service. Therefore, it is important to evaluate the *outage probability*, given by

$$P_{\mathrm{out}} = \Pr\left(r_k < r_{\min}, \forall k\right). \tag{3.9}$$

where $r_k = \log_2(1 + \Gamma_k)$ and $r_{\min} = \log_2(1 + \Gamma_{\min})$.

3.3 PROPOSED IA ALGORITHM

In this thesis, a novel solution for the IA problem based on GA is proposed. The IA problem can be defined as the establishment of an initial connection between the BS and the UE. In this work both BS and UE are equipped with an antenna array, *i.e.*, beamforming is considered. Therefore, for solving the IA problem the BS and the UE need to scan the beam search space to find the best beam alignment. The search space is defined by the codebooks in (3.5) and (3.6). Therefore, there is a finite, although usually very large, number of possible beamformers for the BS and the UE. The possible pairs of beamformers are evaluated according to the performance metrics defined in (3.7) and (3.9), and the best possible beamforming matrices (**U** and **W**) are found.

The proposed method considers a population with L individuals in each generation. In the first generation, the individuals are generated in a completely random way. From the second generation on, the new population is formed with the following composition: N_{f} individuals given by the **Elitism**, $(L - N_{\mathrm{f}})/2$ individuals generated by the **Crossover Operator**, and $(L - N_{\mathrm{f}})/2$ individuals generated by the **Mutation Operator**. The implementation of the proposed beam refinement algorithm for IA is described in **Algorithm 3.1** and, in order to improve the understanding of the proposed

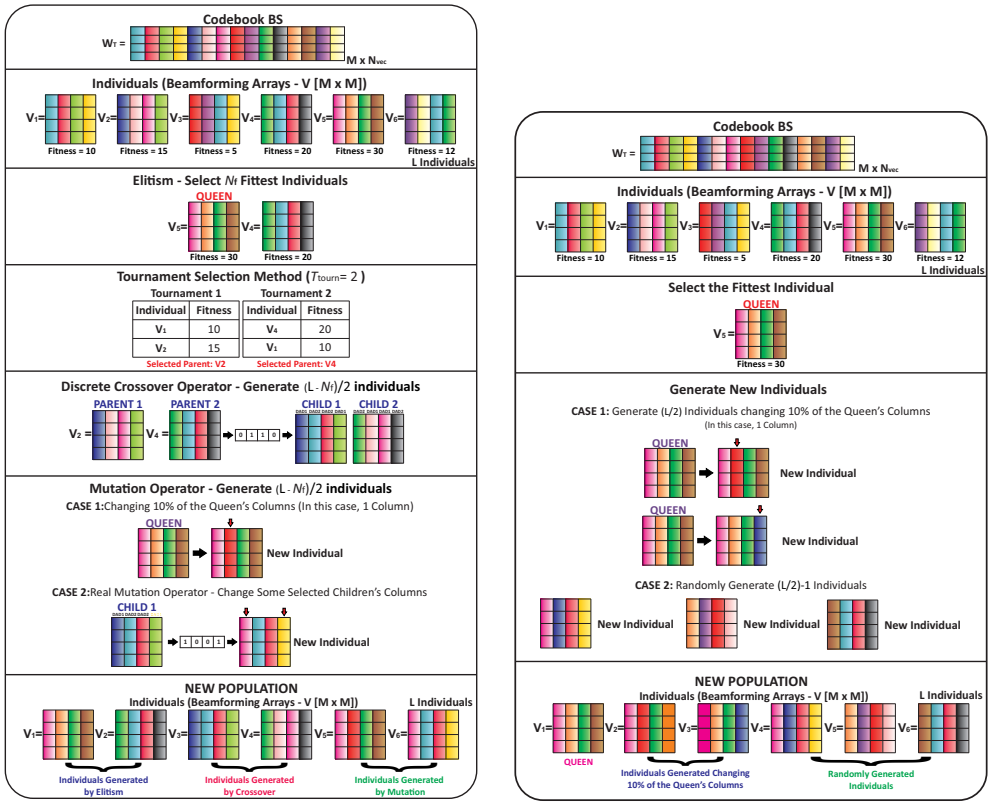

(a) (b)

Figure 3.3 – (a) Steps of the proposed method; (b) Steps of the algorithm proposed in [23–25].

method, Table 3.2 relates the main terms of GA to their meaning in the IA problem. In addition, with the help of Figure 3.3a, the steps of the algorithm are detailed next.

1. Randomly generate L pairs of beamforming arrays (individuals), $(\mathbf{W}_l, \mathbf{U}_l)$, $l = 1, \ldots, L$, taken from the coodebooks $\mathbf{C}_{\mathrm{T}}$ and $\mathbf{C}_{\mathrm{R}}$ of the BS and the UE, respectively, to form the first population.

2. Calculate the fitness of each individual based on the performance metrics presented in Section 3.2.1.

3. **Elitism:** From the L individuals, select the N_{f} fittest ones, which are perpetuated for the next generation.

4. By the Tournament Method, select $(L–N_{\mathrm{f}})/2$ parents from the current generation.

Table 3.2 – The relation between the main GA parameters and their meaning in the IA problem.

GA Parameter	**Meaning in IA**
Gene	The columns of the beamforming matrices (**U**, **W**).
Chromosome	Either beamforming matrix.
Individual	A pair of TX-RX beamforming matrices (**U**, **W**).
Population	A set with L possible solutions (**U**, **W**) for the IA problem.
Parents	Individuals selected in the Selection Method.
Children	Individuals generated by the Crossover Operator.
Fitness Function	Performance metric, defined in (3.7) and (3.9).
Fitness	Output of the fitness function: quality of a beam alignment.
Search Space	The codebooks in (3.5) and (3.6).
Generation	Iteration of the algorithm.

5. **Crossover Operator:** With crossover probability p_{c}, the parents selected in the previous step generate $(L - N_{\mathrm{f}})/2$ children by the Discrete Crossover Operator. Otherwise, with probability $1 - p_{\mathrm{c}}$, the children generated are the same as the selected parents.

6. **Mutation Operator:** Generate each child in the third group as follows. With mutation probability p_{mut}, change $\eta\%$ of the columns of the fittest individual — 10% in the simulations (similar to [23–25]). Otherwise, with probability $1 - p_{\mathrm{mut}}$, randomly select a child generated in Step 5 and submit it to the Real Random Mutation Operator[1]. This step must be run $(L - N_{\mathrm{f}})/2$ times to form the individuals in the third group.

7. The population of the next generation is formed by the union of the individuals in the three groups, generated in Steps 3, 5, and 6. In other words, the pairs of beamforming arrays, $(\mathbf{W}_l, \mathbf{U}_l)$, $l = 1, \ldots, L$, are updated.

8. Check if the stop criterion has been satisfied. In this approach, the maximum number of iterations N_{it} (generations) is considered as the stop criterion. If so, then return the fittest individual. Otherwise, go to Step 2.

[1] Both the mutation and crossover operators are restricted to operate only within the columns of **W** and **U** defined in (3.5) and (3.6), respectively. The following constraints are ensured: Constant modulus and progressive phases in the columns. These constraints ensure the practical feasibility of these beamforming matrices in Uniform Planar Arrays.

Algorithm 3.1: Proposed GA.

Input : Number of antennas at the BS: M
Number of antennas at the UE: N
Size of the population: L
Maximum number of generations (iterations): N_{it}
Mutation probability: p_{mut}
Crossover probability: p_{c}
Number of users in the elitism process: N_{f}
Size of the codebooks: N_{vec}

Output : $\mathbf{U}_{\mathrm{best}}$, $\mathbf{W}_{\mathrm{best}}$

Define the codebook at the BS and UE based on (3.5) and (3.6), respectively.
Randomly initialize the first population: $\mathbf{X}^{\mathrm{BS}}(m,:) = \mathbf{C}_{\mathrm{T}}(\mathrm{randi}(N_{\mathrm{vec}}),:)$, $\mathbf{X}^{\mathrm{UE}}(n,:) = \mathbf{C}_{\mathrm{R}}(\mathrm{randi}(N_{\mathrm{vec}}),:)$ where $m = 1,\ldots,M$ and $n = 1,\ldots,N$.
for $g = 1 : N_{\mathrm{it}}$ **do**
    Determine the fitness of each individual based on (3.7) or (3.9).
    Determine the N_{f} fittest individuals defined as $\mathbf{X}^{\mathrm{BS}}_{\mathrm{elite}}, \mathbf{X}^{\mathrm{UE}}_{\mathrm{elite}}$.
    Determine $(L - N_{\mathrm{f}})/2$ parents by the Tournament Method.
    for $pop = 1 : (L - N_{\mathrm{f}})/2$ **do**
        if $p_c < rand()$ **then**
            Generate two new children by the Discrete Crossover Operator.
            These new generated individuals are defined as $\mathbf{X}^{\mathrm{BS}}_{\mathrm{crossover}}, \mathbf{X}^{\mathrm{UE}}_{\mathrm{crossover}}$.
        else
            The parents selected by the Tournament Method are kept for the next generation.
            These new individuals are defined as $\mathbf{X}^{\mathrm{BS}}_{\mathrm{crossover}}, \mathbf{X}^{\mathrm{UE}}_{\mathrm{crossover}}$.
        end
    end
    for $pop = 1 : (L - N_{\mathrm{f}})/2$ **do**
        if $p_{mut} < \mathrm{rand}()$ **then**
            Change 10% of the columns of the fittest individual.
            These new generated individuals are defined as $\mathbf{X}^{\mathrm{BS}}_{\mathrm{mutation}}, \mathbf{X}^{\mathrm{UE}}_{\mathrm{mutation}}$
        else
            Select a child generated in the previous step;
            Submit the selected child to the Real Random Mutation Operator.
            These new generated individuals are defined as $\mathbf{X}^{\mathrm{BS}}_{\mathrm{mutation}}, \mathbf{X}^{\mathrm{UE}}_{\mathrm{mutation}}$.
        end
    end
    Determine the new population: $\mathbf{X}^{\mathrm{BS}} = [\mathbf{X}^{\mathrm{BS}}_{\mathrm{elite}}\ \mathbf{X}^{\mathrm{BS}}_{\mathrm{crossover}}\ \mathbf{X}^{\mathrm{BS}}_{\mathrm{mutation}}]$, $\mathbf{X}^{\mathrm{UE}} = [\mathbf{X}^{\mathrm{UE}}_{\mathrm{elite}}\ \mathbf{X}^{\mathrm{UE}}_{\mathrm{crossover}}\ \mathbf{X}^{\mathrm{UE}}_{\mathrm{mutation}}]$
end
Determine $\mathbf{U}_{\mathrm{best}}$ and $\mathbf{W}_{\mathrm{best}}$, the fittest individuals in $\mathbf{X}^{\mathrm{UE}}$ and $\mathbf{X}^{\mathrm{BS}}$, according to (3.7) and (3.9).
return $\boldsymbol{U}_{best}$, $\boldsymbol{W}_{best}$

Algorithm 3.2: GA proposed in [23–25].

Input : Number of antennas at the BS: M
Number of antennas at the UE: N
Size of the population: L
Maximum number of generations: N_{it}
Size of the codebooks: N_{vec}

Output : $\mathbf{U}_{\text{best}}$, $\mathbf{W}_{\text{best}}$

Define the codebook at the BS and UE based on (3.5) and (3.6), respectively.

Randomly initialize the first population: $\mathbf{X}^{\text{BS}}(m,:) = \mathbf{C}_{\text{T}}(\text{randi}(N_{\text{vec}}),:)$, $\mathbf{X}^{\text{UE}}(n,:) = \mathbf{C}_{\text{R}}(\text{randi}(N_{\text{vec}}),:)$ where $m = 1,\ldots,M$ and $n = 1,\ldots,N$.

for $g = 1 : N_{it}$ **do**

  Determine the fitness of each individual based on (3.7) or (3.9).

  Determine the fittest individual (*Queen*) defined as $\mathbf{X}^{\text{BS}}_{\text{queen}}, \mathbf{X}^{\text{UE}}_{\text{queen}}$.

  for $pop = 1 : L/2$ **do**

    Generate $L/2$ new individuals changing 10% of the columns of the fittest individual.

    These new generated individuals are defined as $\mathbf{X}^{\text{BS}}_{\text{new}}, \mathbf{X}^{\text{UE}}_{\text{new}}$.

  end

  for $pop = 1 : (L/2) - 1$ **do**

    Generate $(L/2) - 1$ new individuals randomly
    $\mathbf{X}^{\text{BS}}_{\text{random}}(m,:) = \mathbf{C}_{\text{T}}(\text{randi}(N_{\text{vec}}),:)$,
    $\mathbf{X}^{\text{UE}}_{\text{random}}(n,:) = \mathbf{C}_{\text{R}}(\text{randi}(N_{\text{vec}}),:)$.

  end

  Determine the new population: $\mathbf{X}^{\text{BS}} = [\mathbf{X}^{\text{BS}}_{\text{queen}}\ \mathbf{X}^{\text{BS}}_{\text{new}}\ \mathbf{X}^{\text{BS}}_{\text{random}}]$, $\mathbf{X}^{\text{UE}} = [\mathbf{X}^{\text{UE}}_{\text{queen}}\ \mathbf{X}^{\text{UE}}_{\text{new}}\ \mathbf{X}^{\text{UE}}_{\text{random}}]$

end

Determine $\mathbf{U}_{\text{best}}$ and $\mathbf{W}_{\text{best}}$, the fittest individuals in $\mathbf{X}^{\text{UE}}$ and $\mathbf{X}^{\text{BS}}$, according to (3.7) and (3.9).

return $\boldsymbol{U}_{best}$, $\boldsymbol{W}_{best}$

3.3.1 Comparison Between the Proposed IA Algorithm and the Method in [23–25]

The proposed IA method, detailed in **Algorithm 3.1** and Figure 3.3a, is now compared in detail to the one proposed in [23–25], detailed in **Algorithm 3.2** and Figure 3.3b. The main differences in terms of implementation are:

- In the proposed method, the concept of Elitism is considered, where the N_{f} individuals are kept for the next generation. This strategy is not considered in [23–25].
- The proposed method uses the Tournament Method as the selection method. This allows to increase the genetic diversity of the next generation. In [23–25] the new generation is chosen in a random fashion.
- The proposed method uses the Discrete Crossover Operator, from which new individuals are generated from those indicated by the selection method, *i.e.*, the new individuals are generated from the permutation of the genes of individuals selected by the selection method, increasing the probability of generating individuals with greater fitness and increasing the genetic diversity of the new generation. This procedure is not considered in [23–25].
- In [23–25] the Mutation Operator is based on the random change of 10% of the columns of the fittest individual. In the proposed method, first, with a given probability, 10% of the columns of the fittest individual is changed. Then, with a given probability, an individual generated by the Crossover Operator is randomly selected and submitted to the Real Random Mutation Operator. The use of this Mutation Operator can improve the genetic diversity of the new population [27, 34].
- In [23–25] the new population of each generation is formed by: $L/2$ individuals generated by the change of 10% of the columns of the fittest individual; $(L/2) - 1$ individuals generated randomly; and the fittest individual. However, in the proposed method, the new population is formed from the following composition: N_{f} individuals given by **Elitism**, $(L-N_{\mathrm{f}})/2$ individuals generated by the **Crossover Operator**, and $(L-N_{\mathrm{f}})/2$ individuals generated by the **Mutation Operator**. It

is possible to note that in the proposed method the new population is generated by the classical GA principles, and the proposed method does not use random operations to generate the new population. This feature improves convergence, as will be shown in the simulations.

Despite the differences in implementation both methods share the following aspects:

- They are generic. In other words, they can be used for different channel models, performance metrics, and system configurations.
- They do not consider context information, *i.e.*, prior knowledge of the channel, users behavior, or system metrics are not required to solve the IA problem.
- For both the proposed GA and the one in [23–25], it can not be ensured that these methods converge to a global optimum solution. These methods achieve a great performance despite normally converging to a sub-optimum solution. Nonetheless, as will be shown in the numerical results, the proposed GA achieves the same performance as the method in [23–25] with considerably fewer iterations.

From the above, it is possible to observe that the proposed method presents several novel features in its implementation. In addition, as will be demonstrated in the next section, the proposed algorithm outperforms the method in [23–25]. Therefore, the proposed modifications are very relevant to improve the system's performance.

3.4 SIMULATION RESULTS

This section presents simulation results to show the performance of the proposed method. The following simulation parameters are considered: $N_{\mathrm{it}} = 10^3$, $B = 1$ GHz, $L = 10$, and $N_{\mathrm{f}} = 2$. In addition, Table 3.3 lists the parameters considered for the definition of the channel model in (3.2) [4, 61]. In this section, all curves present the average of 10^3 independent channel realizations.

It is important to highlight that, the GA parameters were defined after many simulations. However, due to computational limitations, a detailed calibration of these parameters was not evaluated. In other words, some simulations for different combinations of the GA parameters were run and the combination that presented a better

Table 3.3 – Parameters of the Saleh-Valenzuela channel model [4, 61]

Parameter	**Value**
N_c	5
N_l	10
β_{il}	$\sim CN(0,1)$
ϕ_{il}^{r}	$\sim U[0, 2\pi]$
θ_{il}^{r}	$\sim \mathrm{Laplace}(\mu, 1)$, where $\mu \sim U[-\pi, \pi]$
ϕ_{il}^{t}	$\sim U[0, 2\pi]$
θ_{il}^{t}	$\sim \mathrm{Laplace}(\mu, 1)$, where $\mu \sim U[-\pi, \pi]$
d_{array}	$\lambda/2$

performance in most scenarios configurations was chosen. However, it is important to remark, as it is mentioned in Chapter 1, that the goal of this thesis is to show that Evolutionary Computation can be successfully used to solve relevant and complex emerging problems in B5G systems. Thus, the focus is not to better tune the parameters of the proposed algorithm to achieve the ultimate performance but to demonstrate that it is able to achieve close-to-optimal performance with reasonable complexity and standard configuration. The thin calibration of the GA parameters is left as a potential future work.

In the simulations, the number of antennas at the BS and UE (M and N), codebook size (N_{vec}), and GA mutation probability (p_{mut}), were evaluated. The influence of these parameters in the capacity in (3.7) and outage probability in (3.9) were investigated. In addition, the results are split into two cases. Subsection 3.4.1 presents results ignoring the delay cost for running each iteration of the algorithm (i.e., $\alpha = 0$). Subsection 3.4.2 considers the case of $\alpha \neq 0$. In all simulation results, the proposed algorithm is compared to the GA method in [23–25], while another Meta-Heuristic technique, Tabu Search [31], is also included in some analysis.

3.4.1 Results for $\alpha = 0$

Figure 3.4 presents the convergence[2] analysis for the scenario with $M = 4$, $N = 4$, $P_{\mathrm{T}} = 10$ dBm, and $N_{\mathrm{vec}} = 120$, considering a given channel realization. From the results, it is clear that the proposed algorithm converges with considerably fewer iterations than [23–25]. Other analyses are presented next.

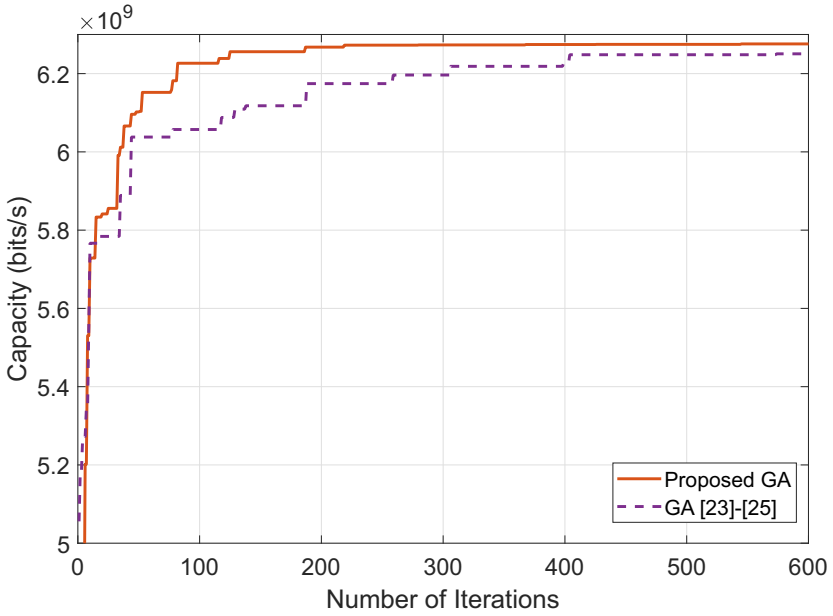

Figure 3.4 – Convergence of the proposed method and the one in [23–25], for $M = 4$, $N = 4$, $N_{\mathrm{vec}} = 120$, $P_{\mathrm{T}} = 10$ dBm, $p_{\mathrm{mut}} = 5\%$, and $\alpha = 0$.

3.4.1.1 Effect of the Number of Antennas at the BS and UE

Now the effect of the number of antennas at the BS (M) and UE (N), considering $N_{\mathrm{vec}} = 120$, $P_{\mathrm{T}} = 10$ dBm, and $p_{\mathrm{mut}} = 5\%$ are investigated. Figure 3.5a shows the capacity versus the number of antennas at the UE, for $M = 64$. As can be seen, increasing the number of antennas at the UE improves the system performance. Moreover, the proposed method is able to achieve the same capacity as in [23–25] with 37.5% fewer antennas at the UE. That is a great reduction in complexity and cost. In

[2] In this thesis, convergence is defined with respect to the fitness function. If the fitness of the best individual at subsequent generations stops changing significantly, then the GA is said to have converged.

addition, Figure 3.5b presents the effect of the number of antennas at the BS (M). The proposed method is able to achieve the same capacity as in [23–25] with 22% fewer antennas at the BS. Moreover, in this comparison another Meta-Heuristic named Tabu Search [31][3] is included. From the results, it is possible to verify that the Tabu Search technique performs worse than the other methods. This result corroborate those in [23–25]. Then, in the rest of this section, the proposed approach only is compared with the method in [23–25].

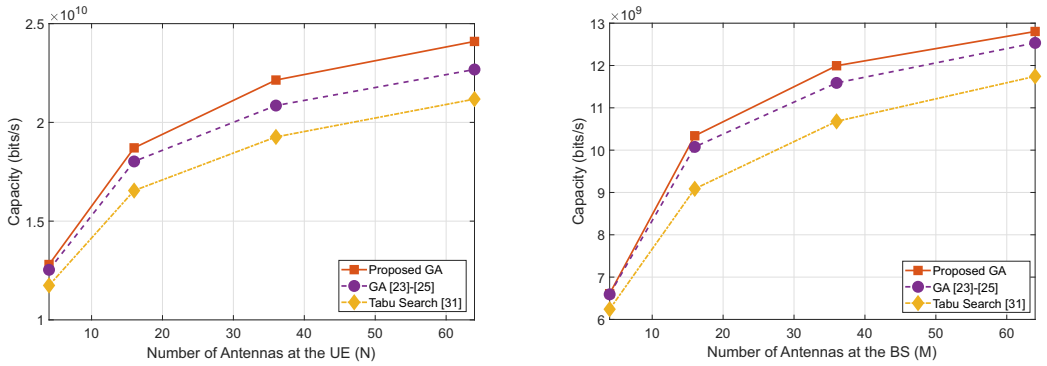

Figure 3.5 – (a) Effect of the number of antennas at the UE (N) on the capacity of the proposed method, the one in [23–25], and Tabu Seach in [31], for $M = 64$, $N_{\text{vec}} = 120$, $P_{\text{T}} = 10$ dBm, $p_{\text{mut}} = 5\%$, and $\alpha = 0$; (b) Effect of the number of antennas at the BS (M) on the capacity of the proposed method and the one in [23–25] for $N = 4$, $N_{\text{vec}} = 120$, $P_{\text{T}} = 10$ dBm, $p_{\text{mut}} = 5\%$, and $\alpha = 0$.

Figure 3.6 shows the capacity versus total transmit power for different number of antennas at the UE. As expected, the performance is improved with the increase in the total transmit power or, as previously observed, the numbers of antennas at the UE. Moreover, for a fixed number of antennas at the UE, and the same capacity, the proposed method uses about 4 dB less power, which may represent a reduction of up to 60%, depending on N, when compared with [23–25]. All these improvements are considered quite significant.

[3] For the Tabu Search, we consider $T_{\text{list}} = 1$ (Tabu List Size) and the number of iteration (N_{it}) as the stop criterion.

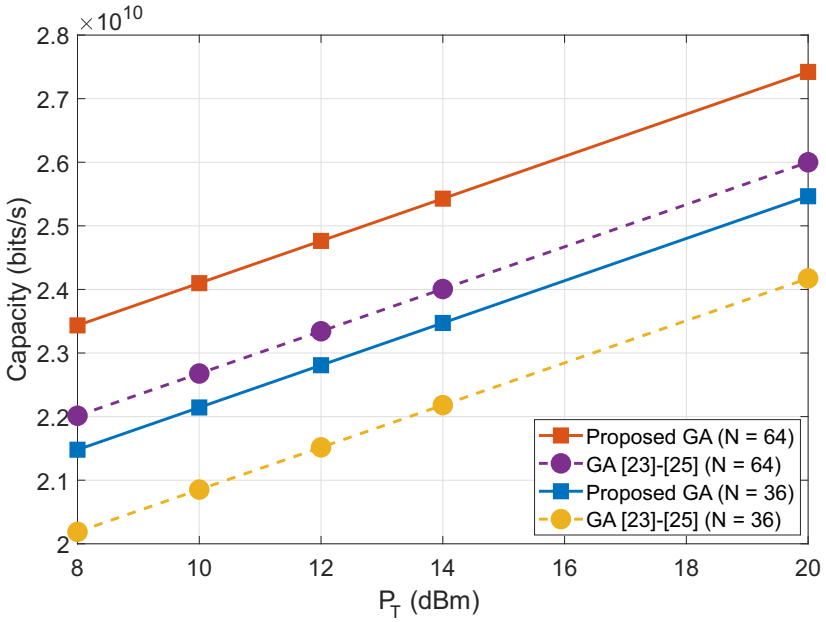

Figure 3.6 – Effect of the power variation (P_{T}) on the capacity of the proposed method and the one in [23–25], for different values of N, with $N_{\mathrm{vec}} = 120$, $M = 64$, $p_{\mathrm{mut}} = 5\%$, and $\alpha = 0$.

3.4.1.2 Effect of the Codebook Size

Choosing the codebook size is an extremely important part of the IA process. The designer is faced with the following trade-off. A large codebook size implies a greater beam refinement during the UE search, increasing the received SNR and reducing the interference. Thus, performance is improved. On the other hand, small codebook sizes are desirable to keep the search delay and the storage requirement small.

Figure 3.7 shows the capacity for the two methods as a function of the codebook size, N_{vec}, for $M = 4$, $N = 4$, $P_{\mathrm{T}} = 10$ dBm, and $p_{\mathrm{mut}} = 5\%$. From the results, it can be seen that the capacity of both methods has a steep growth as the codebook size increases from a small value, but it quickly saturates. This is because the search space becomes very large, and the two GAs, not being able to exploit it completely, converge to a (sub)optimal capacity value. Nonetheless, it is possible to observe that the proposed algorithm presents a superior performance as compared to the GA in [23–25], even for a codebook size as low as $N_{\mathrm{vec}} = 30$. For the proposed method, for $N_{\mathrm{vec}} > 100$ it is not possible to verify any performance improvement. So, a good result

is obtained with a not so large codebook.

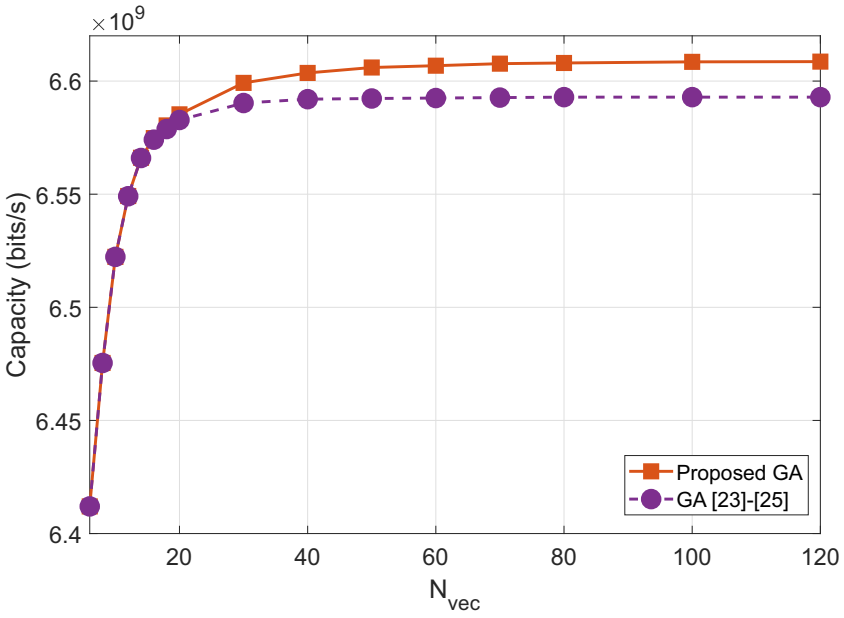

Figure 3.7 – Effect of the codebook size (N_{vec}) on the capacity of the proposed method and the one in [23–25], for $M = 4$, $N = 4$, $P_{\text{T}} = 10$ dBm, $p_{\text{mut}} = 5\%$, and $\alpha = 0$.

3.4.1.3 Effect of the GA Mutation Probability

The mutation operator guarantees the genetic diversity of the population, but it is used with a given probability. For high values of mutation probability, the new individuals are generated randomly, losing the main characteristics of the fittest individuals in the population. To verify the influence of this parameter, the capacity as a function of the number of antennas at the BS for different mutation probabilities is presented in Figure 3.8.

From Figure 3.8, it can be observed that the greater the mutation probability, the worse the performance of the proposed algorithm in terms of convergence speed, and the closer it gets to the performance of the GA in [23–25]. Note that the GA in [23–25] performs almost completely random operations, slowing convergence. The same behavior was observed when considering the evaluation of the capacity as a function of the number of antennas at the UE (not shown here). In addition, it is

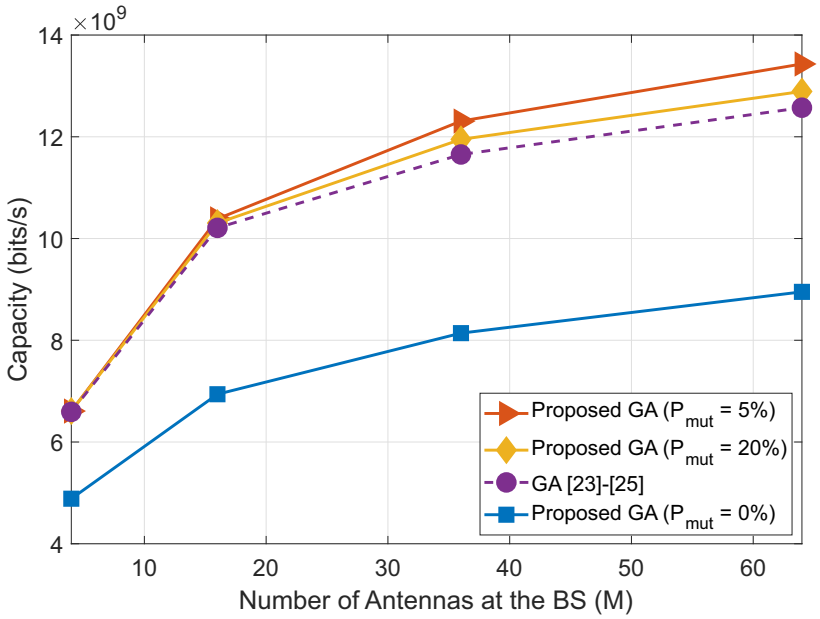

Figure 3.8 – Effect of the GA mutation probability (p_{mut}) on the capacity of the proposed method and the one in [23–25], as a function of number of antennas at the BS, for $N = 4$, $N_{\mathrm{vec}} = 120$, and $P_{\mathrm{T}} = 10$ dBm.

possible to see the importance of the mutation operator, *i.e.*, the system performance decreases considerably for $p_{\mathrm{mut}} = 0\%$ or for an excessive p_{mut}.

Moreover, the impact of the crossover probability was also evaluated. Figure 3.9 shows the impact of the crossover and mutation probabilities. It is possible to conclude that: 1) For $p_{\mathrm{mut}} = 0\%$ and/or $p_{\mathrm{c}} = 0\%$ the system performance decreases considerably; 2) The higher p_{mut}, the higher p_{c} should be set to compensate the reduction of system performance due to the increased randomness; 3) For a large number of antennas at the BS and/or UE, the influence of crossover increases due to the higher complexity of the problem. Therefore, from the previously conclusions, it is possible to note that the adequate selection of crossover and mutation operators are important for improving the system performance and achieving a near-optimum solution. For instance, if there is no mutation then convergence is very slow, but if mutation is excessive then performance decreases as well. Thus, we can conclude that both operators greatly influence the system performance.

Usually, in the literature the value of crossover and mutation probabilities are

around $p_{\mathrm{c}} \geq 50\%$ and $p_{\mathrm{mut}} \leq 10\%$, respectively [27, 41, 65, 66]. This can be better explained by the fact that, if p_{mut} is too high GA becomes a random search [27], while if $p_{\mathrm{c}} = 100\%$ then the old population can not survive for the next generation and the genetic diversity of the new population decreases [27]. Based on the above, and as in the numerical evaluations, $p_{\mathrm{mut}} = 5\%$ yielded a very good performance, as illustrated in Figure 3.9, and therefore, $p_{\mathrm{c}} = 50\%$ and $p_{\mathrm{mut}} = 5\%$ were assumed for all simulation results.

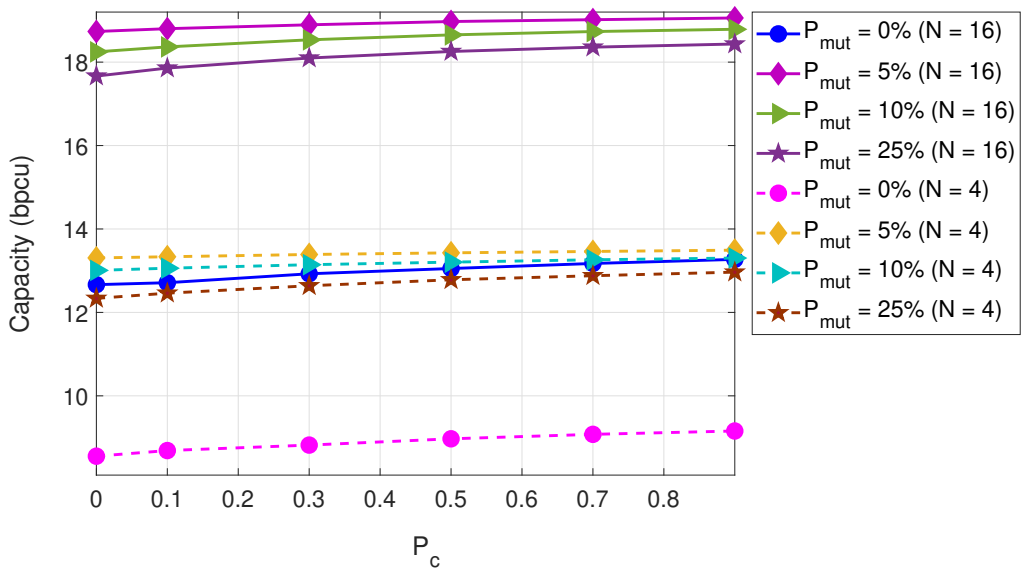

Figure 3.9 – Capacity of the proposed method varying the Crossover probability for different values of mutation probability for $N_{\mathrm{vec}} = 120$, $P_{\mathrm{T}} = 10$ dBm, $M = 64$, $N = 4, 16$, and $\alpha = 0$.

3.4.1.4 Outage Probability Analysis

Simulation results for the outage probability in (3.9) are given in Figure 3.10. The proposed algorithm has lower outage probability than the GA in [23–25], for all considered values of Γ_{min}. Moreover, it is possible to observe that the outage probability decreases with the reduction of Γ_{min}, *i.e.*, as the application requires a lower minimum SNR. Similar behaviour was obtained with $N > 1$.

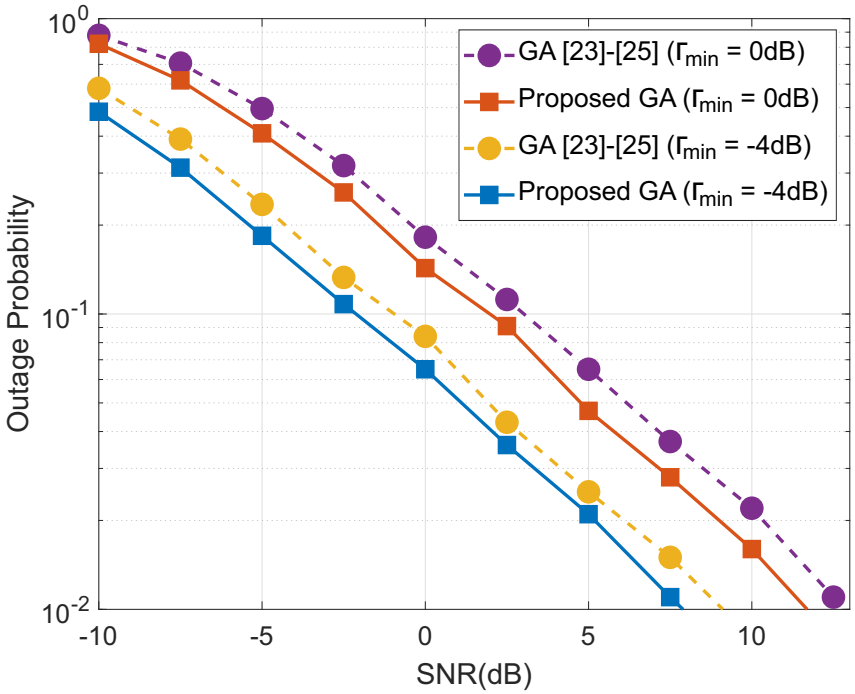

Figure 3.10 – Outage probability of the proposed method and that in [23–25], for $M = 64$, $N = 1$, $N_{\text{vec}} = 120$, $P_{\text{T}} = 10$ dBm, $p_{\text{mut}} = 5\%$, and $\alpha = 0$.

3.4.1.5 Computational Cost

The proposed method uses some different operators when compared with [23–25]. However, unlike the method in [23–25], the proposed method does not make frequent use of a function that generates random numbers. In contrast, the proposed method uses simple operations that require a lower computation time than that required to update a random number generator. In order to exemplify this, the software Matlab® was used to measure the computation time of each function and method. First, it was concluded that the rand function has a computation time approximately 2 times higher than the computation time demanded by some simple math operations. Second, the computation time was measured for each iteration considering both methods, the proposed method obtained an average time per iteration that is less than the method in [23–25], *e.g.*, for 10^4 iterations the average time for the proposed method is 1.8 ms, and the average time for the method in [23–25] is 3.4 ms.

Although the above example is dependent on the particular software/hardware architecture and the programming, it illustrates how hard it is to define an appropriate

and fair measure of complexity and delay. That is the reason why this comparison is not presented in detail. Nevertheless, please note that the proposed method is able to achieve the same performance as the scheme in [23–25] with a smaller number of iterations, *i.e.*, the proposed method can reduce the IA delay. Figure 3.11 shows the number of iterations for a given performance. From these results, and considering the average time for each iteration as discussed above, the IA delay of the proposed method is approximately 261 ms and the IA delay with [23–25] is 680 ms for the same scenario. However, again, please note that these values depend on the particular implementation, and therefore should be seen as an illustration only.

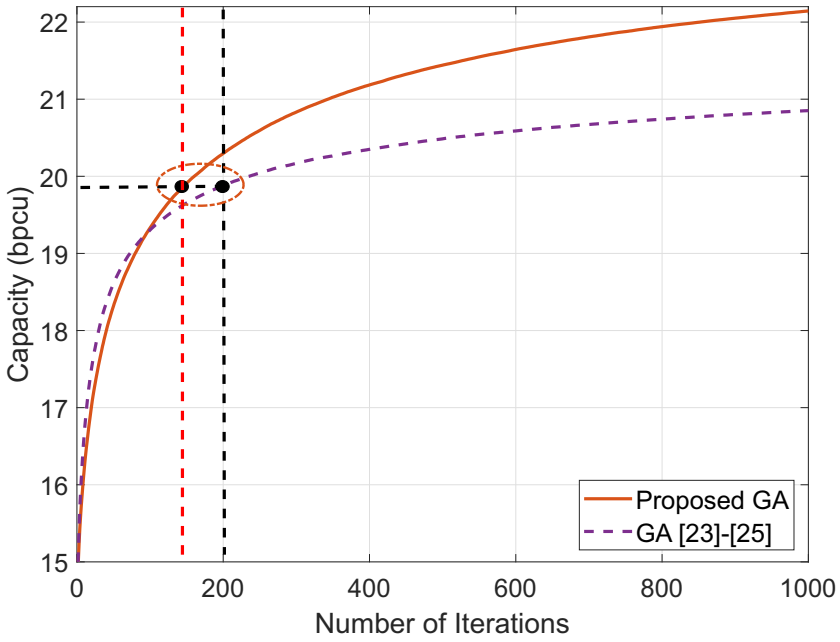

Figure 3.11 – Capacity as a function of the number of iterations for $N_{\text{vec}} = 120$, $P_{\text{T}} = 10$ dBm, $M = 64$, and $N = 36$.

3.4.2 Results for $\alpha \neq 0$

The results discussed in the previous subsection do not consider the execution cost of each iteration of the algorithm ($\alpha = 0$). In other words, from the considerations above, the larger the number of iterations, the better the system performance. Of course, this is not valid in practice due to the delay in the IA process. As a countermeasure,

the authors in [23–25] have introduced a delay cost (α) for running each iteration of the algorithm. This parameter value was arbitrarily chosen in those references. But, as will be shown next, it can be properly chosen depending on the desirable capacity and the delay that can be tolerated by the application.

Next, it is performed two analyses under these delay constraints. First, Figure 3.12 presents the convergence of the proposed algorithm and of the GA in [23–25] for a fixed, nonzero value of α, for a given channel realization. Then, in Figure 3.13, the system performance for different values of α was evaluated. As can be seen from Figure 3.12, increasing the number of iterations without limit does not improve the system performance, since it directly influences the search delay. In addition, the convergence of the proposed algorithm is verified.

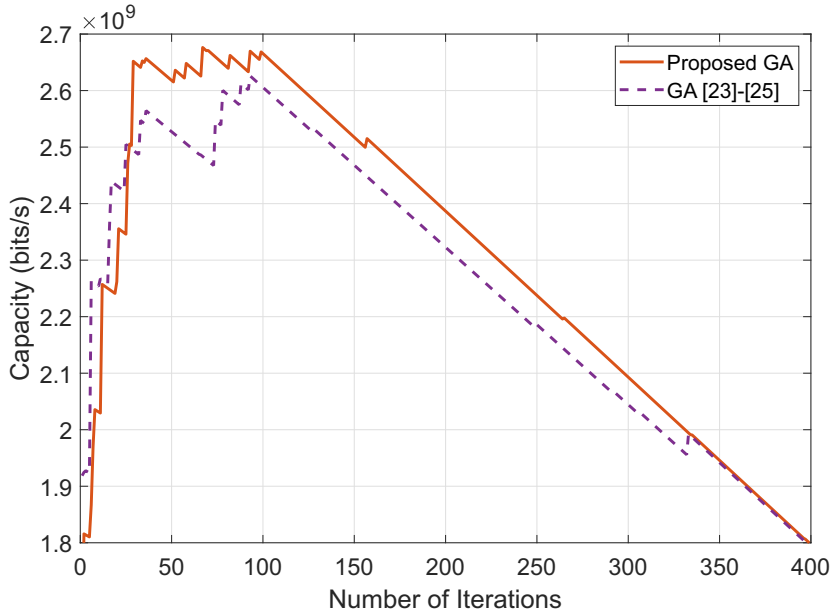

Figure 3.12 – Convergence analysis of the proposed GA and GA in [23–25] for $M = 4$, $N = 4$, $N_{\text{vec}} = 120$, $P_{\text{T}} = 10$ dBm and $\alpha = 10^{-3}$

Figure 3.13 shows the variation of α analysis for $M = 64$, $N = 64$, $N_{\text{vec}} = 120$, $P_{\text{T}} = 10$ dBm, and $p_{\text{mut}} = 5\%$. The values of α are defined, in practical scenarios, by the application requirements. Thus, in this work, we randomly choose different values of α to evaluate the performance of the proposed solution. From the results, it is possible to verify that the proposed algorithm presents initially a slower convergence,

as compared to the GA in [23–25], but it then reaches maximum capacity values higher than those achieved by the GA in [23–25] for most of the values of α. This certifies the proposed algorithm for practical applications, where a trade-off exists between performance and delay of beam refinement. The results presented in this section show that it is possible to achieve (sub)optimal performance with a few iterations.

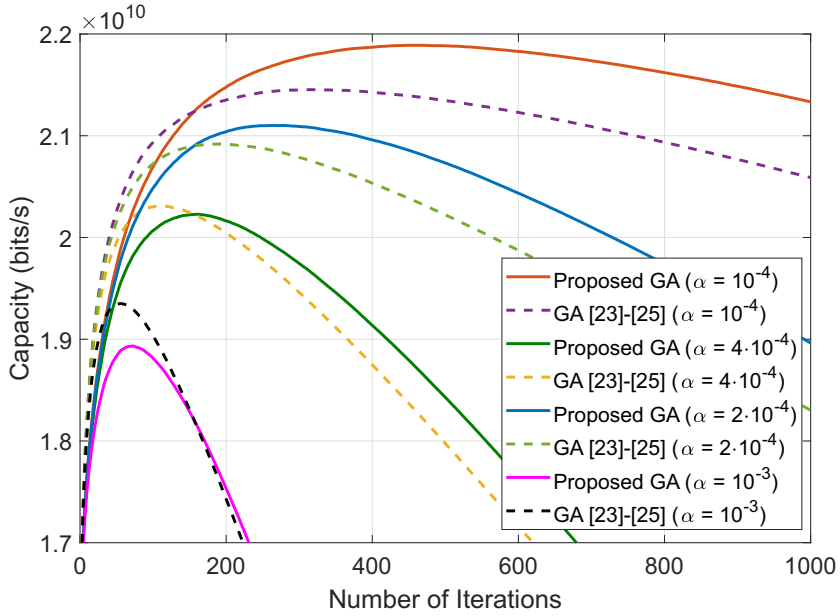

Figure 3.13 – Variation of α for $M = 64$, $N = 64$, $N_{\text{vec}} = 120$, $P_{\text{T}} = 10$ dBm and $p_{\text{mut}} = 5\%$.

3.5 CONCLUSION

In this chapter, the proposed beam search method based on GA, which aims to reduce the delay of the directional search in IA, was evaluated considering scenarios with and without delay constraints. The proposed method was evaluated in different scenarios, including variable number of antennas at the BS and UE, codebook size, and power consumption. The simulation results show that the proposed method presents an excellent performance when compared to the method in [23–25], and can reach the same results as ES in small scenarios. In addition, the proposed algorithm is generic, as it can be applied to different scenarios. To finish, it is important to remark that

the proposed algorithm can reduce the cellular search delay introduced by the use of beamforming at the BS and UE.

Chapter 4

IRS Beamforming Design

4.1 INTRODUCTION

B5G wireless systems aim to meet application requirements of verticals like Industry 4.0, Smart Grids, and Smart Cities [67]. This requires to considerably increase the network capacity and provide ubiquitous wireless connectivity for a very large number of devices. To achieve these goals, many technologies have been developed during the last years, such as mmWave communications, massive MIMO systems, and ultra-dense networks (UDN) [68]. As presented in the previous chapter, the mmWave communications allow the use of large active antenna arrays at the BS and UE, *i.e.*, narrow beams and flexible antenna configurations can be considered, which enable spatially dense network layouts by reducing co-channel interference. In addition, the mmWave communications exhibit a huge available bandwidth that provides multi-Gbps rates. These advantages notwithstanding, the use of active antenna arrays at the BS and UE represents a large implementation cost and/or huge energy consumption. To overcome this problem, recently, an energy-efficient and low-cost technology, IRS, which is a meta-surface equipped with a large number of low-cost passive elements [11, 12], was developed to increase the network capacity. This technology is a promising new paradigm to achieve smart and reconfigurable wireless radio propagation environments for B5G communication systems.

An IRS is a planar surface comprising a large number of passive reflecting elements, each of which is able to reflect the incident signal with a given phase or amplitude shift. By densely deploying IRSs in wireless communication networks and

intelligently coordinating their phase and amplitude shifts, the reflected and direct signals can be optimized to add constructively at the UE, and the wireless channels can be smartly controlled to achieve desired realization and/or distributions, which provides a new paradigm to tackle the wireless channel fading impairment and interference issue, potentially improving capacity and reliability [11, 69]. In addition, the main practical advantages of the employment of IRSs in a wireless communication system are presented next [69].

1. IRS consists of only passive elements that can reflect the impinging signals without the need of any RF chain, leading to a great reduction in the energy consumption and hardware cost when compared to traditional active antenna arrays [11, 69].

2. Different from the full-duplex (FD) relays, IRSs operate in FD mode but do not suffer from antenna noise amplification and self interference [11, 69, 70].

3. IRSs usually are low profile, lightweight, and have conformal geometry. They can be easily mounted or removed from objects [11].

4. The IRSs can be transparently employed in the wireless networks, *i.e.*, they can be integrated into the existing wireless system without deep modifications in the UE and BS [69].

Therefore, motivated by the above advantages of IRSs, next, this emerging technology is considered to assist and wireless communication system and its performance is evaluated.

4.1.1 Related Work

Some recent works studied the beamforming design at the IRS and/or BS [10, 12, 18, 19, 21, 71–74]. In [12], the beamforming at the IRS and power allocation were jointly optimized to maximize the energy efficiency of the system. In [19, 71] the authors designed the beamforming at the BS and IRS aiming to minimize the transmit power at the BS. In addition, an IRS-enhanced orthogonal frequency division multiplexing system was proposed in [75] in order to maximize the downlink achievable rate by optimizing the beamforming at the IRS and power allocation at the BS. The above

works considered continuous phases at the IRS, while [10, 21, 73, 74] extended the setups to discrete phases at the IRS. In addition, in [72] the authors take into account a practical phase shift model that captures the phase-dependent amplitude variation in the element-wise reflection coefficient.

It is important to underline that all the mentioned works consider the perfect knowledge of the instantaneous channel state information (I-CSI) at the BS, which is difficult to obtain in practice due to the large number of elements at the IRS and requires that each element at the IRS be equipped with an RF chain. However, estimating the CSI between the IRS and BS or between the IRS and UE is a challenge. Some works have presented possible solutions for this problem, however, they have the following possible drawbacks: (*i*) the IRS needs to be equipped with multiple RF chains [7, 76]; (*ii*) the IRS needs to implement not only phase control but also amplitude control, which increases the system complexity [77, 78]; (*iii*) the channel must be sparse, which in general is experienced only in mmWave and LOS-dominant sub-6 GHz systems [60, 79]; (*iv*) the training overhead scales up with the number of elements at the IRS and/or BS [7, 75–78, 80–82].

In order to overcome these issues, currently, a few works started exploring the statistical channel state information (S-CSI) [83–85], which is easier to estimate thanks to its much slower variation in time. Accordingly, in [85], the authors designed the beamforming only at the IRS in order to verify its effect on the ergodic spectral efficiency for different propagation scenarios. In [85], the authors proposed an optimal beamforming design based on the upper bound of the ergodic spectral efficiency and the S-CSI. In addition, in [83, 84], a new two-timescale transmission protocol was proposed in order to maximize the achievable average sum-rate for an IRS-aided multi-user system. Specifically, the IRS phase-shifts are first optimized based on the S-CSI of all links, while the transmit beamforming vector at the BS is then designed to cater to the I-CSI of the users effective channels. Finally, in [86], the authors considered a multi-pair communication system assisted by an IRS, and a method based on GA was proposed in order to maximize the system achievable rate by solely optimizing the discrete or continuous phase shifts at the IRS considering S-CSI. From the above, it can be seen that most part of the literature considers the perfect CSI knowledge at the BS/IRS and there are a few works exploring the S-CSI in order to reduce the training overhead required by the beamforming design.

4.1.2 Contributions

Motivated by the above issues, the communication between a multiple antenna BS and a single antenna UE, assisted by an IRS, is considered. Then, two different approaches are proposed in order to solve the beamforming optimization problem at the IRS and BS without considering any I-SCSI knowledge. The proposed approaches are described as follows.

1. A joint beamforming optimization at the BS and IRS based on PSO is introduced. This approach is not dependent on CSI acquisition. In addition, the proposed solution aims to minimize the transmit power at the BS while meeting a minimum received SNR requirement through beamforming optimization. In this approach, continuous phase shifts at the IRS elements are considered.

2. Considering discrete phase shifts at the IRS, in order to solve the beamforming optimization problem at the IRS and the BS, two different solutions based on GA are proposed. In the first, it was not considered any CSI knowledge at the IRS and/or BS. Then, in the second approach, only the S-CSI knowledge is assumed. The main goal of this approach is to maximize the system achievable rate while meeting a maximum transmit power requirement at the BS through beamforming optimization at the IRS and BS.

This chapter is split into two parts. First, the approach based on PSO is detailed in **Section 4.2**, named *"Novel Approach Considering Continuous Phases at the IRS"*, and its system model and simulation results are presented. Next, the approach based on GA is presented in detail in **Section 4.3**, named *"Novel Approach Considering Discrete Phases at the IRS"*.

4.2 NOVEL APPROACH CONSIDERING CONTINUOUS PHASES AT THE IRS

In this approach, the communication between a multiple antenna BS and a single antenna user, assisted by an IRS, is considered. The main goal of the proposed approach is to optimize the beamforming at the BS and IRS without CSI, by minimizing the transmit power, subject to a minimum SNR. To solve this problem, a new method

based on the PSO technique is proposed. The system model considered and the results obtained for this approach are presented in this section.

4.2.1 System Model

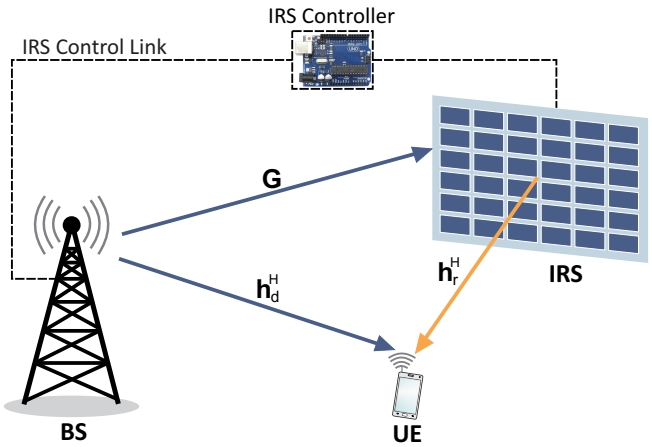

Figure 4.1 – An IRS-assisted single-user communication system.

In Figure 4.1, we consider a downlink system including a BS equipped with a Uniform Linear Array (ULA) with M transmit antennas, an IRS equipped with an UPA with K reflecting elements, and a single antenna UE. It is assumed that mobility is limited or very limited, so that the channels change slowly. This is a valid premise as IRS is employed in practice mainly to support low-mobility scenarios [75]. In addition, no CSI knowledge at the BS and/or the IRS is assumed.

The received signal at the UE can be written as [19]

$$y = (\mathbf{h}_{\mathrm{r}}{}^{\mathrm{H}}\Theta\mathbf{G} + \mathbf{h}_{\mathrm{d}}{}^{\mathrm{H}})\mathbf{w}s + n, \tag{4.1}$$

where $\mathbf{h}_r^{\mathrm{H}} \in \mathbb{C}^{1\times K}$ denotes the channel vector from the IRS to the UE (IRS-UE), $\mathbf{G} \in \mathbb{C}^{K\times M}$ is the channel matrix from the BS to the IRS (BS-IRS), $\mathbf{h}_d^{\mathrm{H}} \in \mathbb{C}^{1\times M}$ is the channel vector from the BS to the UE (BS-UE), $\mathbf{w} \in \mathbb{C}^{M\times 1}$ is the beamforming vector at the BS, s is the transmitted data, an independent random variable with zero mean and unit variance, while n denotes the additive white Gaussian noise at the user with power σ^2. Moreover, $\Theta = \mathrm{diag}(\xi_1 e^{j\theta_1}, ..., \xi_K e^{j\theta_K})$ where $\theta = [\theta_1, ..., \theta_K]$ denotes the phase shift vector with $\theta_k \in [0, 2\pi)$, and $\xi_k \in [0, 1]$ for $(k = 1, \ldots, K)$

is the amplitude reflection coefficient. For simplicity, it is considered $\xi_k = 1$, *i.e.*, maximum signal reflection for each element of the IRS.

In this thesis, the Rician fading and log-distance path loss for all channels are considered in accordance to [19]. It is important to note that the signals reflected two or more times by the IRS are ignored [19]. Thus, the BS-IRS, BS-UE and IRS-UE links are denoted as

$$\mathbf{G} = \sqrt{P_{\mathrm{L}}^{\mathrm{BI}}}\left(\sqrt{\frac{\beta_{\mathrm{BI}}}{1+\beta_{\mathrm{BI}}}}\mathbf{G}^{\mathrm{LoS}}\right), \tag{4.2}$$

$$\mathbf{h}_{\mathrm{d}} = \sqrt{P_{\mathrm{L}}^{\mathrm{BU}}}\left(\sqrt{\frac{\beta_{\mathrm{BU}}}{1+\beta_{\mathrm{BU}}}}\mathbf{h}_{\mathrm{d}}^{\mathrm{LoS}} + \sqrt{\frac{1}{1+\beta_{\mathrm{BU}}}}\mathbf{h}_{\mathrm{d}}^{\mathrm{NLoS}}\right), \tag{4.3}$$

$$\mathbf{h}_{\mathrm{r}} = \sqrt{P_{\mathrm{L}}^{\mathrm{IU}}}\left(\sqrt{\frac{\beta_{\mathrm{IU}}}{1+\beta_{\mathrm{IU}}}}\mathbf{h}_{\mathrm{r}}^{\mathrm{LoS}} + \sqrt{\frac{1}{1+\beta_{\mathrm{IU}}}}\mathbf{h}_{\mathrm{r}}^{\mathrm{NLoS}}\right), \tag{4.4}$$

where $P_{\mathrm{L}}^{i} = C_0 d^{-\alpha_i}$ for $i \in \{BI, BU, IU\}$ is the path loss. α_i is the path loss exponent of the BS-IRS, BS-UE, IRS-UE links, respectively. Moreover, $\mathbf{G}^{\mathrm{LoS}}$, $\mathbf{h}_{\mathrm{r}}^{\mathrm{LoS}}$ and $\mathbf{h}_{\mathrm{d}}^{\mathrm{LoS}}$ denote the deterministic LoS components. Moreover, $\mathbf{h}_{\mathrm{d}}^{\mathrm{NLoS}}$ and $\mathbf{h}_{\mathrm{r}}^{\mathrm{NLoS}}$ are the Rayleigh fading of the BS-UE and IRS-UE links, respectively, and β_{BI}, β_{IU} and β_{BU} are the Rician factors. It is important to underline that it is considered a LoS link between the BS and IRS, which is a reasonable assumption in practical scenarios [75, 87–89]. Finally, the SNR at the UE is given by

$$\Gamma = \frac{|(\mathbf{h}_{\mathrm{r}}{}^{\mathrm{H}}\Theta\mathbf{G} + \mathbf{h}_{\mathrm{d}}{}^{\mathrm{H}})\mathbf{w}|^2}{\sigma^2} \tag{4.5}$$

The achievable rate at the UE in bps/Hz is given by

$$R = \log_2(1+\Gamma). \tag{4.6}$$

4.2.1.1 Optimization Problem

The main goal of this work is to minimize the total transmit power at the BS by jointly optimizing the beamforming at the BS and the phase shifts at the

IRS considering a minimum SNR constraint, without CSI estimation. This non-convex optimization problem can be formulated as [19]

$$\begin{aligned} \underset{\mathbf{w},\theta}{\text{Minimize}} \quad & ||\mathbf{w}||^2 \\ \text{Subject to} \quad & |(\mathbf{h}_{\mathrm{r}}{}^{\mathrm{H}}\Theta\mathbf{G} + \mathbf{h}_{\mathrm{d}}{}^{\mathrm{H}})\mathbf{w}|^2 \geq \Gamma_{\min}\sigma^2, \\ & 0 \leq \theta_k \leq 2\pi, \ k = 1, ..., K \end{aligned} \tag{4.7}$$

where $\Gamma_{\min}$ is the minimum SNR constraint. Although the objective function of the optimization problem in (4.7) is convex, the minimum SNR constraint is non-convex where the beamforming at the BS and UE are coupled. So, there is not a standard method to solve it. Therefore, in this thesis, a new method based on the PSO is proposed and its operation is described next.

4.2.2 Proposed Method based on PSO

In this thesis, a novel method based on PSO was developed in order to solve the non-convex optimization problem in (4.7), without knowledge of CSI at the IRS and BS. Although the proposed solution is based on PSO its operation presents some differences when compared to the basic PSO described in Chapter 2. Specifically, the proposed method differs from the classic PSO in the way that a new swarm is generated in each iteration. More precisely, a classic PSO generates a new swarm in each iteration only by updating the velocity and position of each particle using (2.1) and (2.2), respectively. However, in the new method, the first $L/2$ particles are generated by updating the velocity and position of each particle using (2.1) and (2.2), respectively. The other $L/2$ particles are generated in two possible different ways: For a given probability, a new particle is generated by randomly changing some columns of the best particle $\left(g_{\mathrm{best}} = [\mathbf{x}_{\mathrm{best}}, \mathbf{v}_{\mathrm{best}}]\right)$, otherwise a new particle is randomly generated. For a better understanding the proposed method is presented in **Algorithm 4.1** and its steps are detailed next.

1. Randomly generate L particles, or beamforming vector pairs, $(\mathbf{w}_l, \theta_l)$, $l = 1, \ldots, L$. The beamformings vector pairs are also the "positions" of the particles in the PSO nomenclature.

2. For each particle, if the SNR at the UE is larger than $\Gamma_{\min}$, then the fitness of that particle is $||\mathbf{w}||^2$.

3. Update p_{best} and g_{best} from the fitness computed in the previous step: p_{best} is the best fitness obtained for each particle up to the current iteration, and g_{best} is the best fitness obtained for all particles up to the current iteration. In our approach, the fittest particle is the particle with the smallest $||\mathbf{w}||^2$.

4. In this step, L new particles are generated as follows. Generate $L/2$ particles from the updating of the velocity and position of each particle using (2.1) and (2.2), respectively. Generate the $L/2$ remaining particles by the following steps: (a) With a given probability p^*_{PSO}, generate a new particle by operating on each column of the best particle as follows: With a given probability p_{PSO} randomly change the column of the best particle ($g_{\text{best}} = [\mathbf{x}_{\text{best}}, \mathbf{v}_{\text{best}}]$), otherwise, with probability $(1-p_{\text{PSO}})$, this column is maintained; (b) With probability $(1-p^*_{\text{PSO}})$, randomly generate a whole new particle. The swarm of the next iteration is formed by the particles generated in this step, *i.e.*, from this operation, the beamforming at the BS and the IRS are updated to form the new pairs (or particles).

5. Check if the stop criterion is met. If so, then return the fittest particle $(\mathbf{w}_{\text{best}}, \theta_{\text{best}})$. Otherwise, go to Step 2.

The main parameters used in **Algorithm 4.1** are: $N_{\text{it}} = 1000$, $L = 10$, $\ell_1 = \ell_2 = 1.2$, $\omega_{\min} = 0.1$, $\omega_{\max} = 0.6$, $p^*_{\text{PSO}} = 0.2$ and $p_{\text{PSO}} = 0.1$. In the proposed method, the pairs of beamforming vectors at the BS and IRS to be tested are defined at the BS, while the IRS beamforming are sent by the BS to the controller shown in Figure 4.1. Then, for each beamforming pair, the feedback of the SNR at the UE is received at the BS, and the current beamforming pair is evaluated based on $||\mathbf{w}||^2$. This process is performed for all pairs. Note that the BS/IRS/UE channels are not explicitly estimated. Therefore, it does not require one RF chain at each IRS element and do not require any channel estimation process, thus solving the challenges of CSI estimation of IRS systems, as mentioned in [11].

Algorithm 4.1: Proposed solution based on PSO.

Input : System parameters: M, K
Main PSO parameters: L, N_{it}, ℓ_1, ℓ_2, $\omega_{\min}$, $\omega_{\max}$
Probabilities: p_{mut1} and p_{mut2}.

Output : $\mathbf{w}_{\text{best}}$, θ_{best}

Initialize position $[\mathbf{x}_{\text{BS}}]_m = [\mathbf{w}_{\text{BS}}]_m$ and velocity $[\mathbf{v}_{\text{BS}}]_m$
Initialize position $[\mathbf{x}_{\text{IRS}}]_k = \theta_k$ and velocity $[\mathbf{v}_{\text{IRS}}]_k$
$[\mathbf{x}]_i = ([\mathbf{x}_{\text{BS}}]_m,\ [\mathbf{x}_{\text{IRS}}]_k)$; $[\mathbf{v}]_i = ([\mathbf{v}_{\text{BS}}]_m,\ [\mathbf{v}_{\text{IRS}}]_k)$
$i = 1, \ldots, L, \quad m = 1, \ldots, M$ and $k = 1, \ldots, K$
Find the global g_{best} and local p_{best} best solutions.
for $t = 1 : N_{it}$ **do**
    Calculate ω following (2.3)
    for $i = 1 : L/2$ **do**
        Update $[\mathbf{v}]_i^t$ based on (2.1).
        Update $[\mathbf{x}]_i^t$ based on (2.2).
        Update p_{best}
    end
    for $i = L/2 + 1 : L$ **do**
        if $(\text{rand}(\ ) < p_{\text{PSO}}^*)$ **then**
            $[\mathbf{x}]_i^t = [\mathbf{x}_{\text{best}}]^t$
            $[\mathbf{v}]_i^t = [\mathbf{v}_{\text{best}}]^t$
            for *m = 1:K* **do**
                if $(\text{rand}(\ ) < p_{\text{PSO}})$ **then**
                    Generate a new particle from randomly changing the column of $[\mathbf{x}_{\text{IRS}}]_{m,i}^t$ and $[\mathbf{v}_{\text{IRS}}]_{m,i}^t$.
                end
            end
            for *n = 1:M* **do**
                if $(\text{rand}(\ ) < p_{\text{PSO}}^*)$ **then**
                    Generate a new particle from randomly changing the column of $[\mathbf{x}_{\text{BS}}]_{n,i}^t$ and $[\mathbf{v}_{\text{BS}}]_{n,i}^t$.
                end
            end
        else
            Randomly generate a new particle $([\mathbf{x}]_i^t, [\mathbf{v}]_i^t)$.
        end
        Update p_{best}
    end
    Update $g_{\text{best}} = \mathbf{x}_{\text{best}}$
end
$\mathbf{w}_{\text{best}} = g_{\text{best}}$, $\theta_{\text{best}} = g_{\text{best}}$
return $\boldsymbol{w}_{best}$, θ_{best}

4.2.3 Simulation Results

All curves in this section are the average of 10^3 different realizations. The simulation setup described in Figure 4.2 is considered, where d is the BS-UE horizontal distance. Therefore, the BS-UE and IRS-UE link distances are $d_1 = \sqrt{d^2 + d_{\mathrm{v}}^2}$ and $d_2 = \sqrt{(d_{\mathrm{h}} - d)^2 + d_{\mathrm{v}}^2}$, respectively. The simulation parameters are $M = 4$ (if not specified otherwise), $\beta_{\mathrm{BU}} = \beta_{\mathrm{IU}} = 0$, $\beta_{\mathrm{BI}} \to \infty$, $\alpha_{\mathrm{BI}} = 3.5$, $\alpha_{\mathrm{BI}} = 2.0$, $\alpha_{\mathrm{BI}} = 2.8$, $C_0 = -30$ dBm, $\sigma^2 = -80$ dBm, $d_{\mathrm{v}} = 2$ m, $d_{\mathrm{h}} = 51$ m and $P_{\mathrm{T}} = 10$ dBm. In this section, the following benchmarks are evaluated: *i*) The optimal beamforming design with perfect CSI in [19], which is a lower bound for (4.7). This benchmark is obtained from solving the optimization problem in [19, Eq. (19)] by the CVX technique as in [19]; *ii*) Random phase shifts, where $\theta \in [0, 2\pi]$ and the beamforming at the BS is the optimal transmit beamforming; *iii*) Without IRS, where it does not consider the IRS and the bemforming at the BS is the optimal transmit beamforming. Moreover, for the sake of simplicity, in this work, the maximum number of iterations N_{it} is considered as the stop criterion.

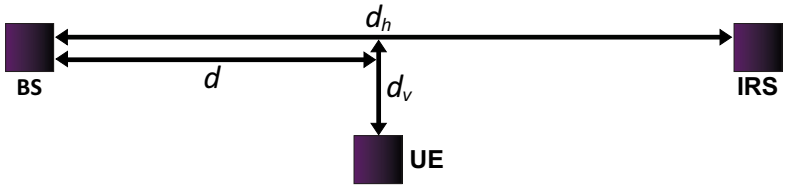

Figure 4.2 – Simulation setup.

First of all, in order to illustrate the performance of the proposed method, Figure 4.3 presents its convergence considering $K \in \{20, 40, 60\}$ and $L = 10$. From the results, it can be verified that the proposed method converges in few iterations (around 100) for different IRS sizes. It is important to note that the number of iterations does not noticeably increase with K, which fortunately leads to a relatively low training overhead for complex scenarios (*i.e.* for large K). Figure 4.4 compares the transmit power at the BS versus the BS-UE distance for the PSO and the lower bound [19]. For $L = 30$ particles the proposed method achieves similar performance as that of perfect CSI case. Moreover, for $d = 20$ m, *i.e.*, when the UE is near to the BS, the required transmit power is the least among the considered distances. The power increases with d till $d = 40$, then decreases again. From this figure, it is possible to observe the

importance of the IRS as d increases, *i.e.*, the UE is close to the IRS and far from the BS. The above results show the importance of the correct design of the beamforming at the IRS. Well designed beamforming can considerably increase the signal coverage even without CSI estimation.

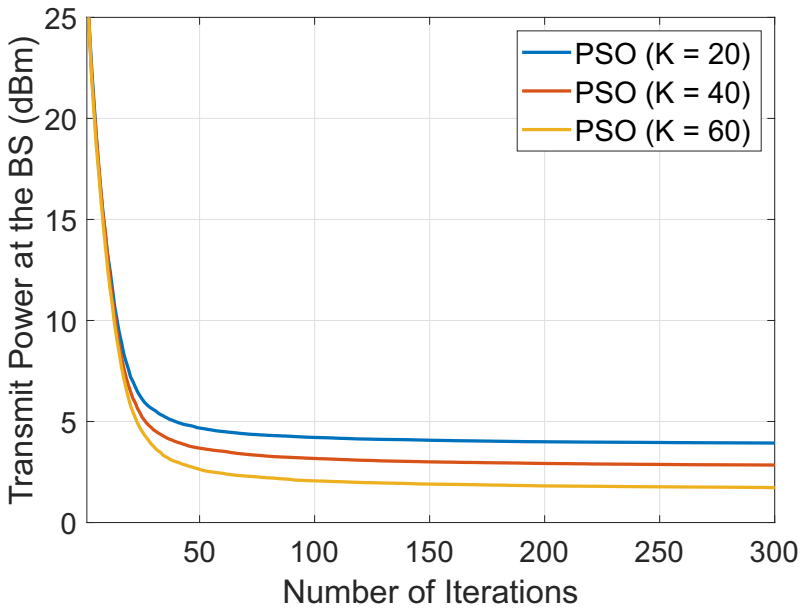

Figure 4.3 – Convergence of the proposed PSO for $L = 10$ and $M = 4$

Figure 4.5 shows the transmit power at the BS versus the number of reflecting elements at the IRS for $d \in \{15, 40, 50\}$ m. It can be seen from the results that: i) for $d = 15$ m in Figure 4.5a, in which the UE is close to the BS but far from the IRS, if increasing K, the transmit power remains almost constant; (ii) for $d = 40$ m in Figure 4.5b, when the UE is far from the BS and the IRS, the transmit power slowly decreases with K; (iii) for $d = 50$ m in Figure 4.5c, as the UE is very close to the IRS but far from the BS, the transmit power greatly decreases with increasing K due to the IRS; (iv) when it is considered a scenario without the IRS or with random phase shifts at the IRS the transmit power at the BS remains almost constant with K, since it does not explore the beamforming gain at the IRS. In addition, in accordance with [19, Proposition 2], the transmit power scales down with K almost in the order of K^2. This squared gain can be explained as the IRS leads to a beamforming gain of order K both at the user link and at the BS-IRS link [19].

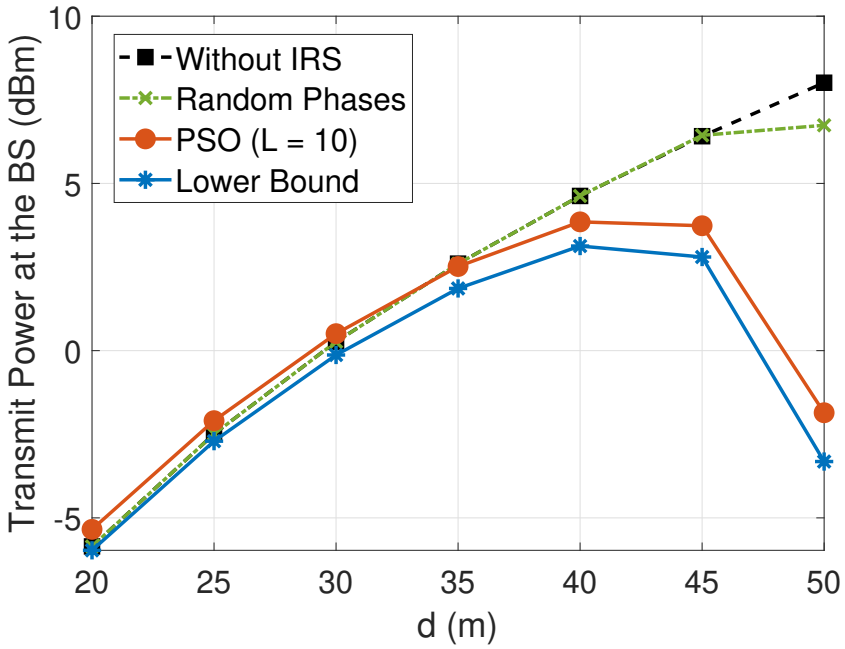

Figure 4.4 – Transmit power at the BS versus BS-UE distance for $K = 20$.

As the main goal of the proposed method is to design the beamforming at the BS and at the IRS without any CSI, it is necessary to consider an amount of feedback from the user, which is given by $N_{\text{it}}L$ and adds some training overhead to the system. It would be of practical importance to have an amount of feedback from the user that is not larger than the number of pilots that would be necessary to estimate the channel, *i.e.*, $N_{\text{it}}L < (MK + 1)$ [90]. Therefore, in order to prove the efficiency of the proposed method, Figure 4.6 shows the training overhead considering $M = 32$ and $d = 50$ m. From the results, it can be observed that for large K, the proposed solution achieves a close to ideal performance with a smaller amount of feedback from the user $(N_{\text{it}}L)$ than the number of pilots necessary to estimate the channel, more specifically, $N_{\text{it}}L = 0.7 \times (MK + 1)$. In addition, from the results, it can be seen that for large K the performance difference between the lower bound and the proposed solution with $N_{\text{it}}L = 0.7 \times (MK + 1)$ and even with $N_{\text{it}}L = 0.5 \times (MK + 1)$ decreases.

Therefore, from the results, it can be concluded that the proposed solution achieves a close to ideal performance with a reasonable amount of feedback from the user in complex scenarios, differently from [7, 75–78, 80] where the training overhead

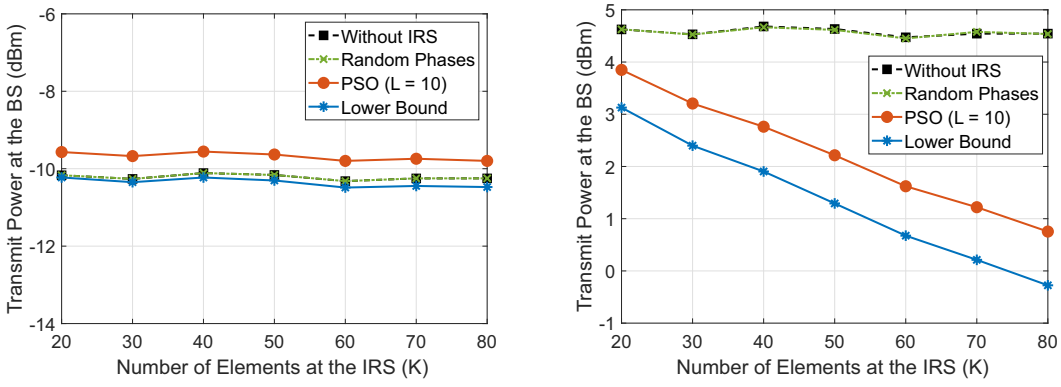

(a) $d = 15$m (b) $d = 40$m

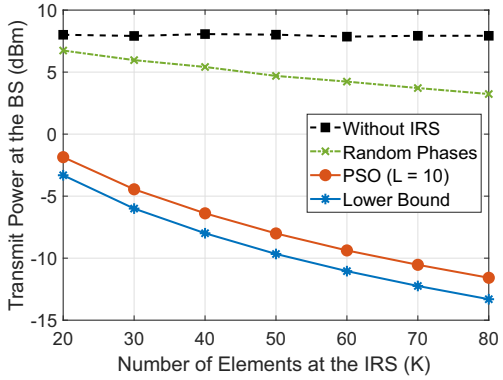

(c) $d = 50$m

Figure 4.5 – Transmit power at the BS versus the number of reflecting elements (K) at the IRS

scales up with MK. In addition, the proposed method can be applied in LoS and NLoS systems because, differently from [60, 79], it does not assume sparse channels. Finally, it is essential to note that the proposed method does not require either active elements at the IRS as in [7, 76] or separate amplitude control at each IRS element as in [77, 78].

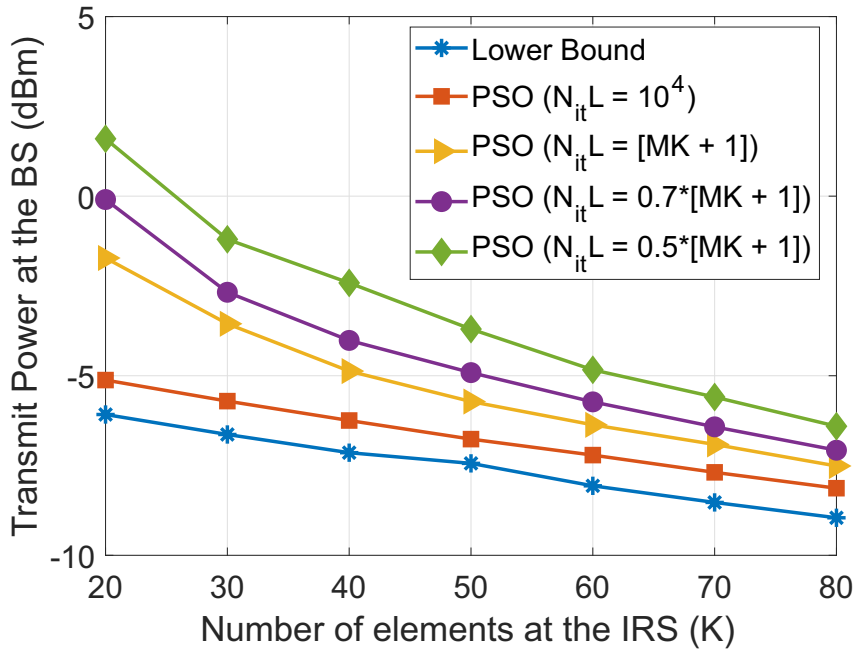

Figure 4.6 – Training overhead analysis $d = 50$ m.

4.3 NOVEL APPROACH CONSIDERING DISCRETE PHASES AT THE IRS

In the previous section, the beamforming design problem is evaluated considering continuous phase shifts at the IRS, which are practically difficult to achieve for an IRS with a large number of passive elements, due to the high cost of manufacturing each reflecting element with high-resolution phase shifts to yield (quasi) continuous phases. To overcome this problem, in this section, two different approaches considering finite-resolution discrete phase shifts at the IRS are proposed and presented in detail. The main goal of the proposed approaches is to maximize the user achievable rate subject to a maximum transmit power constraint. In addition, in this section, the effect of the S-CSI knowledge in the system performance is evaluated and new solutions based on GA are presented. In the rest of this section, the proposed approaches and their simulation results are described.

4.3.1 System Model

In this approach, the same IRS-assisted wireless communication system presented in Figure 4.1 and described in Section 4.2.1 is evaluated. However, different from the approach in the previous section, where continuous phase shifts at the IRS are considered, here, discrete phase shifts at the IRS are assumed in the beamforming design problem. Thus, the set of all possible discrete phases is given by

$$\theta_k \in \mathcal{T} = \left\{ 0, \frac{2\pi}{T}, \ldots, \frac{2\pi(T-1)}{T} \right\} \tag{4.8}$$

where $T = 2^b$, and b denotes the number of bits per each element at the IRS. Moreover, for the sake of simplicity and in accordance to [19, 71], it is considered $[\xi]_k = 1$ for $(k = 1, \ldots, K)$, *i.e.*, maximum signal reflection for each element of the IRS.

Furthermore, as previously mentioned, in this section, two different approaches are presented. First, none CSI prior knowledge is considered in the optimization process and, second, only the knowledge of S-CSI is evaluated. The S-CSI is defined by the deterministic LoS components of the channels $(\mathbf{G}^{\mathrm{LoS}}, \mathbf{h}_{\mathrm{d}}^{\mathrm{LoS}}, \mathbf{h}_{\mathrm{r}}^{\mathrm{LoS}})$. Since, low-mobility users are assumed, the S-CSI changes slowly. In addition, different from the previous section, where the LoS components are given by a complex Gaussian random variable with zero mean and unit variance, here, in order to improve the system model, the LoS components of all links are expressed by the antenna array responses at the IRS and at the BS which are dependent on the array geometry [85]. In this approach, both the IRS and the BS are equipped with an ULA as in [85, 91][1], thus the LoS components of the BS-IRS, BS-UE and IRS-UE links are given by

$$\mathbf{G}^{\mathrm{LoS}} = \mathbf{a}_{\mathrm{IRS}}^{\mathrm{H}}(\phi_{\mathrm{AoA}})\mathbf{a}_{\mathrm{BS}}(\phi_{\mathrm{AoD}}), \tag{4.9}$$

$$\mathbf{h}_{\mathrm{d}}^{\mathrm{LoS}} = \mathbf{a}_{\mathrm{BS}}(\varphi_{\mathrm{AoD}}), \tag{4.10}$$

$$\mathbf{h}_{\mathrm{r}}^{\mathrm{LoS}} = \mathbf{a}_{\mathrm{IRS}}(\psi_{\mathrm{AoD}}), \tag{4.11}$$

[1] Although it is considered an ULA at the IRS, the proposed solution can be easily extended for scenarios with an UPA at the IRS.

where ϕ^{AoA} is the AoA to the ULA at the IRS from the BS, ϕ^{AoD} is the AoD from the ULA at the BS towards the IRS, while φ^{AoD} and ψ^{AoD} are the AoD from the ULA at the BS and at the IRS towards the UE, respectively. In addition, the ULA responses at the IRS and BS are given by

$$\mathbf{a}_{\mathrm{IRS}}(\vartheta) = \frac{1}{K}\left[1, \mathrm{e}^{j\pi\cos(\vartheta)}, \ldots, \mathrm{e}^{j\pi(K-1)\cos(\vartheta)}\right], \tag{4.12}$$

$$\mathbf{a}_{\mathrm{BS}}(\vartheta) = \frac{1}{M}\left[1, \mathrm{e}^{j\pi\cos(\vartheta)}, \ldots, \mathrm{e}^{j\pi(M-1)\cos(\vartheta)}\right], \tag{4.13}$$

where we consider that the distance between the array elements is $\lambda/2$.

4.3.1.1 Optimization Problem

The main goal of the proposed approaches is to maximize the achievable rate at the UE by jointly optimizing the beamforming at the BS and the phase shifts at the IRS considering a maximum transmit power constraint. This non-convex optimization problem can be formulated as

$$\begin{aligned} \underset{\mathbf{w},\boldsymbol{\theta}}{\text{Maximize}} \quad & R = \log_2(1+\Gamma) \\ \text{Subject to} \quad & ||\mathbf{w}||^2 \leq P_{\mathrm{T}}, \\ & [\theta]_k \in \mathcal{T},\ k = 1, \ldots, K. \end{aligned} \tag{4.14}$$

where P_{T} is the transmit power at the BS. In this optimization problem, it is important to underline that although the constraints are convex the optimization problem is non-convex due to the fact that the beamforming at the BS and IRS are coupled. Thus, there is not a standard method to solve it. Therefore, a novel solution based on GA is proposed and described next.

It is important to note that the optimization problem in (4.14) is a discrete problem and although the proposed PSO presented in Section 4.2 achieves a close-to-optimum performance, PSO is suited to continuous optimization problems. Moreover, PSO needs to be deeply modified to solve discrete optimization problems and usually does not present a great performance for complex problems of such kind. On the other hand, GA is discrete by nature, *i.e.*, it is preferable to use GA to solve discrete optimization problems. Therefore, a solution based on GA is more suited to solve

the optimization problem in (4.14). In addition, it is important to underline that as Meta-heuristic techniques are generic they present the same efficiency for different performance metrics.

4.3.2 Proposed Solution

In this section the new proposed method based on GA to solve (4.14) is described. Two different approaches are followed. First, the CSI knowledge at the IRS and at the BS are not considered. Then, the knowledge of the S-CSI at the BS is exploited. These approaches are explained in more details in the following.

4.3.2.1 Beamforming without CSI

In this section, a new method based on GA to solve (4.14) without any prior CSI knowledge at the BS or at the IRS is presented. In this scenario, the beamforming vectors at the BS and IRS to be tested are defined at the BS, while the IRS beamformings are sent by the BS to the controller shown in Figure 4.1. Then, for each beamforming pair, the feedback of the SNR at the UE is received at the BS, and the current beamforming pair is evaluated based on (4.6). This process is performed for all pairs. In addition, in order to speed up convergence of the proposed solution and to reduce the overhead, since it is assumed a limited mobility scenario, in the process of generating the first population of the proposed method, it is considered the knowledge of the best pair of beamformings computed in the previous channel realization. Note that, in this approach, the BS/IRS/UE channels are not explicitly estimated. Therefore, it is not required one RF chain at each IRS element and any explicit channel estimation process is needed. The proposed method is summarized in **Algorithm 4.2** and its steps are detailed next.

1. Randomly generate $(L-1)$ pairs of beamforming (individuals) and generate the first population. The first population is formed by the $(L-1)$ pairs of beamforming randomly generated, and the best beamforming pair from the previous channel realization[2].

[2] In the first initialization there is no previous beamforming to be used, and therefore L individuals should be randomly generated.

2. Compute the fitness of each individual defined by (4.6), where the SNR at UE is given in (4.5).

3. Select the N_{f} fittest individuals $\Big(\mathbf{w}_f, \theta_f \mid f = 1, \ldots, N_{\mathrm{f}}\Big)$, which are perpetuated for the next generation.

4. **Selection Process:** By the *Tournament Method*, select $(L - N_{\mathrm{f}})/2$ parents from the current generation.

5. **Crossover Operator:** With crossover probability p_{c}, generate $(L - N_{\mathrm{f}})/2$ children from the crossing of the selected parents. Otherwise, with probability $1 - p_{\mathrm{c}}$, the children are the same as the selected parents. The generated individuals are stored in $\Big(\mathbf{w}_c, \theta_c \mid c = 1, \ldots, (L - N_{\mathrm{f}})/2\Big)$.

6. **Mutation Operator:** With mutation probability p_{mut}, select the fittest individual. Otherwise, with probability $1 - p_{\mathrm{mut}}$, randomly select a child generated in Step 5. In either case, submit the selected individual to the Real Random Mutation Operator with probability p_{mut}. This step must be run $(L - N_{\mathrm{f}})/2$ times and the following individuals are generated $\Big(\mathbf{w}_p, \theta_p \mid p = 1, \ldots, (L - N_{\mathrm{f}})/2\Big)$.

7. The population of the next generation is formed by the union of the individuals generated in Steps 3, 5, and 6, $\Big(\mathbf{w}_l, \theta_l = (\mathbf{w}_f, \theta_f), (\mathbf{w}_c, \theta_c), (\mathbf{w}_p, \theta_p) \mid l = 1, \ldots, L\Big)$.

8. Check if the stop criterion has been satisfied. In this work, it is considered the maximum number of iterations N_{it} (generations) as the stop criterion. If so, then return the fittest individual $(\mathrm{w}_{\mathrm{best}}, \theta_{\mathrm{best}})$. Otherwise, go to Step 2.

Algorithm 4.2: Proposed method based on GA for beamforming design without CSI.

Input : Number of antennas at the BS: M
Number of elements at the IRS: K
Size of the population: L
Maximum number of iterations: N_{it}
Mutation probabilities: p_{mut}
Crossover probability: p_{c}
Number of users in the elitism process: N_{f}

Output : $\mathbf{w}_{\text{best}}$, θ_{best}

for $g = 1 : N_{\text{it}}$ **do**
  if $(g = 1)$ **then**
    Generate de first population $\left(\text{w}_l, \theta_l \mid l = 1, \ldots, L\right)$;
  end
  Determine the fitness of each individual based on (4.14).
  Determine the N_{f} fittest individuals defined as $\left(\mathbf{w}_f, \theta_f \mid f = 1, \ldots, N_{\text{f}}\right)$.
  Select $(L - N_{\text{f}})/2$ parents by the Tournament Method.
  for $k = 1 : (L - N_{\text{f}})/2$ **do**
    if $p_{\text{c}} < rand()$ **then**
      Generate two new children by the Discrete Crossover Operator.
    else
      The parents selected by the Tournament Method are kept for the next generation.
    end
  end
  The individuals generated by the *Crossover Operator* are given by $\left(\mathbf{w}_c, \theta_c \mid c = 1, \ldots, (L - N_{\text{f}})/2\right)$;
  for $k = 1 : (L - N_{\text{f}})/2$ **do**
    if $(p_{\text{mut}} < \text{rand}())$ **then**
      Select the fittest individual $(\mathbf{w}_{\text{fittest}}, \theta_{\text{fittest}})$.
      if $(p_{\text{mut}} < \text{rand}())$ **then**
        Submit the fittest individual to the Real Mutation Operator.
      else
        The fittest individual is kept without changes for the next generation.
      end
    else
      Randomly select a child $\left(\mathbf{w}_c, \theta_c \mid c = 1, \ldots, (L - N_{\text{f}})/2\right)$.
      if $(p_{\text{mut}} < \text{rand}())$ **then**
        Submit the selected child to the Real Mutation Operator.
      else
        The selected child is kept without changes for the next generation.
      end
    end
  end
  The individuals generated by the *Mutation Operator* are given by $\left(\mathbf{w}_p, \theta_p \mid p = 1, \ldots, (L - N_{\text{f}})/2\right)$;
  Determine the new population:
  $\mathbf{w} = [\mathbf{w}_f, \mathbf{w}_c, \mathbf{w}_p]$, $\theta = [\theta_f, \theta_c, \theta_p]$.
end
Determine $\mathbf{w}_{\text{best}}$ and θ_{best} according to (4.14).
return $\text{w}_{\text{best}}, \theta_{\text{best}}$

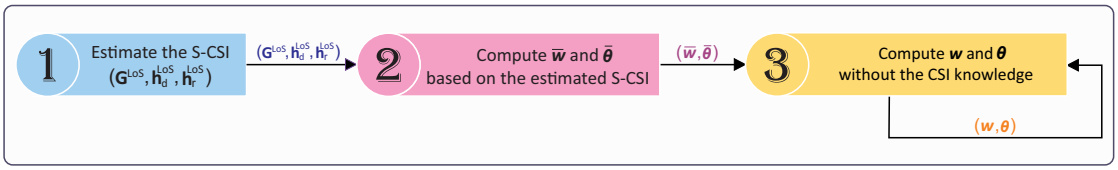

Figure 4.7 – Diagram of the proposed solution.

4.3.2.2 Beamforming with S-CSI

In this case, the S-CSI is exploited during the beamforming design process. The proposed solution is divided into three phases, as illustrated in Figure 4.7. In the first phase, S-CSI is acquired using standard estimation techniques [92, 93] and fedback to the BS[3]. In the second phase, the pairs of beamforming vectors at the BS and IRS to be tested are defined at the BS and the best beamforming pair is computed considering only the S-CSI. To finish, in the third phase, the best beamforming pair computed in the second phase and the best beamforming pair computed in the previous channel realizations are exploited as an initial position of the proposed method. In order to improve the understanding about the proposed approach, these main phases are described next.

1. **Estimate the S-CSI**: In this phase, it is considered that the IRS is in the sensing mode and the S-CSI of all links $\left(\mathbf{G}^{\text{LoS}}, \mathbf{h}_{\text{d}}^{\text{LoS}}, \mathbf{h}_{\text{r}}^{\text{LoS}}\right)$ can be estimated by considering dedicated sensors/receiving circuits at the IRS and using standard estimation techniques [92, 93].

2. **Compute $\overline{\mathbf{w}}$ and $\overline{\theta}$**: Based on the estimated S-CSI, in this phase **Algorithm** 4.3 is considered to compute $\overline{\mathbf{w}}$ and $\overline{\theta}$. To better explain the operation of **Algorithm** 4.3, its main steps are detailed next.

    I. Randomly generate L beamforming vectors at the IRS $\left(\overline{\theta}_l,\ l = 1, \ldots, L\right)$. For each $\overline{\theta}_l$, compute the Maximum-Ratio Transmission (MRT) beamform-

[3] The acquisition of the S-CSI is left for future work. Here the focus is to analyse the influence of the S-CSI knowledge on the optimization problem.

ing vector [94] given by,

$$\overline{w}_l = \frac{\sqrt{P_{\mathrm{t}}}\left[\left(\mathbf{h}_{\mathrm{r}}^{\mathrm{LoS}}\right)^{\mathrm{H}}\Theta\mathbf{G}^{\mathrm{LoS}} + \left(\mathbf{h}_{\mathrm{d}}^{\mathrm{LoS}}\right)^{\mathrm{H}}\right]^{\mathrm{H}}}{\left\|\left(\mathbf{h}_{\mathrm{r}}^{\mathrm{LoS}}\right)^{\mathrm{H}}\Theta\mathbf{G}^{\mathrm{LoS}} + \left(\mathbf{h}_{\mathrm{d}}^{\mathrm{LoS}}\right)^{\mathrm{H}}\right\|}. \tag{4.15}$$

It is important to highlight that, for a given $\overline{\theta}_l$, $\overline{w}_l$ is the optimal transmit beamforming at the BS considering only the S-CSI. Here, each individual in the proposed GA is defined as a beamforming vector at the IRS $\left(\overline{\theta}\right)$.

II. Calculate the fitness defined by (4.6) of each individual, where the SNR at the UE is given by

$$\mathrm{SNR} = \frac{\left|\left(\mathbf{h}_{\mathrm{r}}^{\mathrm{H}}\Theta\mathbf{G}^{\mathrm{LoS}} + \mathbf{h}_{\mathrm{d}}^{\mathrm{H}}\right)\overline{\mathbf{w}}\right|^2}{\sigma^2}, \tag{4.16}$$

where $\Theta = \mathrm{diag}\left(\mathrm{e}^{j[\overline{\theta}]_1}, \ldots, \mathrm{e}^{j[\overline{\theta}]_K}\right)$.

III. Select the N_{f} fittest individuals $\left(\overline{\theta}_f \mid f = 1, \ldots, N_{\mathrm{f}}\right)$, which are perpetuated for the next generation.

IV. By the *Tournament Method*, select $(L - N_{\mathrm{f}})$ parents from the current generation.

V. With crossover probability p_{c}, generate $(L - N_{\mathrm{f}})$ children from the crossing of the selected parents. Otherwise, with probability $1 - p_{\mathrm{c}}$, the children are the same as the selected parents. The following individuals are generated $\left(\overline{\theta}_c \mid c = 1, \ldots, L - N_{\mathrm{f}}\right)$.

VI. With mutation probability p_{mut} select one children generated in Step V and submit it to the Real Random Mutation Operator. Otherwise, the selected children is perpetuated for the next generation. This step is run $(L - N_{\mathrm{f}})$ times. The following individuals are generated $\left(\overline{\theta}_p \mid p = 1, \ldots, L - N_{\mathrm{f}}\right)$.

VII. The population of the next generation is formed by the union of the individuals generated in Steps III and VI $\left[\overline{\theta}_f, \overline{\theta}_p\right]$. In other words, the L beamforming vectors, $\left(\overline{\theta}_l,\ l = 1, \ldots, L\right)$, are updated.

VIII. Check if the stop criterion has been satisfied. In this work, the stop criterion is defined as the maximum number of iterations N_{it} (generations). If so, then return the fittest individual. Otherwise, go to Step II.

Note that, comparing **Algorithm 4.2** and **Algorithm 4.3**, there is a difference in the way that a new population is generated in each generation. In **Algorithm 4.3** the new population (Step VII) is generated following the basic principles of GAs [34]. However, in **Algorithm 4.2**, some modifications are proposed in the Mutation Operator (Step 6) and consequently in the generation of a new population (Step 7). These modifications were made after extensive tests for obtaining maximum performance.

3. **Compute w and** θ: As illustrated in Figure 4.7, this phase is similar to the approach without CSI described in the Subsection 4.3.2.1. The **Algorithm 4.2** is applied in this phase with the following modification in the generation of the first population (Step 1 in **Algorithm 4.2**):

   - In this phase, the first population is generated by the following individuals: (*i*) $(L-2)$ pairs of beamforming (individuals) randomly generated; (*ii*) The beamforming pair generated in the first phase $(\overline{\mathbf{w}}, \overline{\theta})$ considering S-CSI; and (*iii*) The best beamforming pair from the previous channel realization $(\mathbf{w}, \theta)$.

   The other steps remain the same. It is important to note that the proposed solution exploits the S-CSI knowledge as an initial point of the beamforming search in order to improve its convergence. With this approach, as will be shown next, it is possible to achieve a close-to-optimal solution with reasonable overhead.

Algorithm 4.3: Proposed method based on GA exploiting S-CSI.

Input : Number of antennas at the BS: M
Number of elements at the IRS: K
Size of the population: L
Maximum number of iterations: N_{it}
Mutation probability: p_{mut}
Crossover probability: p_{c}
Number of users in the elitism process: N_{f}

Output : $\overline{\mathbf{w}}_{\mathrm{best}}$, $\overline{\theta}_{\mathrm{best}}$

Randomly initialize the first population: $(\overline{\theta}_l \mid l = 1, \ldots, L)$.
For each $\overline{\theta}_l$, compute $\overline{\mathbf{w}}_l$ based on (4.15).
for $g = 1 : N_{\mathrm{it}}$ **do**
    Determine the fitness of each individual based on (4.14).
    Determine the N_{f} fittest individuals defined as $(\overline{\theta}_f \mid f = 1, \ldots, N_{\mathrm{f}})$.
    Select $(L - N_{\mathrm{f}})$ parents by the Tournament Method.
    for $k = 1 : (L - N_{\mathrm{f}})$ **do**
        if $p_{\mathrm{c}} < rand()$ **then**
            Generate two new children by the Discrete Crossover Operator.
        else
            The parents selected by the Tournament Method are kept for the next generation.
        end
    end
    The individuals generated by the *Crossover Operator* are defined as $(\overline{\theta}_c \mid c = 1, \ldots, L - N_{\mathrm{f}})$.
    for $k = 1 : (L - N_{\mathrm{f}})$ **do**
        if $p_{\mathrm{mut}} < \mathrm{rand}()$ **then**
            Submit the child $([\overline{\theta}_c]_k)$to the Real Mutation Operator.
        else
            The child is kept without changes for the next generation.
        end
    end
    The individuals generated by the *Mutation Operator* are defined as $(\overline{\theta}_p \mid p = 1, \ldots, L - N_{\mathrm{f}})$.
    Determine the new population: $\overline{\theta} = [\overline{\theta}_f, \overline{\theta}_p]$.
end
Determine $\overline{\theta}_{\mathrm{best}}$, the fittest individual, according to (4.14).
Compute $\overline{\mathbf{w}}_{\mathrm{best}}$ based on (4.15) for $\overline{\theta}_{\mathrm{best}}$.
return $\overline{w}_{\mathrm{best}}$, $\overline{\boldsymbol{w}}_{\mathrm{best}}$

4.3.3 Simulation Results

In order to show the performance of the proposed solution, this subsection presents the simulation results obtained considering the simulation setup presented in Figure 4.2, where d is the BS-UE distance. Therefore, the BS-UE and IRS-UE link distances are $d_1 = \sqrt{d^2 + d_{\mathrm{v}}^2}$ and $d_2 = \sqrt{(d_{\mathrm{h}} - d)^2 + d_{\mathrm{v}}^2}$, respectively. The simulation parameters considered in this section are described in Table 4.1, unless specified otherwise, and all curves present the average of 10^3 different realizations. It is important to highlight, that the GA parameters were defined after extensive simulations. Numerical results are shown for three beamforming solutions: (*i*) *Upper Bound*, the optimal beamforming using continuous phase shifts at the IRS and optimal beamforming at the BS. This benchmark is obtained from solving the optimization problem in ([95], Eq. 12) using CVX [96], and the resulting achievable rate is an upper bound for the optimization problem in (4.14); (*ii*) *GA - without CSI*, the proposed solution in Subsection 4.3.2.1, which does not consider any CSI knowledge; (*iii*) *GA - with S-CSI*, the proposed solution presented in Subsection 4.3.2.2, exploiting the S-CSI knowledge.

Table 4.1 – Simulation parameters.

Parameter	**Value**
M	10
N_{it}	10^3
N_{f}	2
N_{tourn}	2
p_{mut}	8%
p_{c}	90%
d_{v} [19]	2 m
d_{h} [19]	50 m
$\beta = \beta_{\mathrm{BU}} = \beta_{\mathrm{IU}}$	1
α_{BU} [19]	3.5
α_{BI} [19]	2.0
α_{IU} [19]	2.8
C_0 [19]	-30 dBm
σ^2 [19]	-80 dBm

4.3.3.1 Number of Phase Bits

First of all, in this section, it was considered a more practical scenario with discrete phase shifts at each reflecting element at the IRS. Due to the large number of elements at the IRS, it is important to achieve a close-to-optimal performance with a small number of controlling bits b [82]. Therefore, Figure 4.8 presents the convergence of the proposed solutions for different values of b. From the results, it can be verified that it is possible to achieve a close-to-optimal performance with only $b = 3$ bits when the S-CSI knowledge (Figure 4.8a) is considered. In addition, as the ideal continuous phase shifts are not energy efficient and are difficult to achieve due to hardware limitations. Therefore, it can be concluded that the proposed solution can be applied in practical scenarios with low-resolution phase shifts. In the rest of this subsection, all results are evaluated considering $b = 3$ bits.

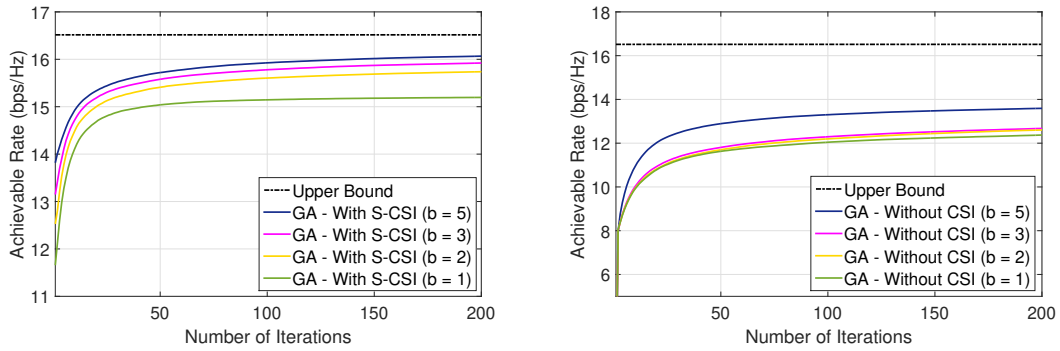

(a) (b)

Figure 4.8 – Analyse of the number of controlling bits at each element at the IRS with and without the S-CSI knowledge.

4.3.3.2 Influence of LoS and Topology

Figure 4.9 presents the convergence of the proposed solution with and without S-CSI considering $\beta \in \{1, 2\}$. From the results, it is possible to verify that the proposed solution considering S-CSI knowledge achieves a better performance with considerably fewer iterations (at least $\sim 95\%$ less iterations for the same achievable rate). Figure 4.10 compares the system achievable rate versus the BS-UE distance considering $K = 80$

reflecting elements at the IRS. From the results, it can be seen that the proposed solution achieves a close-to-optimal performance and the influence of the knowledge of the S-CSI increases when d increases.

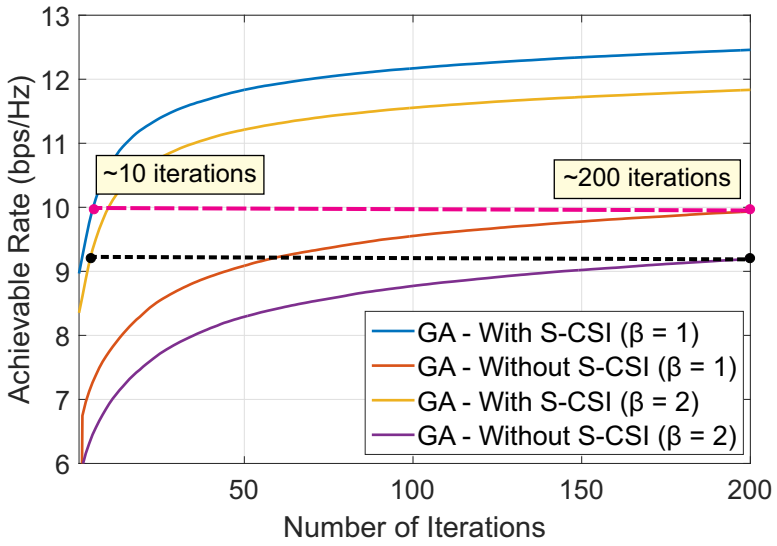

Figure 4.9 – Convergence of the proposed solution for $d = 40$ m, and $K = 80$.

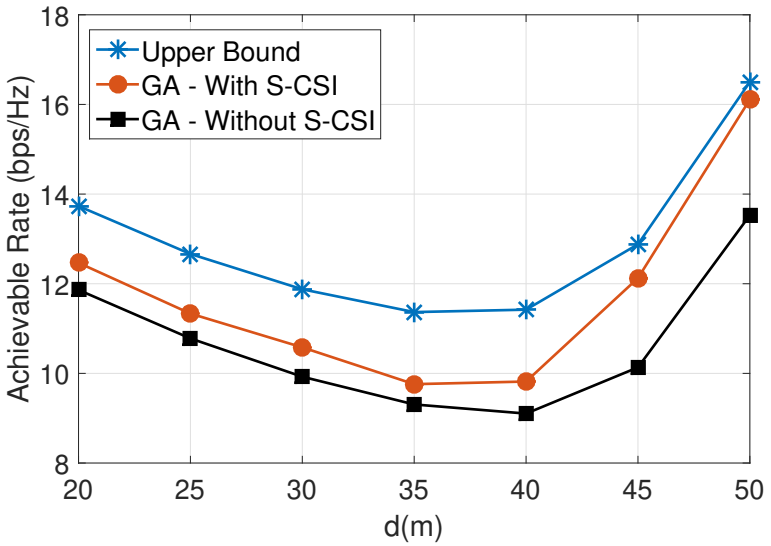

Figure 4.10 – Achievable Rate versus BS-UE distance for $K = 20$.

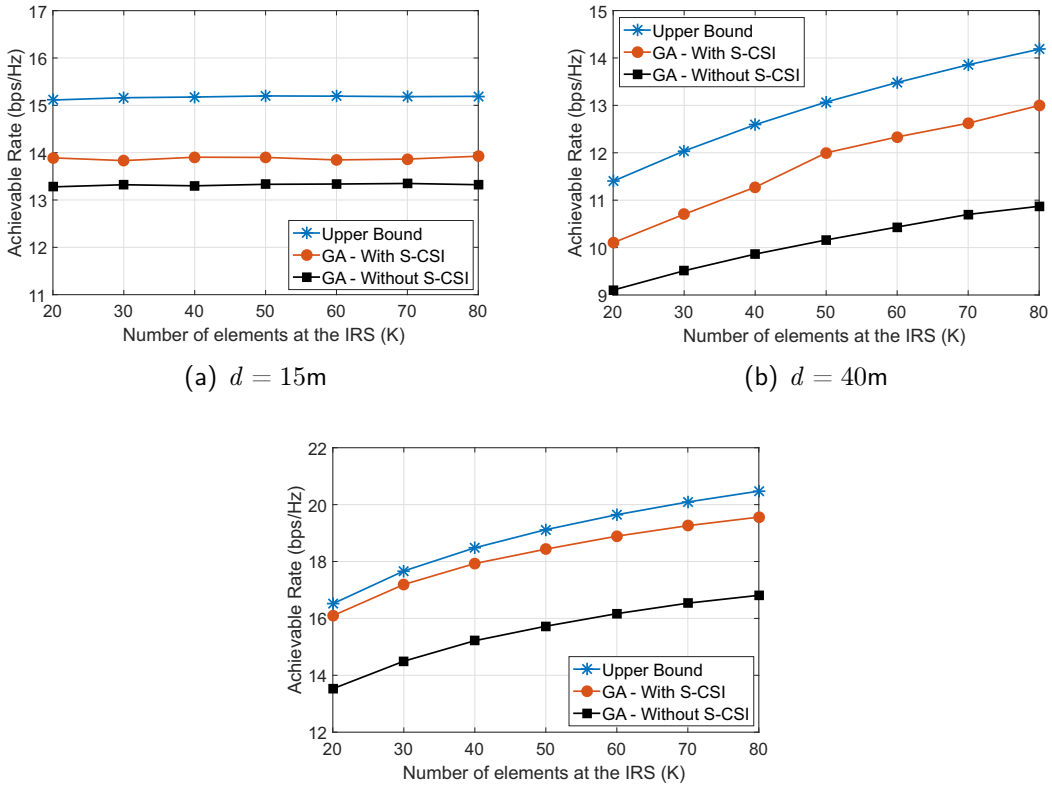

(a) $d = 15$m

(b) $d = 40$m

(c) $d = 50$m

Figure 4.11 – Transmit power at the BS versus the number of reflecting elements (K) at the IRS.

Figure 4.11 shows the achievable rate versus the number of reflecting elements at the IRS for $d \in \{15, 40, 50\}$ m. It can be seen, from the results, that: i) for $d = 15$ m in Figure 4.11a, in which the UE is close to the BS but far from the IRS, if increasing K, the achievable rate remains almost constant. This can be explained due to the fact that, as the UE is far from to the IRS, increasing K does not increase the achievable rate at the UE. In this case, the achievable rate is more dependent of the beamforming at the BS; (ii) for $d > 15$ m in Figures 4.11b and 4.11c when the UE is far from the BS, the achievable rate greatly increases with K; (iii) when the UE is close to the IRS, the proposed solution achieves a close-to-ideal performance with discrete phases at each IRS element and only a few number of controlling bits. In addition, from the results, it is possible to verify that the position of the UE has a considerable influence,

this can be related to the gain of the beamforming at the BS or at the IRS that the UE can exploit when it is close to the BS or IRS. This conclusion is ratified in Figure 4.10, where it is possible to note the importance of the UE position.

4.3.3.3 Amount of Feedback

It is important to measure the amount of feedback required from the user, which is given by $N_{\text{it}}L$ and adds some overhead to the system. It is very desirable that this amount of feedback is not larger than the number of pilots that would be required by a solution that explicitly estimates the channel, which is $(MK + 1)$ [90]. Therefore, Figure 4.12 presents the training overhead of the proposed solution in terms of the number of pilots that would be necessary to estimate the channel. The proposed solution, even when using only 30% of the training overhead that would be necessary to estimate the channel, besides do not requiring additional RF chains at the IRS elements, performs close to the upper bound. Moreover, it is important to emphasize that the upper bound considers continuous phases at the IRS and the proposed solution considers a more realistic scenario with discrete phases at the IRS elements. Therefore, it is possible to conclude that the proposed solution achieves a close-to-ideal performance with a reasonable amount of feedback from the user.

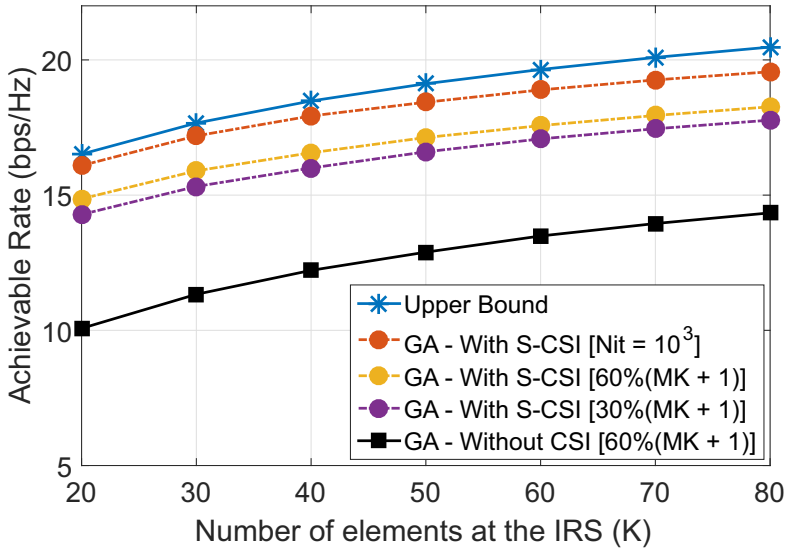

Figure 4.12 – Training overhead analysis $d = 50$ m and $M = 10$.

4.3.3.4 Imperfect S-CSI Knowledge

The previous results consider perfect S-CSI knowledge. Thus, in order to investigate the robustness of the proposed solution, next the following model for imperfect S-CSI knowledge [97] is considered, taking the BS-IRS link as an example:

$$\overline{\mathbf{G}}^{\mathrm{LoS}} = (\sqrt{1-\tau})\mathbf{G}^{\mathrm{LoS}} + (\sqrt{\tau})\mathbf{E}, \tag{4.17}$$

where $\mathbf{G}^{\mathrm{LoS}}$ is the LoS component of the BS-IRS link and $\overline{\mathbf{G}}^{\mathrm{LoS}}$ represents the imperfect estimation of the LoS component of the BS-IRS link, while $\mathbf{E}$ represents the estimation error, whose entries are i.i.d. zero mean circularly symmetric complex Gaussian random variables with zero mean and unit variance. Moreover, $\tau \in [0, 1]$ is the estimation accuracy, *i.e.*, if $\tau = 1$ there is no correlation between $\overline{\mathbf{G}}^{\mathrm{LoS}}$ and $\mathbf{G}^{\mathrm{LoS}}$, otherwise, if $\tau = 0$ there is perfect S-CSI estimation. In this work, it is considered that the imperfect estimation of the LoS components or all links (BS-UE and IRS-UE) are generated in the same way.

Figure 4.13 presents the convergence of the proposed solution for different values of τ considering the following schemes: (*i*) Proposed solution with perfect S-CSI; (*ii*) Proposed solution with imperfect S-CSI; and (*iii*) Proposed solution without any CSI. In all cases, it is considered $\beta = 1$, *i.e.*, both LoS and NLoS components present the same influence on all links. From the results, it is possible to verify that imperfect S-CSI knowledge degrades the performance, but the proposed solution with imperfect S-CSI still achieves a considerably better performance than in the case without S-CSI.

4.4 CONCLUSION

In this chapter, two different scenarios are considered. In the first, a new method based on PSO to minimize the transmit power at the BS by jointly optimizing the BS and IRS beamforming, with a minimum SNR constraint, is proposed. The solution achieves a close-to-ideal performance with a reasonable amount of feedback from the UE, allowing the use of IRS without the need of one RF chain per reflecting element, since CSI acquisition is not required, reducing cost and energy consumption. In the second, two different solutions based on GA are proposed to optimize the beamforming at the BS and IRS, with a maximum transmit power constraint and discrete phase shifts

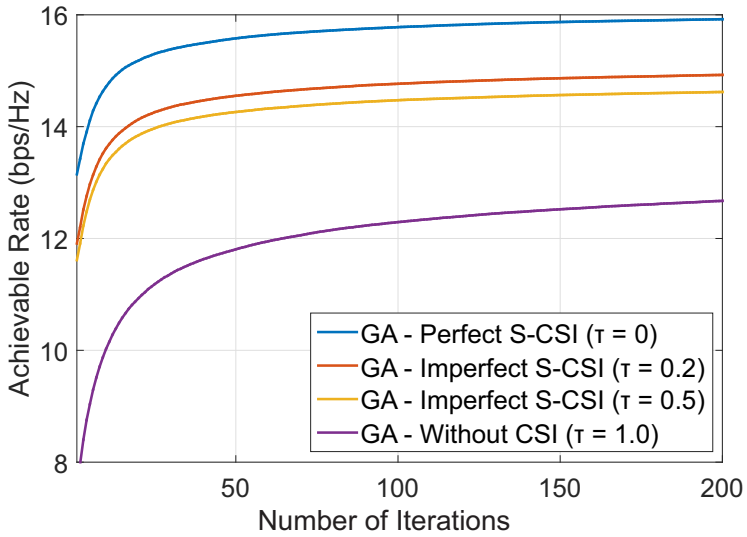

Figure 4.13 – Convergence of the proposed solution with perfect and imperfect S-CSI for $d = 50$ m, and $K = 20$.

at the IRS. First, a novel solution without any knowledge of the CSI at the BS/IRS is proposed, and a sub-optimum design of the beamforming at the BS and IRS is performed. Next, another solution to solve the beamforming problem only by exploiting the S-CSI knowledge is introduced. The novel solutions are evaluated considering different setups, and from the results it is possible to conclude that they achieve a close-to-ideal performance considering discrete phases with a few numbers of controlling bits at each element and with a reasonable amount of feedback from the UE. This shows that the proposed solutions are very attractive in practice.

Chapter 5

Conclusions

In this thesis, both the IA in mmWave systems and the beamforming design in IRS-assisted wireless systems are addressed. One of the main contributions of this thesis is to show that Evolutionary Computation can be successfully used to solve these relevant optimization problems in B5G wireless systems.

In Chapters 3 and 4, different B5G-emerging optimization problems have been presented and successfully solved using Evolutionary Computation. More specifically, in Chapter 3 a beam refinement method based on GA was proposed in order to reduce the delay of the directional search in the IA procedure in mmWave systems, considering scenarios with and without delay constraints. The proposed method was evaluated in different scenarios. The simulation results have shown that the proposed method presents an excellent performance when compared to the one in [23–25], and can reach the same results as ES. In addition, the proposed algorithm is generic, as it can be applied to different scenarios. The proposed algorithm can reduce the cellular search delay introduced by the use of beamforming at the BS and UE.

Moreover, in Chapter 4, the deployment of IRSs in a wireless system was studied and some different approaches were evaluated. First, a new method based on PSO was implemented in order to minimize the transmit power at the BS by jointly optimizing the BS and IRS beamforming considering continuous phases at the IRS elements, with a minimum SNR constraint for the UE. The proposed solution achieved a close-to-ideal performance with a reasonable amount of feedback from the UE, allowing the use of IRS without the need of one RF chain per reflecting element, since CSI acquisition is

not required, reducing cost and energy consumption. Second, a more realistic scenario was evaluated, with discrete phase shifts at the IRS. Then, two different solutions were proposed. First, a method based on GA, that does not consider any knowledge of the CSI at the BS, was proposed. A sub-optimum design of the beamforming at the BS and IRS, considering discrete phase shifts at the IRS, was presented. Next, another solution based on GA was proposed in order to solve the beamforming problem by exploiting the S-CSI knowledge only. The novel solutions were evaluated considering different setups, and, from the results, it can be concluded that they achieved a great performance considering discrete phases with a few number of controlling bits at each element and with a reasonable amount of feedback from the UE. Therefore, the proposed solutions are very attractive in practice and they can be applied to low-mobility LoS and NLoS scenarios.

From the results presented in this thesis, it is possible to confirm the efficiency of the Evolutionary Computation techniques in solving non-convex emerging optimization problems related to B5G wireless systems.

5.1 FUTURE WORKS

This thesis showed that Evolutionary Computation can be successfully used to solve the IA problem in mmWave communications and the beamforming design in an IRS-assisted wireless system. However, some practical scenarios, parameters optimization, and other emerging optimization problems are not investigated and are left for the future due to the lack of time.

This thesis has been mainly focused on the Computation Evolutionary, leaving the study of other methods in the Artificial Intelligence area as potential future works. Moreover, the development of B5G wireless systems is in its infancy, thus there are many challenges to overcome and, consequently, many emerging open problems [98–100] that could be effectively solved using these techniques. Therefore, the following future works can be addressed:

- With respect to IA in mmWave communications:
  - It would be interesting to extend the proposed scenario considering multiple mobile systems. This extension would considerably increase the complexity

of the optimization problem and it is a more practical problem. In addition, the use of different multiple access techniques could be evaluated in order to improve the system rate [101–103].

- This thesis has considered analog beamforming at the BS and UE and DFT-codebooks at the BS and UE. However, it could be interesting to investigate how to design an optimum codebook for the BS and UE. In addition, the performance of the digital and hybrid beamforming at the BS and UE could be investigated and the energy consumption evaluated [103–106].

- Regarding IRS-assisted wireless systems:

  - An interesting extension is to analyze a more practical scenario considering multiple UEs and BSs assisted by multiple IRSs and to solve the beamforming design problem for this scenario [107, 108]. This extension increases considerably the complexity of the optimization problem. In addition, in order to improve the system performance, the use of different clustering and multiple access techniques could be investigated [109–111]. To the best of the author's knowledge, there is no work in the literature that considers such broad scenario.
  - It would be very relevant to investigate the employment of IRSs in a mmWave wireless system [112–114]. The beam search problem could be solved using Evolutionary Computation and the obtained results could be compared with those in Chapter 3.
  - The IRSs are considered an revolutionizing technology that is able to significantly improve the performance of wireless networks, to achieve the stringent requirements of the B5G wireless systems, and consequently to enable the deployment of demanding applications. For instance, the study of the employment of IRSs to enable the Internet of Things (IoT) [115] is a relevant future work.

- Finally, as mentioned in Chapter 1, in this thesis, the detailed optimization of the parameters involved in PSO and GA has not been done, and therefore it could be carried out as a future work.

BIBLIOGRAPHY

[1] S. Yong and C. Chong. "An Overview of Multigigabit Wireless through Millimeter Wave Technology: Potentials and Technical Challenges". In: *EURASIP Journal on Wireless Communications and Networking* 2007.1 (Dec. 2006), p. 078907. ISSN: 1687-1499. DOI: 10.1155/2007/78907. Available from: https://doi.org/10.1155/2007/78907.

[2] Z. Pi and F. Khan. "An introduction to millimeter-wave mobile broadband systems". In: *IEEE Communications Magazine* 49.6 (June 2011), pp. 101–107. ISSN: 0163-6804. DOI: 10.1109/MCOM.2011.5783993.

[3] S. Sun, G. R. MacCartney, M. K. Samimi, S. Nie, and T. S. Rappaport. "Millimeter wave multi-beam antenna combining for 5G cellular link improvement in New York City". In: *2014 IEEE International Conference on Communications (ICC)*. June 2014, pp. 5468–5473. DOI: 10.1109/ICC.2014.6884191.

[4] M. R. Akdeniz, Y. Liu, M. K. Samimi, S. Sun, S. Rangan, T. S. Rappaport, and E. Erkip. "Millimeter Wave Channel Modeling and Cellular Capacity Evaluation". In: *IEEE Journal on Selected Areas in Communications* 32.6 (June 2014), pp. 1164–1179. ISSN: 0733-8716. DOI: 10.1109/JSAC.2014.2328154.

[5] T. Bai and R. W. Heath. "Coverage and Rate Analysis for Millimeter-Wave Cellular Networks". In: 14.2 (Feb. 2015), pp. 1100–1114. ISSN: 1536-1276. DOI: 10.1109/TWC.2014.2364267.

[6] O. Özdogan and E. Björnson. "Deep Learning-based Phase Reconfiguration for Intelligent Reflecting Surfaces". In: *CoRR* (2020). arXiv: 2009.13988 [eess.SP]. Available from: https://arxiv.org/abs/2009.13988.

[7] Abdelrahman Taha, Muhammad Alrabeiah, and Ahmed Alkhateeb. "Enabling Large Intelligent Surfaces with Compressive Sensing and Deep Learning". In: (2019). arXiv: 1904.10136. Available from: http://arxiv.org/abs/1904.10136.

[8] C. Liaskos, S. Nie, A. Tsioliaridou, A. Pitsillides, S. Ioannidis, and I. Akyildiz. "A New Wireless Communication Paradigm through Software-Controlled Metasurfaces". In: *IEEE Communications Magazine* 56.9 (2018), pp. 162–169. DOI: 10.1109/MCOM.2018.1700659.

[9] Harsh Tataria, Mansoor Shafi, Andreas F. Molisch, Mischa Dohler, Henrik Sjöland, and Fredrik Tufvesson. *6G Wireless Systems: Vision, Requirements, Challenges, Insights, and Opportunities*. 2020. arXiv: 2008.03213 [eess.SP].

[10] Q. Wu and R. Zhang. "Beamforming Optimization for Intelligent Reflecting Surface with Discrete Phase Shifts". In: *ICASSP 2019 - 2019 IEEE International Conference on Acoustics, Speech and Signal Processing (ICASSP)*. 2019, pp. 7830–7833.

[11] Q. Wu and R. Zhang. "Towards Smart and Reconfigurable Environment: Intelligent Reflecting Surface Aided Wireless Network". In: (Nov. 2020), pp. 1–7. ISSN: 1558-1896. DOI: 10.1109/MCOM.001.1900107.

[12] C. Huang, A. Zappone, G. C. Alexandropoulos, M. Debbah, and C. Yuen. "Reconfigurable Intelligent Surfaces for Energy Efficiency in Wireless Com-

munication". In: 18.8 (Aug. 2019), pp. 4157–4170. ISSN: 1558-2248. DOI: 10.1109/TWC.2019.2922609.

[13] M. Di Renzo, A. Zappone, M. Debbah, M. -S. Alouini, C. Yuen, J. de Rosny, and S. Tretyakov. "Smart Radio Environments Empowered by Reconfigurable Intelligent Surfaces: How It Works, State of Research, and The Road Ahead". In: *IEEE Journal on Selected Areas in Communications* 38.11 (2020), pp. 2450–2525. DOI: 10.1109/JSAC.2020.3007211.

[14] M. Giordani, M. Mezzavilla, C. N. Barati, S. Rangan, and M. Zorzi. "Comparative analysis of initial access techniques in 5G mmWave cellular networks". In: *2016 Annual Conference on Information Science and Systems (CISS)*. Mar. 2016, pp. 268–273. DOI: 10.1109/CISS.2016.7460513.

[15] C. Jeong, J. Park, and H. Yu. "Random access in millimeter-wave beamforming cellular networks: issues and approaches". In: *IEEE Communications Magazine* 53.1 (Jan. 2015), pp. 180–185. ISSN: 0163-6804. DOI: 10.1109/MCOM.2015.7010532.

[16] J. G. Andrews, S. Buzzi, W. Choi, S. V. Hanly, A. Lozano, A. C. K. Soong, and J. C. Zhang. "What Will 5G Be?" In: *IEEE Journal on Selected Areas in Communications* 32.6 (June 2014), pp. 1065–1082. ISSN: 0733-8716. DOI: 10.1109/JSAC.2014.2328098.

[17] M. Giordani, M. Mezzavilla, and M. Zorzi. "Initial Access in 5G mmWave Cellular Networks". In: *IEEE Communications Magazine* 54.11 (Nov. 2016), pp. 40–47. ISSN: 0163-6804. DOI: 10.1109/MCOM.2016.1600193CM.

[18] Y. Yang, S. Zhang, and R. Zhang. "IRS-Enhanced OFDM: Power Allocation and Passive Array Optimization". In: *2019 IEEE Global Communications Conference (GLOBECOM)*. 2019, pp. 1–6.

[19] Q. Wu and R. Zhang. "Intelligent Reflecting Surface Enhanced Wireless Network via Joint Active and Passive Beamforming". In: 18.11 (Nov. 2019), pp. 5394–5409. ISSN: 1558-2248. DOI: 10.1109/TWC.2019.2936025.

[20] Chandan Pradhan, Ang Li, Lingyang Song, Branka Vucetic, and Yonghui Li. "Hybrid Precoding Design for Reconfigurable Intelligent Surface aided mmWave Communication Systems". In: *IEEE Wireless Communications Letters* (2020), pp. 1–1. ISSN: 2162-2345. DOI: 10.1109/lwc.2020.2980225. Available from: http://dx.doi.org/10.1109/lwc.2020.2980225.

[21] Q. Wu and R. Zhang. "Beamforming Optimization for Wireless Network Aided by Intelligent Reflecting Surface with Discrete Phase Shifts". In: (Dec. 2019), pp. 1–1. ISSN: 1558-0857. DOI: 10.1109/TCOMM.2019.2958916.

[22] Boya Di, Hongliang Zhang, Lingyang Song, Yonghui Li, Zhu Han, and H. Vincent Poor. *Hybrid Beamforming for Reconfigurable Intelligent Surface based Multi-user Communications: Achievable Rates with Limited Discrete Phase Shifts*. 2019. arXiv: 1910.14328 [cs.IT]. Available from: https://arxiv.org/abs/1910.14328.

[23] H. Guo, B. Makki, and T. Svensson. "A genetic algorithm-based beamforming approach for delay-constrained networks". In: *2017 15th International Symposium on Modeling and Optimization in Mobile, Ad Hoc, and Wireless Networks (WiOpt)*. May 2017, pp. 1–7. DOI: 10.23919/WIOPT.2017.7959905.

[24] H. Guo, B. Makki, and T. Svensson. "A comparison of beam refinement algorithms for millimeter wave initial access". In: *2017 IEEE 28th Annual International Symposium on Personal, Indoor, and Mobile Radio Communications (PIMRC)*. Oct. 2017, pp. 1–7. DOI: 10.1109/PIMRC.2017.8292686.

[25] J. Chen, H. Guo, B. Makki, and T. Svensson. "Genetic Algorithm-Based Beam Refinement for Initial Access in Millimeter Wave Mobile Networks". In: *Wireless*

Communications and Mobile Computing 2018 (2018), 10 pages. DOI: https://doi.org/10.1155/2018/5817120.

[26] Quoc-Viet Pham, Dinh C. Nguyen, Seyedali Mirjalili, Dinh Thai Hoang, Diep N. Nguyen, Pubudu N. Pathirana, and Won-Joo Hwang. *Swarm Intelligence for Next-Generation Wireless Networks: Recent Advances and Applications*. 2020. arXiv: 2007.15221 [cs.NI].

[27] S.N. Sivanandam and S. N. Deepa. *Introduction to Genetic Algorithms*. Vol. 1. Springer-Verlag Berlin Heidelberg, 2008.

[28] J. Qiao, X. Shen, J. W. Mark, and Y. He. "MAC-Layer Concurrent Beamforming Protocol for Indoor Millimeter-Wave Networks". In: *IEEE Transactions on Vehicular Technology* 64.1 (Jan. 2015), pp. 327–338. ISSN: 0018-9545. DOI: 10.1109/TVT.2014.2320830.

[29] S. Hur, T. Kim, D. J. Love, J. V. Krogmeier, T. A. Thomas, and A. Ghosh. "Multilevel millimeter wave beamforming for wireless backhaul". In: *2011 IEEE GLOBECOM Workshops (GC Wkshps)*. Dec. 2011, pp. 253–257. DOI: 10.1109/GLOCOMW.2011.6162448.

[30] L. Chen, Y. Yang, X. Chen, and W. Wang. "Multi-stage beamforming codebook for 60GHz WPAN". In: *2011 6th International ICST Conference on Communications and Networking in China (CHINACOM)*. Aug. 2011, pp. 361–365. DOI: 10.1109/ChinaCom.2011.6158179.

[31] X. Gao, L. Dai, C. Yuen, and Z. Wang. "Turbo-Like Beamforming Based on Tabu Search Algorithm for Millimeter-Wave Massive MIMO Systems". In: *IEEE Transactions on Vehicular Technology* 65.7 (July 2016), pp. 5731–5737. ISSN: 0018-9545. DOI: 10.1109/TVT.2015.2461440.

[32] A. K. Sangaiah, Z. Zhang, and M. Sheng. *Computational Intelligence for Multimedia Big Data on the Cloud with Engineering Applications*. Elsevier Science, 2018. ISBN: 978-0-12-813314-9.

[33] C. A. Darwin. *Origem das Especies*. Martin Claret, São Paulo, Brazil, 2005.

[34] D. R. Goldberg. *Genetic Algorithms in Search, Optimization, and Machine Learning*. Addison Wesley Longman Inc., New York, 1989.

[35] M. Mitchell. *An Introduction to Genetic Algorithms*. MIT Press, Cambridge, MA, USA, 1998.

[36] M. Gen and R. Cheng. *Genetic Algorithms and Engineering Optimization*. Vol. 1. John Wiley & Sons Inc, USA, 1999.

[37] J. Kennedy and R. Eberhart. "Particle swarm optimization". In: *Proceedings of ICNN'95 - International Conference on Neural Networks*. Vol. 4. Nov. 1995, 1942–1948 vol.4. DOI: 10.1109/ICNN.1995.488968.

[38] Russell Eberhart, Yuhui Shi, and James Kennedy. *Swarm Intelligence*. English (US). Morgan Kaufmann Publishers, 2001. ISBN: 9781493303588.

[39] J. Kennedy and R. Mendes. "Population structure and particle swarm performance". In: *Proceedings of the 2002 Congress on Evolutionary Computation. CEC'02 (Cat. No.02TH8600)*. Vol. 2. 2002, 1671–1676 vol.2. DOI: 10.1109/CEC.2002.1004493.

[40] J. Xiong, W. Wang, H. Shao, and H. Chen. "Frequency Diverse Array Transmit Beampattern Optimization With Genetic Algorithm". In: *IEEE Antennas and Wireless Propagation Letters* 16 (2017), pp. 469–472. ISSN: 1536-1225. DOI: 10.1109/LAWP.2016.2584078.

[41] C. Cui, W. T. Li, X. T. Ye, and X. W. Shi. "Hybrid Genetic Algorithm and Modified Iterative Fourier Transform Algorithm for Large Thinned Array Synthesis". In: *IEEE Antennas and Wireless Propagation Letters* 16 (2017), pp. 2150–2154. ISSN: 1536-1225. DOI: 10.1109/LAWP.2017.2700865.

[42] Y. Chang, X. Yuan, B. Li, D. Niyato, and N. Al-Dhahir. "A Joint Unsupervised Learning and Genetic Algorithm Approach for Topology Control in Energy-Efficient Ultra-Dense Wireless Sensor Networks". In: *IEEE Communications Letters* 22.11 (Nov. 2018), pp. 2370–2373. ISSN: 1089-7798. DOI: 10.1109/LCOMM.2018.2870886.

[43] J. A. Martins, A. Mazayev, N. Correia, G. Schütz, and A. Barradas. "GACN: Self-Clustering Genetic Algorithm for Constrained Networks". In: *IEEE Communications Letters* 21.3 (Mar. 2017), pp. 628–631. ISSN: 1089-7798. DOI: 10.1109/LCOMM.2016.2641420.

[44] A. Alkhateeb, Y. Nam, M. S. Rahman, J. Zhang, and R. W. Heath. "Initial Beam Association in Millimeter Wave Cellular Systems: Analysis and Design Insights". In: 16.5 (May 2017), pp. 2807–2821. ISSN: 1536-1276. DOI: 10.1109/TWC.2017.2666806.

[45] L. Wei, Q. Li, and G. Wu. "Exhaustive, Iterative and Hybrid Initial Access Techniques in mmWave Communications". In: *2017 IEEE Wireless Communications and Networking Conference (WCNC)*. Mar. 2017, pp. 1–6. DOI: 10.1109/WCNC.2017.7925666.

[46] C. Liu, M. Li, S. V. Hanly, I. B. Collings, and P. Whiting. "Millimeter Wave Beam Alignment: Large Deviations Analysis and Design Insights". In: *IEEE Journal on Selected Areas in Communications* 35.7 (July 2017), pp. 1619–1631. ISSN: 0733-8716. DOI: 10.1109/JSAC.2017.2699360.

[47] H. Soleimani, R. Parada, S. Tomasin, and M. Zorzi. "Statistical Approaches for Initial Access in mmWave 5G Systems". In: *CoRR* abs/1711.05456 (2017). arXiv: 1711.05456. Available from: http://arxiv.org/abs/1711.05456.

[48] C. Liu, M. Li, I. B. Collings, S. V. Hanly, and P. Whiting. "Design and Analysis of Transmit Beamforming for Millimeter Wave Base Station Discovery". In: *IEEE Transactions on Wireless Communications* 16.2 (Feb. 2017), pp. 797–811. ISSN: 1536-1276. DOI: 10.1109/TWC.2016.2630681.

[49] A. Abdelreheem, E. M. Mohamed, and H. Esmaiel. "Location-Based Millimeter Wave Multi-Level Beamforming Using Compressive Sensing". In: *IEEE Communications Letters* 22.1 (Jan. 2018), pp. 185–188. ISSN: 1089-7798. DOI: 10.1109/LCOMM.2017.2766629.

[50] A. Capone, I. Filippini, and V. Sciancalepore. "Context Information for Fast Cell Discovery in mm-wave 5G Networks". In: *Proceedings of European Wireless 2015; 21th European Wireless Conference*. May 2015, pp. 1–6.

[51] W. B. Abbas and M. Zorzi. "Context information based initial cell search for millimeter wave 5G cellular networks". In: *2016 European Conference on Networks and Communications (EuCNC)*. June 2016, pp. 111–116. DOI: 10.1109/EuCNC.2016.7561015.

[52] R. Parada and M. Zorzi. "Cell discovery based on historical user's location in mmWave 5G". In: *European Wireless 2017; 23th European Wireless Conference*. May 2017, pp. 1–6.

[53] I. Filippini, V. Sciancalepore, F. Devoti, and A. Capone. "Fast Cell Discovery in mm-Wave 5G Networks with Context Information". In: *IEEE Transactions on Mobile Computing* 17.7 (July 2018), pp. 1538–1552. ISSN: 1536-1233. DOI: 10.1109/TMC.2017.2772881.

[54] F. Devoti, I. Filippini, and A. Capone. "Facing the Millimeter-Wave Cell Discovery Challenge in 5G Networks With Context-Awareness". In: *IEEE Access* 4 (2016), pp. 8019–8034. ISSN: 2169-3536. DOI: 10.1109/ACCESS.2016.2628917.

[55] F. Devoti, I. Filippini, and A. Capone. "MM-wave Initial Access: A Context Information Overview". In: *IEEE 19th International Symposium on "A World of Wireless, Mobile and Multimedia Networks* (June 2018), pp. 1–9. ISSN: 0163-6804. DOI: 10.1109/WoWMoM.2018.8449790.

[56] Y. Chen, W. Cheng, and L. Wang. "Learning-assisted beam search for indoor mmWave networks". In: *2018 IEEE Wireless Communications and Networking Conference Workshops (WCNCW)*. Apr. 2018, pp. 320–325. DOI: 10.1109/WCNCW.2018.8369007.

[57] A. Alkhateeb, S. Alex, P. Varkey, Y. Li, Q. Qu, and D. Tujkovic. "Deep Learning Coordinated Beamforming for Highly-Mobile Millimeter Wave Systems". In: *IEEE Access* 6 (2018), pp. 37328–37348. ISSN: 2169-3536. DOI: 10.1109/ACCESS.2018.2850226.

[58] M. K. Samimi and T. S. Rappaport. "3-D statistical channel model for millimeter-wave outdoor mobile broadband communications". In: *2015 IEEE International Conference on Communications (ICC)*. June 2015, pp. 2430–2436. DOI: 10.1109/ICC.2015.7248689.

[59] Y. Zou, Q. Li, G. Yang, and X. Cheng. "Analog beamforming for millimeter-wave MIMO systems via stochastic optimization". In: *2016 8th International Conference on Wireless Communications Signal Processing (WCSP)*. Oct. 2016, pp. 1–5. DOI: 10.1109/WCSP.2016.7752743.

[60] J. Chen. "Hybrid Beamforming With Discrete Phase Shifters for Millimeter-Wave Massive MIMO Systems". In: *IEEE Transactions on Vehicular Technology* 66.8 (2017), pp. 7604–7608.

[61] M. Rebato, L. Resteghini, C. Mazzucco, and M. Zorzi. "Study of Realistic Antenna Patterns in 5G mmWave Cellular Scenarios". In: *2018 IEEE International Conference on Communications (ICC)*. May 2018, pp. 1–6. DOI: 10.1109/ICC.2018.8422746.

[62] L. Wan, X. Zhong, Y. Zheng, and S. Mei. "Adaptive codebook for limited feedback MIMO system". In: *2009 IFIP International Conference on Wireless and Optical Communications Networks*. Apr. 2009, pp. 1–5. DOI: 10.1109/WOCN.2009.5010525.

[63] C. Liu, M. Li, S. V. Hanly, P. Whiting, and I. B. Collings. "Millimeter-Wave Small Cells: Base Station Discovery, Beam Alignment, and System Design Challenges". In: *IEEE Wireless Communications* 25.4 (Aug. 2018), pp. 40–46. ISSN: 1536-1284. DOI: 10.1109/MWC.2018.1700392.

[64] S. Lien, S. Shieh, Y. Huang, B. Su, Y. Hsu, and H. Wei. "5G New Radio: Waveform, Frame Structure, Multiple Access, and Initial Access". In: *IEEE Communications Magazine* 55.6 (June 2017), pp. 64–71. ISSN: 0163-6804. DOI: 10.1109/MCOM.2017.1601107.

[65] M. Srinivas and L. M. Patnaik. "Adaptive probabilities of crossover and mutation in genetic algorithms". In: *IEEE Transactions on Systems, Man, and Cybernetics* 24.4 (Apr. 1994), pp. 656–667. ISSN: 0018-9472. DOI: 10.1109/21.286385.

[66] R. M. Ramos, R. R. Saldanha, R. H. C. Takahashi, and F. J. S. Moreira. "The real-biased multiobjective genetic algorithm and its application to the design of wire antennas". In: *IEEE Transactions on Magnetics* 39.3 (May 2003), pp. 1329–1332. ISSN: 0018-9464. DOI: 10.1109/TMAG.2003.810505.

[67] H. Tullberg, P. Popovski, Z. Li, M. A. Uusitalo, A. Hoglund, O. Bulakci, M. Fallgren, and J. F. Monserrat. "The METIS 5G System Concept: Meeting the 5G Requirements". In: 54.12 (Dec. 2016), pp. 132–139. ISSN: 0163-6804. DOI: 10.1109/MCOM.2016.1500799CM.

[68] M. Shafi, A. F. Molisch, P. J. Smith, T. Haustein, P. Zhu, P. De Silva, F. Tufvesson, A. Benjebbour, and G. Wunder. "5G: A Tutorial Overview of Standards, Trials, Challenges, Deployment, and Practice". In: 35.6 (June 2017), pp. 1201–1221. ISSN: 0733-8716. DOI: 10.1109/JSAC.2017.2692307.

[69] Q. Wu, S. Zhang, B. Zheng, C. You, and R. Zhang. "Intelligent Reflecting Surface Aided Wireless Communications: A Tutorial". In: *IEEE Transactions on Communications* (2021), pp. 1–1. DOI: 10.1109/TCOMM.2021.3051897.

[70] E. Björnson, Ö. Özdogan, and E. G. Larsson. "Reconfigurable Intelligent Surfaces: Three Myths and Two Critical Questions". In: *IEEE Communications Magazine* 58.12 (2020), pp. 90–96. DOI: 10.1109/MCOM.001.2000407.

[71] Q. Wu and R. Zhang. "Intelligent Reflecting Surface Enhanced Wireless Network: Joint Active and Passive Beamforming Design". In: *2018 IEEE Global Communications Conference (GLOBECOM)*. 2018, pp. 1–6. DOI: 10.1109/GLOCOM.2018.8647620.

[72] S. Abeywickrama, R. Zhang, Q. Wu, and C. Yuen. "Intelligent Reflecting Surface: Practical Phase Shift Model and Beamforming Optimization". In: *IEEE Transactions on Communications* 68.9 (2020), pp. 5849–5863. DOI: 10.1109/TCOMM.2020.3001125.

[73] H. Guo, Y. Liang, J. Chen, and E. G. Larsson. "Weighted Sum-Rate Maximization for Intelligent Reflecting Surface Enhanced Wireless Networks". In: *2019 IEEE Global Communications Conference (GLOBECOM)*. 2019, pp. 1–6. DOI: 10.1109/GLOBECOM38437.2019.9013288.

[74] B. Di, H. Zhang, L. Song, Y. Li, Z. Han, and H. V. Poor. "Hybrid Beamforming for Reconfigurable Intelligent Surface based Multi-User Communications: Achievable Rates With Limited Discrete Phase Shifts". In: *IEEE Journal on Selected Areas in Communications* 38.8 (2020), pp. 1809–1822. DOI: 10.1109/JSAC.2020.3000813.

[75] B. Zheng and R. Zhang. "Intelligent Reflecting Surface-Enhanced OFDM: Channel Estimation and Reflection Optimization". In: *IEEE Wireless Communications Letters* 9.4 (Dec. 2019), pp. 518–522.

[76] Minchae Jung, Walid Saad, and Gyuyeol Kong. "Performance Analysis of Large Intelligent Surfaces (LISs): Uplink Spectral Efficiency and Pilot Training". In: (2019). arXiv: 1904.00453. Available from: http://arxiv.org/abs/1904.00453.

[77] D. Mishra and H. Johansson. "Channel Estimation and Low-complexity Beamforming Design for Passive Intelligent Surface Assisted MISO Wireless Energy Transfer". In: *ICASSP 2019 - 2019 IEEE International Conference on Acoustics, Speech and Signal Processing (ICASSP)*. May 2019, pp. 4659–4663. DOI: 10.1109/ICASSP.2019.8683663.

[78] Z. He and X. Yuan. "Cascaded Channel Estimation for Large Intelligent Metasurface Assisted Massive MIMO". In: *IEEE Wireless Communications Letters* 9.2 (Feb. 2020), pp. 210–214. ISSN: 2162-2345. DOI: 10.1109/LWC.2019.2948632.

[79] H. Liu, X. Yuan, Y. Jun, and Zhang. *Matrix-Calibration-Based Cascaded Channel Estimation for Reconfigurable Intelligent Surface Assisted Multiuser MIMO*. 2019. arXiv: 1912.09025 [cs.IT]. Available from: https://arxiv.org/abs/1912.09025.

[80] T. L. Jensen and E. De Carvalho. "An Optimal Channel Estimation Scheme for Intelligent Reflecting Surfaces Based on a Minimum Variance Unbiased Estimator". In: *ICASSP 2020 - 2020 IEEE International Conference on Acoustics, Speech and Signal Processing (ICASSP)*. Apr. 2020, pp. 5000–5004.

[81] C. You, B. Zheng, and R. Zhang. *Intelligent Reflecting Surface with Discrete Phase Shifts: Channel Estimation and Passive Beamforming*. 2019. arXiv: 1911.03916 [cs.IT]. Available from: https://arxiv.org/abs/1911.03916.

[82] C. You, B. Zheng, and R. Zhang. "Channel Estimation and Passive Beamforming for Intelligent Reflecting Surface: Discrete Phase Shift and Progressive Refinement". In: *IEEE Journal on Selected Areas in Communications* 38.11 (2020), pp. 2604–2620. DOI: 10.1109/JSAC.2020.3007056.

[83] M.-M. Zhao, Q. Wu, M. -J. Zhao, and R. Zhang. "Intelligent Reflecting Surface Enhanced Wireless Network: Two-Timescale Beamforming Optimization". In: *IEEE Transactions on Wireless Communications* (2020), pp. 1–1. DOI: 10.1109/TWC.2020.3022297.

[84] M. Zhao, Q. Wu, M. Zhao, and R. Zhang. "Two-timescale Beamforming Optimization for Intelligent Reflecting Surface Enhanced Wireless Network". In: *2020 IEEE 11th Sensor Array and Multichannel Signal Processing Workshop (SAM)*. 2020, pp. 1–5. DOI: 10.1109/SAM48682.2020.9104346.

[85] Y. Han, W. Tang, S. Jin, C. Wen, and X. Ma. "Large Intelligent Surface-Assisted Wireless Communication Exploiting Statistical CSI". In: *IEEE Transactions on Vehicular Technology* 68.8 (2019), pp. 8238–8242. DOI: 10.1109/TVT.2019.2923997.

[86] Zhangjie Peng, Tianshu Li, Cunhua Pan, Hong Ren, Wei Xu, and Marco Di Renzo. *Analysis and Optimization for RIS-Aided Multi-Pair Communications Relying on Statistical CSI*. 2020. arXiv: 2007.11704 [eess.SP]. Available from: https://arxiv.org/abs/2007.11704.

[87] Yanyu Cheng, Kwok Hung Li, Yuanwei Liu, Kah Chan Teh, and H. Vincent Poor. "Downlink and Uplink Intelligent Reflecting Surface Aided Networks: NOMA and OMA". In: (2020). arXiv: 2005.00996 [eess.SP]. Available from: https://arxiv.org/abs/2005.00996.

[88] M. Zeng, X. Li, G. Li, W. Hao, and O. A. Dobre. "Sum Rate Maximization for IRS-Assisted Uplink NOMA". In: *IEEE Communications Letters* 25.1 (2021), pp. 234–238. DOI: 10.1109/LCOMM.2020.3025978.

[89] Z. Ding and H. Vincent Poor. "A Simple Design of IRS-NOMA Transmission". In: *IEEE Communications Letters* 24.5 (2020), pp. 1119–1123.

[90] A. Zappone, M. Di Renzo, F. Shams, X. Qian, and M. Debbah. "Overhead-Aware Design of Reconfigurable Intelligent Surfaces in Smart Radio Environments". In: *IEEE Transactions on Wireless Communications* 20.1 (2021), pp. 126–141. DOI: 10.1109/TWC.2020.3023578.

[91] Zhendong Li, Wen Chen, and Qingqing Wu. "Joint Beamforming Design and Power Splitting Optimization in IRS-Assisted SWIPT NOMA Networks". In: *CoRR* (2020). arXiv: 2011.14778 [cs.IT]. Available from: https://arxiv.org/abs/2011.14778.

[92] X. Mestre. "Improved Estimation of Eigenvalues and Eigenvectors of Covariance Matrices Using Their Sample Estimates". In: *IEEE Transactions on Information Theory* 54.11 (2008), pp. 5113–5129. DOI: 10.1109/TIT.2008.929938.

[93] K. Werner, M. Jansson, and P. Stoica. "On Estimation of Covariance Matrices With Kronecker Product Structure". In: *IEEE Transactions on Signal Processing* 56.2 (2008), pp. 478–491. DOI: 10.1109/TSP.2007.907834.

[94] T. K. Y. Lo. "Maximum ratio transmission". In: *IEEE Transactions on Communications* 47.10 (1999), pp. 1458–1461. DOI: 10.1109/26.795811.

[95] Q. Wu and R. Zhang. "Intelligent Reflecting Surface Enhanced Wireless Network: Joint Active and Passive Beamforming Design". In: *2018 IEEE Global Communications Conference (GLOBECOM)*. Dec. 2018, pp. 1–6. DOI: 10.1109/GLOCOM.2018.8647620.

[96] Michael Grant and Stephen Boyd. *CVX: Matlab software for disciplined convex programming, version 2.1*. 2014.

[97] B. Nosrat-Makouei, J. G. Andrews, and R. W. Heath. "MIMO Interference Alignment Over Correlated Channels With Imperfect CSI". In: *IEEE Transactions on Signal Processing* 59.6 (2011), pp. 2783–2794. DOI: 10.1109/TSP.2011.2124458.

[98] L. U. Khan, I. Yaqoob, M. Imran, Z. Han, and C. S. Hong. "6G Wireless Systems: A Vision, Architectural Elements, and Future Directions". In: *IEEE Access* 8 (2020), pp. 147029–147044. DOI: 10.1109/ACCESS.2020.3015289.

[99] L. Bariah, L. Mohjazi, S. Muhaidat, P. C. Sofotasios, G. K. Kurt, H. Yanikomeroglu, and O. A. Dobre. "A Prospective Look: Key Enabling Technologies, Applications and Open Research Topics in 6G Networks". In: *IEEE Access* 8 (2020), pp. 174792–174820. DOI: 10.1109/ACCESS.2020.3019590.

[100] M. Z. Chowdhury, M. Shahjalal, S. Ahmed, and Y. M. Jang. "6G Wireless Communication Systems: Applications, Requirements, Technologies, Challenges, and Research Directions". In: *IEEE Open Journal of the Communications Society* 1 (2020), pp. 957–975. DOI: 10.1109/OJCOMS.2020.3010270.

[101] L. Zhu, J. Zhang, Z. Xiao, X. Cao, D. O. Wu, and X. Xia. "Joint Tx-Rx Beamforming and Power Allocation for 5G Millimeter-Wave Non-Orthogonal Multiple Access Networks". In: *IEEE Transactions on Communications* 67.7 (2019), pp. 5114–5125. DOI: 10.1109/TCOMM.2019.2906589.

[102] L. Zhu, J. Zhang, Z. Xiao, X. Cao, D. O. Wu, and X. Xia. "Joint Power Control and Beamforming for Uplink Non-Orthogonal Multiple Access in 5G Millimeter-Wave Communications". In: *IEEE Transactions on Wireless Communications* 17.9 (2018), pp. 6177–6189. DOI: 10.1109/TWC.2018.2855151.

[103] Z. Wei, L. Zhao, J. Guo, D. W. K. Ng, and J. Yuan. "Multi-Beam NOMA for Hybrid mmWave Systems". In: *IEEE Transactions on Communications* 67.2 (2019), pp. 1705–1719. DOI: 10.1109/TCOMM.2018.2879930.

[104] C. Xu, R. Ye, Y. Huang, S. He, and C. Zhang. "Hybrid Precoding for Broadband Millimeter-Wave Communication Systems With Partial CSI". In: *IEEE Access* 6 (2018), pp. 50891–50900. DOI: 10.1109/ACCESS.2018.2862432.

[105] B. Ning, Z. Chen, X. Wang, and W. Mei. "Codebook-Based Hybrid Beamforming Design for MISOME Wiretap Channel". In: *IEEE Wireless Communications Letters* 8.1 (2019), pp. 57–60. DOI: 10.1109/LWC.2018.2852618.

[106] F. Sohrabi and W. Yu. "Hybrid Digital and Analog Beamforming Design for Large-Scale Antenna Arrays". In: *IEEE Journal of Selected Topics in Signal Processing* 10.3 (2016), pp. 501–513. DOI: 10.1109/JSTSP.2016.2520912.

[107] Mustafa A. Kishk and Mohamed-Slim Alouini. *Exploiting Randomly-located Blockages for Large-Scale Deployment of Intelligent Surfaces*. 2020. arXiv: 2001.10766 [cs.IT].

[108] Cunhua Pan, Hong Ren, Kezhi Wang, Wei Xu, Maged Elkashlan, Arumugam Nallanathan, and Lajos Hanzo. *Multicell MIMO Communications Relying on Intelligent Reflecting Surface*. 2020. arXiv: 1907.10864 [eess.SP].

[109] Xidong Mu, Yuanwei Liu, Li Guo, Jiaru Lin, and Naofal Al-Dhahir. "Exploiting Intelligent Reflecting Surfaces in NOMA Networks: Joint Beamforming Optimization". In: *IEEE Transactions on Wireless Communications* 19.10 (Oct. 2020), pp. 6884–6898. ISSN: 1558-2248. DOI: 10.1109/twc.2020.3006915. Available from: http://dx.doi.org/10.1109/TWC.2020.3006915.

[110] B. Zheng, Q. Wu, and R. Zhang. "Intelligent Reflecting Surface-Assisted Multiple Access With User Pairing: NOMA or OMA?" In: *IEEE Communications Letters* 24.4 (2020), pp. 753–757. DOI: 10.1109/LCOMM.2020.2969870.

[111] Y. Cheng, K. H. Li, Y. Liu, K. C. Teh, and H. Vincent Poor. "Downlink and Uplink Intelligent Reflecting Surface Aided Networks: NOMA and OMA". In:

IEEE Transactions on Wireless Communications (2021), pp. 1–1. DOI: 10.1109/TWC.2021.3054841.

[112] Peilan Wang, Jun Fang, Xiaojun Yuan, Zhi Chen, and Hongbin Li. "Intelligent Reflecting Surface-Assisted Millimeter Wave Communications: Joint Active and Passive Precoding Design". In: *IEEE Transactions on Vehicular Technology* 69.12 (Dec. 2020), pp. 14960–14973. ISSN: 1939-9359. DOI: 10.1109/tvt.2020.3031657. Available from: http://dx.doi.org/10.1109/TVT.2020.3031657.

[113] C. Jia, H. Gao, N. Chen, and Y. He. "Machine learning empowered beam management for intelligent reflecting surface assisted MmWave networks". In: *China Communications* 17.10 (2020), pp. 100–114. DOI: 10.23919/JCC.2020.10.007.

[114] J. Zuo, Y. Liu, E. Basar, and O. A. Dobre. "Intelligent Reflecting Surface Enhanced Millimeter-Wave NOMA Systems". In: *IEEE Communications Letters* 24.11 (2020), pp. 2632–2636. DOI: 10.1109/LCOMM.2020.3009158.

[115] G. Yu, X. Chen, C. Zhong, D. W. Kwan Ng, and Z. Zhang. "Design, Analysis, and Optimization of a Large Intelligent Reflecting Surface-Aided B5G Cellular Internet of Things". In: *IEEE Internet of Things Journal* 7.9 (2020), pp. 8902–8916. DOI: 10.1109/JIOT.2020.2996984.